School of Science and Engineering

Department of Petroleum Engineering

A Decision Support Model for Differential Sticking Avoidance

by

Affonso Marcelo Fernandes Lourenço

This thesis is presented for the Degree of

Doctor of Philosophy

of

Curtin University

January 2012

Declaration

To the best of my knowledge and belief this thesis contains no material previously published by any other person except where due acknowledgment has been made.

This thesis contains no material which has been accepted for the award of any other degree or diploma in any university.

Signature: . . . . . .

Date: . . . .

Contents

List of Tables

List of Figures

Abstract

An innovative theoretical model to quantify the risk of differential sticking is presented. The proposed risk assessment is based on the concept of likelihood versus consequence. The likelihood of the problem's occurrence in a given wellbore segment (case) is evaluated from a knowledge-based model and translated by a similarity measure of relevant operational conditions between the target case and historical cases with known outcomes. The stand alone module performed satisfactorily and predicts the likelihood of occurrence by more than a chance probability, demonstrated by a rate of sixty eight percent (68%) correct predictions against field data from forty four wells drilled by different operators in several fields. The consequence assessment is performed through an unidimensional mechanistic model that predicts the downhole overpull (differential sticking force) and performed well while estimating reported overpulls from known field instances of the problem. Together, the models serve as a risk assessment tool able to correctly describe risk operational trends while designing or drilling wells, with critical situations being defined as high likelihood plus high potential overpulls. Both models utilizes unique experimental data about mechanical properties of drilling fluids filtercakes (hardness, torque resistance and adhesion-cohesion strength) under simulated downhole conditions, raised through the HTHP Mudcake Characterization Equipment developed during the course of this research work. Moreover, the study contributes towards the development of modern predictive models aiming at combining large amount of available operational drilling data (LWD, PWD, mudlogging, survey, drilling reports, etc), expert's knowledge, laboratory data and phenomenological models in order to optimize drilling operations.

Acknowledgment

I thank Curtin University, in special, the Department of Petroleum Engineering, the Commonwealth Scientific and Industrial Research Organization (CSIRO) and the government of Western Australia for the continuous support and funding that enabled the conclusion of this work.

I would like to express my sincere gratitude to my supervisor, Dr. Jorge H. B. Sampaio Jr., for the solid supervision, friendship and patience offered to me during the course of this work. My special thanks to Dr. Brian Evans, head of the Department of Petroleum Engineering, for the trust deposited on me and for accommodating so well numerous personal and management-related requests that handled in any other way could have jeopardized the conclusion of this research work. I extend my gratitude to Dr. Edson Y. Nakagawa for the opportunities, support and authorizations given within CSIRO, Mr. Bruce Maney for his dedication and sharing of his technical skills while designing and building the HPHT Mudcake Characterization Equipment and Mr. Dean Waly for contributing with field data gathering, database organization and helpful thoughts and hands during the development of the HPHT MCCE, calibration and conduction of experiments.

Furthermore, I thank all involved in Petrobras/Cenpes and Genesis Petroleum for providing valuable field data, software tools and continuous technical support that became integral part of this dissertation. Special thanks to Carlos Damski, CEO of Genesis Petroleum, for granting full access to the Genesis Petroleum Suite throughout the research work.

My sincere thanks to Curtin University and CSIRO supporting staff and colleagues for receiving me so well and for the daily dose of encouragement, fruitful conversations, cultural enrichment, special moments and laughs.

Finally, I would like to thank my wife for her love, encouragement and patience.

For my Beloved Mother Elza Fernandes Lourenço

Chapter 1

Introduction

Conventional drilling operations of oil and gas wells are carried out by rotating a drillstring attached to a drill bit submitted to compressive load. The drillstring is composed by sections of pipes of standard dimensions and other mechanical characteristics that are connected in sequence as the hole advances. A drilling fluid, often containing suspended solids, is circulated in the well while drilling. The drilling fluid is pumped throughout the drillstring, passes through nozzles in the drill bit and returns to the surface through the annular space between the borehole wall and the drillstring. The drilling fluid has many functions, including providing enough pressure to hold the borehole wall stable and to prevent fluids (liquids and gases) present in the permeable formations being drilled to enter the well[1]. For this purpose, the density of the drilling fluid is adjusted in order to provide pressure greater than that of the fluids present in the pores of the geological formations and smaller than the formation's fracture pressure. As a consequence, filtration of drilling fluid occurs through the borehole wall into the formation, leaving a filtercake (or mudcake) formed by the suspended solids on the borehole wall. The filtercake acts as a seal between the borehole and the formation. Its thickness and characteristics are dictated by the characteristics of the drilling fluid, formation and operational scenario such as magnitude of differential pressure and flow rate. Although the sealing effect is not perfect, the filtercake prevents significant losses of drilling fluid to the formation and undesirable physical-chemical interactions between drilling fluid components and the formation. The circulation of the drilling fluid also carries the drilled cuttings generated by the bit to the surface, keeping the bottom hole clean.

Stuck pipe is a general term used, particularly among drillers, to describe

[1]This technique is called "overbalanced drilling" (OBD). Drilling with borehole pressure smaller than formation pressure is also possible and called "underbalanced drilling" (UBD). UBD is considered a non-conventional drilling technique.

the problem of loosing the ability to move the drillstring assembly. The causes of stuck pipe are many and they can be classified into two categories: mechanical and differential sticking. The classification is based on the physical mechanism causing the problem, and therefore mechanical sticking refers to the cases where the movement of the drillstring is prevented by mechanical means. The most common causes of mechanical sticking are accumulation of drilled cuttings (inadequate hole cleaning), borehole instability (pack off), the closing of borehole by reactive formations (clay swelling), the drilling of unsymmetrical sections of the borehole (key seating) and the presence of *junk*[2] in the well. Differential sticking is different. The locking mechanism is caused by a force, acting radially, that pushes the drillstring against the borehole wall. This force is generated whenever a positive differential pressure exists between the borehole and the formation being drilled. The drillstring becomes exposed to the differential force whenever it is embedded in the filtercake formed by solids present in the drilling fluid and deposited on the borehole wall during filtration through a permeable formation.

This dissertation is about differential sticking, an old drilling problem that resurged with more significant consequences due to the expansion of the horizons of hydrocarbon exploration from onshore shallow vertical wells to deep offshore wells with complex trajectories. The time to free a stuck pipe can range from hours to weeks, rapidly becoming a very expensive exercise with disastrous consequences to the cost of drilling campaigns, particularly when drilling offshore. Despite of responding to a significant percentage of overall drilling problems[3], a theoretical methodology able to predict its occurrence with more than a chance probability across different fields and drilling conditions remains to be developed and recognized by the industry. In addition, the number of works conducted in oil companies or academia, dedicated to explicitly predicting its occurrence in the field, are rather the exception than the rule when compared to the number of investigations tackling a particular aspect of it, for example, a variable or phenomenon that indirectly affects the problem. In these cases, the approach is usually purely analytical while in the other it is often purely statistical. Although this work does not innovate in attempting to anticipate the problem given certain drilling operational conditions, it certainly does on its approach. An effort was made in proposing a engineering methodology aimed at computing a risk score for any given drilling scenario. The novel

[2]Expression referring to any undesirable object left in the well; for example: a tool or a broken piece of the the drillstring.

[3]Stuck pipe occurrences are responsible for around 35% of overall drilling problems and 11% of unproductive time. Differential sticking responds to about 30% of stuck pipe occurrences[4].

contribution lies in attempting to compute this risk score combining the results of approximate analytical models describing the physical phenomenon and an optimized analysis and history match of available drilling data from historical wells via a classical likelihood versus consequence risk definition. The result is neither a purely statistical non-physically based model nor a purely analytical model that fails in addressing the uncertain nature of its variables. Instead, the combination leads to a more robust and potentially more exact model, which explicits the physics behind the problem while treating its innate uncertainties utilizing techniques such as case-based reasoning and theory of fuzzy sets. These mathematical artifices enable easier and adequate use of available field data and translation of expert knowledge into crisp numerical answers to unavailable information. Finally, the soft computing methodology developed, here applied to the problem for the first time, can be used as a problem solving platform for other drilling problems.

Chapter 2

Statement of the Problem

The difficulties behind avoiding differential sticking becomes clear upon a detailed analysis of the physical phenomenon.

Fig. 2.1 shows an inclined section of a wellbore being drilled and details of the drillpipes and bottom hole assembly (BHA), where d is the chord over the cross section of the drillstring defined by the extent of embedment in the mudcake. The length h is the effective length of the drillstring in contact with the borehole wall and consequently with the mudcake. As mentioned previously, differential sticking only occurs upon embedment of the drillstring in the drilling fluid mudcake, creating the necessary physical exposure to the differential pressure existing between the borehole and the formation being drilled. Before being covered by the mudcake, the wellbore pressure acts uniformly on the body of the drillstring and no net force is observed. Drilling fluid filtration starts in the moment the drilling fluids makes contact with the permeable formation and continues through a filtercake of solids formed on the borehole wall as a consequence of filtration. It is at this permeable interface, acting as a partial seal between the borehole and formation, that severe pressure drop exists and that the phenomenon takes place. A net force in radial direction and towards the borehole wall is generated whenever embedment occurs. It can be verified from Fig. 2.1 that the greater the projected exposed area, i.e., the product between d and h, the greater the sticking force. If the sum of the weight of the drillstring plus the drag force along the wellbore plus the differential sticking force surpasses the tensile strength (Yield Point) of the drillpipes, the drillstring will be stuck[1]. One can also conclude from the same figure that the maximum value of d is the outer diameter of the drillstring and the maximum value of h is the length of drillstring. Despite of the limit in the magnitude

[1]Tensile loads near the Yield Point are usually avoided and the tolerated limit varies from case to case. In spite of that, rupture of drillstring because of excessive overpull is not a rare event.

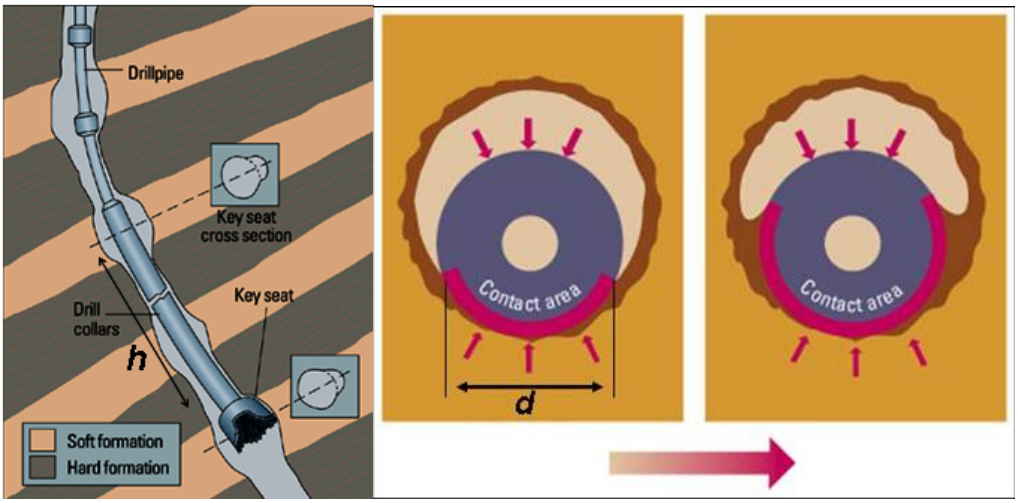

Figure 2.1: Differential Sticking

of the differential sticking force, a stuck pipe event worsens proportionally to the fraction of drillstring surface covered by mudcake. The reason is related to the increase in drag and torsional resistance to be overcome in order to free the drillstring.

The problem lies exactly in evaluating the two variables defining the size of the exposed area of the drillstring to the differential pressure. For a given bottomhole pressure, this area will define the magnitude of the differential sticking force. The variable d is a function of mudcake thickness and the extent of embedment of the drillstring in its matrix. The modeling required to elucidate these two effects is very difficult given the complexity of involved physics and variety of drilling fluid compositions. Moreover, although several studies about drilling fluid filtration [43, 16, 55, 48]were conducted with models able to predict filtercake thickness, some rigorously mechanistically developed [36, 52]„ they are usually based on unrealistic hypothesis, or difficult and time consuming to be solved. They are also often function of variables that are not easily available in the field. Those without these latter problem rely on empirical correlations or experimental parameters to compute their outputs. Even more complicated is the estimation of the embedment depth δ , and the reason resides on the fact that few attempts are found to mechanically characterize the mudcake [48, 32, 6] and its interaction with the drillstring. For these reasons it was decided that the computation of these variables would be based on a experimental program to assess both filtration and mechanical properties of mudcakes under simulated downhole conditions. That decision led to the development of a unique high pressure and high temperature mudcake characterization equipment that enables the assessment of embedment resistance,

torsional resistance and adhesion strength of mudcakes. Filtration properties among other relevant effects could also be studied. Chapter 5 brings the details.

Another challenge in correctly evaluating the area exposed to the differential pressure relates to the effective length of contact of the drillstring with the borehole wall. Where and to what extent does the drilling assembly touches the mudcake? The answer to this question provides h in Fig. 2.1 and the path to find it passes through analysis of deformation of a multicomponent drillstring under stress and its interaction with curved boreholes of different sizes.

In conjunction with this analytical stepwise analysis made so far, one can also imagine the added difficulty to the unfolding problem related to the dynamics and procedures of conventional rotary drilling[2]. While drilling, annular flow exists and the drillstring rotates, usually not uniformly from surface to the bottom or concentric to the well, constantly eroding part of the ever growing mudcake. Every stand length (usually about twenty seven meters long) a new connection needs to be made and the drillstring pulled slightly from the bottom while the whole system is usually brought to a halt during a few minutes. The sequence of these events not only directly affects the previously mentioned relevant variables, but also add random and systematic uncertainties to them, which are difficult to quantify due to the lack of perfect repeatability and changes in drilling scenario as operation progresses (depth, formation characteristics, trajectory, downhole pressures, drilling fluid and flow characteristic, stresses on drillstring, etc).

The final variable with considerable amount of uncertainty is the friction coefficient between the drillstring and the borehole (or cased hole). Field tests can be conducted while drilling to assess this parameter for different operational conditions, but it is time consuming and by no means accurate enough. In addition, other methods must be used during the well design phase of the project in order to devise a problem-free drilling campaign.

It is now clear why the problem remains unsolved and the difficulties behind the development of a rigorous theoretical model for its prediction and consequence avoidance. It is also reasonably easy to realize that its frequency of occurrence increased with the advance of extended reach wells, many horizontal, where deeper wells (higher pressures), and increased exposure of the drillstring to drilled formations (drillstring lies on the bottom of the well and for long periods of time) are necessary.

As a consequence of these difficulties, academia and industry members

[2]Several modern variations exist such as the practice of using downhole motors with a non-rotating drillstring

attempted to avoid the problem through statistical models [39, 19, 24]. Indeed, these models were able to include a greater variety and amount of variables in the analysis of the problem, aiming at capturing, for example, the previously described dynamics of rotary drilling, effect of human errors and effects too difficult to be seen or translated into equations by physics and mathematics. Some models succeeded and even outperformed analytical models in their task to identify the problem based on specific historical data, but the interrelation between variables are never explained and extrapolation of results for new datasets, i.e., different fields, proved unreliable. Real time predictions are also difficult and unknown relations between variables makes it difficult for engineers to correct the course of a likely stuck pipe event.

The subsequent chapters intend to demonstrate the attempt of unifying the advantages of the two approaches, with the remark that purely statistical models are replaced with knowledge-based models or models where mathematical techniques classified as artificial intelligence are deployed as an alternative or support to analytical models depending on its intended role.

Chapter 3

Literature Review

3.1 Works on Analytical Predictive Models

Differential sticking is an old drilling problem and simplified models can be found in classic petroleum engineering textbooks [57], but as heavily stressed across the dissertation the challenge lies on evaluating certain variables and relevant operational aspects that affect the problem. Aadnoy [3] developed analytical equations to determine the depth of stuck point in deviated wellbores based on pull and torsion tests. Analytical equations are derived to compute forces in the drillstring from top to bottom and methods to free the pipe investigated. The model accounts for friction forces [10] in any well geometry and the problem of differential sticking was also contemplated. In spite of standing as one of the most complete works in terms of analytical description of stuck pipe and a practical engineering method to estimate the depth to the stuck point, it does not attempt to solve the derived differential sticking equation in detail given the difficulties in evaluating terms depending on the contact between the drillstring and mudcake. The same equation is carefully examined in Chapter 7 as Eq. 7.1.

De Souza et al. [33] worked specifically on differential sticking in non-conventional wells and described a valuable attempt in utilizing analytical methods to solve the problem. One of the contributions come from integrating a cross-flow microfiltration analytical model to calculate mudcake growth [52] with simulated results of velocity profiles in non-Newtonian eccentric annular flow, obtained from ANSYS®, a commercial program for computational fluid flow modeling. This analysis aimed at calculating a final dynamic mudcake thickness for a given drilling condition. Finally, a qualitative numerical analysis on the nature of contact between the drillstring and mudcake is provided also using ANSYS®. The results were used in estimating torque and drag force

levels necessary to free the drillstring for stipulated types of contact, i.e., two-dimensional (2D) contact between flexible surfaces with adhesion, cohesion effect and dry friction. Material properties for drillstring and mudcake were guessed. Unfortunately, the studies are not combined in order to formulate a methodology for differential sticking prediction in drilling operations. Moreover, the resulting analysis reveals the difficulties in dealing with quantities such as diameter of solids particles in the mudcake[1], volume fraction on the surface and in the bulk of the mudcake as well as assumptions regarding various hydrodynamic effects taking place as the fluid, concomitantly, filtrates through the borehole wall and erodes the surface of the formed mudcake. In addition to the known numerical instabilities and computational time involved in solving finite element numerical schemes, the authors stress the difficulties in obtaining representative mechanical properties for the mudcakes and its importance to properly assess the contact problem.

Empirical models complete the array of analytical methods available in the literature dedicated to development of predictive models to be used in well design or well development. Two relevant works are discussed here: the first purely empirical and the other semi-empirical. Magaji et al. [40] developed two correlations aimed at reducing the likelihood of stuck pipe. The "stuck pipe risk function" ($SPRF$) is a correlation based on operational variables to assess the risk of stuck pipe for a given drilling scenario. The correlation was developed based on the correlated data from various stuck pipe instances in the Niger Delta and includes mechanical sticking too. According to the authors, the correlation tries to incorporate variables from instances of stuck pipe coming from wellbore instabilities, borehole geometry and differential sticking. Eq. 3.1 shows the proposed function.

$$SPRF = 0.2\left(\log 0,1L\right)^{2.5}\left[0.25\left(\sin\theta\right)^{2} + 0.2\left(\sin t_h\right)^{2}\cdots\right]$$

$$\left[\cdots + 0.35 f_n^{0.08}\left(\cos\alpha\right)^{4}\left(1+\frac{200}{f_d}\right)\cdots\right]$$

$$\left[\cdots\left(1+10ABS(M_1-M_2)^{1.6} + 0.2\log\left(100\max\triangle G\right)\right]\right. \tag{3.1}$$

$$M_1 = P_0 + 0.04 + 0.02\sin\theta + 0.00168\left(\log L\right)^{3}\cdots$$

$$\cdots\left(\sin\theta\right)^{2}\left(\cos\alpha\right)^{3} K_{mud}\left(\log t_h\right)^{2} 0.02 f_n \tag{3.2}$$

[1] the mudcake is actually composed by a mixture of various solid materials with different shapes, sizes and physicochemical properties.

Where L is the shale length, θ is the borehole inclination, t_h the open hole exposure time, f_n number of faults in one kilometer radius, α is the difference between well and maximum in-situ stress directions (in degrees), f_d is a filter-cake quality factor not clearly explained, M_2 is the actual mud weight gradient (in $\frac{psi}{ft}$), $\triangle G$ is the overbalance gradient (in $\frac{psi}{ft}$), P_0 is the pore pressure (in psi) and K_{mud} a coefficient (0.003 for oil-based muds and 0.013 for water-based muds). Thresholds of $SPRF$ values are determined from plotting the function versus stuck pipe unproductive time and are used as risk scores. Results revealed that $SPRF$ scores of less than 0.4 are related to safe operational conditions, while scores above 0.7 demonstrated high risk levels of stuck pipe and well plan should be revised. Similarly, a risk analysis is performed based on the required mud weight to stabilize shales, i.e., M_1. An optimum mud weight gradient of 0.56 $\frac{psi}{ft}$ was proposed with wellbore instabilities tendencies gradually increased for mud weights less than that value and differential sticking tendencies for values above. The model showed good agreement against local field data, but extrapolations of the method to other areas seem inappropriate given the nature of the correlation.

The second relevant work was developed by Underhill et al. [34] while investigating differential sticking instances of formation logging tools in the Gulf of Mexico. An interesting semi-analytical model is proposed in the form of a function called "sticking probability". As far as differential sticking is concerned, exact models were proposed to estimate the level of contact L_{cyl} between the cable, or tool, and the mudcake. Mudcake filtration and mechanical properties are expressed through a "mudcake thickness parameter" β and a "stickance factor" S, that are measured with a laboratory device called "stickance tester" [48] which is detailed in the next section. These models, together with the differential pressure, provide the necessary inputs for the calculation of the required axial pull force to keep the tool free.

$$F_{op} = 2L_{cyl}De^{\frac{1}{2}}\beta^{\frac{1}{2}}\tau_0 t^{\frac{1}{4}} \tag{3.3}$$

$$De = \frac{D}{1 - \frac{D}{D_w}} \tag{3.4}$$

$$M_0 = \frac{2}{3}\pi D_{ball}^{\frac{3}{2}}\beta^{\frac{3}{2}}\tau_0 t^{\frac{3}{4}} \tag{3.5}$$

$$S = \frac{2}{3}\pi D_{ball}^{\frac{3}{2}}\beta^{\frac{3}{2}}\tau_0 \tag{3.6}$$

Where F_{op} was called overpull force, D is the object (cable or tool) diameter,

D_w is the borehole diameter and t is the stationary time. In Eq. 3.5 concerning the "stickance" tester, M_0 is the torque required to rotate a sphere with diameter D_{ball} embedded in the mudcake, and τ_0 is the drilling fluid yield stress.

As far as practical application is concerned, empirical correlations were developed to estimate the "stickance factor" for water-based and oil-based drilling fluids since measurements for the "stickance tester" were not available. The so called probability function estimates the likelihood of stuck tool instance that is considered to be proportional to the magnitude of axial pull forces required keep the tool or cable free for a given operational condition. The method accounts for differential sticking and key seating. Unfortunately, the form of the probability function was not revealed preventing proper assessment from being conducted and consequently its use. The published model results were compared to fishing frequencies and considered satisfactory in terms of providing valuable information prior to new logging runs conducted in the company. This work presents similarities with the chosen approach in this dissertation. The difference lies in dealing with a drillstring assembly instead of a cable, the use of a more comprehensive array of measured mudcake properties, a robust and yet adaptable risk assessment methodology based on field data and independence of empirical correlations.

3.1.1 Works on Drilling Fluid Filtercakes (Mudcake)

Nascimento et al. [28] published a recent review paper on differential sticking. In addition to emphasizing the high percentage contribution of the problem to unproductive time and costs, the paper focus in the drilling fluid. Changes to drilling fluid properties are probably the easiest among the few options the driller has to reduce the risk of differential sticking. The work reviews the experimental procedures and apparatus developed to date to investigate wellbore filtration and mudcake in order to optimize them and reduce sticking risk. The next sections present in more detail some of the relevant works in field.

3.1.1.1 Filtration and Growth

Fisher et al. [36] published a comprehensive modeling work on mudcake growth from Non-Newtonian fluid filtration in drilling operations. In addition to a complete literature review on the subject, two three-dimensional finite element models were developed: one for the non-Newtonian flow in annuli (between drillstring and borehole wall) with effect of drillstring rotation and the other for the fluid base permeation into the permeable formation. These were coupled

with a crossflow microfiltration model to predict mudcake thickness build up with time. The importance of this work when compared to other flow models or filtration models is the fact it was developed specifically for drilling operations, with effects such as drillstring eccentricity and boundaries conditions tailored to the drilling realm. The coupling of axial hydrodynamic effects with the radial multiphase filtration phenomenon completes its relevance. The model allows tracking of mudcake thickness with time for a given set of drilling fluid composition, drilling fluid rheological properties, fluid flow rate and drillstring eccentricity data. In addition, the model provides velocity and radial saturation profiles of the invading fluid. The crossflow microfiltration model is from the previously mentioned Stamatakis and Tien [52]. In this work a force balance on a single particle is calculated on the rough surface of the mudcake and an adhesion probability calculated. This probability measures the chance for the deposition of the particle on the cake surface rather than being carried away by the drilling fluid crossflow (shear flow). An important conclusion is the influence of eccentricity on mudcake growth. Increasing eccentricity leads to a wider variation of mudcake growth around the wellbore, with minimum/maximum values occurring either side of the minimum distance between the borehole wall and the rotating drillstring. The complexity of the model is a reason for praise and a disadvantage at the same time. In one hand it enables the detailed study of variables on the problem, but in the other hand it makes it difficult to use since input variables are often unavailable and calculated parameters carries significant uncertainty, such as particle diameter or solids volume fraction in the mudcake and roughness of cake surface, respectively.

Experiments on static or dynamic filtration have been the subject of a number of investigations [43, 42, 29, 16]. Arthur [43] and Peng [42] emphasized the impact of mudcake compressibility on filtrate loss while investigating the effects of drilling fluid composition, differential pressure, filter medium and temperature on filtration properties of water-based drilling fluids (KCl + Polymer and Gypsum + Ferrochrome Lignosulphonate (GFL)) and oil-based systems by adding diesel to the GFL drilling fluid. Results suggest a decrease of mudcake compressibility and increase in thickness with increase of solids concentration, particularly barite; increase of fluid loss with temperature and increase of cake compressibility with increase in bentonite concentration. Formation permeability — simulated by filter papers of different permeabilities — had little effect on filtration rates when compared to cake permeability. It is worth mentioning Peng's experimental procedure of intercalating dynamic and static filtration intervals to simulate the interruption of flow during connections. A gradual decrease in fluid loss was observed during the static filtration intervals deemed

because of an increase in mudcake thickness in the absence of crossflow. The effect of polymer type was superficially investigated, but Xantham Gum (XC) was reported to lead to lower spurt losses[2] when compared to Carboximetilcelulose (CMC). Filtration curves derived from Darcy's law and typically used in the field demonstrated good agreement with data.

Lomba et al. [16] conducted further investigation on the effect of polymeric solution type and rheology and solids shape on filtration properties of Drill-In [3] fluids. Static filtration experiments were conducted in unconsolidated porous bed (mixture of sand and sintered bauxite) and depth of fluid invasion plus thickness of internal and external filtercakes were measured. Experiments were performed with two sets of drilling fluid: polymeric fluid containing different kinds of bridging materials[4] and a fluid with a fixed amount of calcium carbonate with different polymers. One of the results is an ordered sequence for types of polymers regarding their influence on the degree of fluid invasion into the formation and filtration velocity. Invasion increased according to the following sequence: Schleroglucan < HMHAG < XC < PHPA < HPG << CMC . While filtration velocity presented the following increasing sequence: Schleroglucan < HMHAG < XC < PHPA < HPG << CMC.

Other two important conclusions should be highlighted. Firstly, granular, laminated and fiber-like bridging materials behave very differently regarding filtration and its effect is relevant to predict filtration behavior. Secondly, results strongly suggests, except for CMC, that besides viscosity other rheological parameters should be considered in the modeling of static and dynamic filtration behavior. The authors refer to elastic responses, chiefly elongational flow, since much more energy was spent while flowing through the sand bed than predicted by Darcy flow considering the 100 s^{-1} viscosity, that typically characterize flow through porous media. These results are in full agreement with the ones from Durst et al. [20] that affirmed pressure drop of a porous media flow is only due to a small extent to the shear force term usually employed to derive Darcy's law. A term to account for elongational flow needs to be incorporated in the flow equation to lead to correct results. A theoretically derived flow equation is presented with both effects and experimental results used to back the presented flow model. In fact, the particularly important works of Jones and Walters [54], Martins et al. [13] and Barree and Conway [12] corroborates with the idea, emphasizing the importance of extensional viscosity specially in

[2]Filtrate volume observed during the initial phases of filtration, usually measured 30 seconds beginning of filtration.

[3]Fluids used to drill through the reservoir zone.

[4]Solids used to plug pores-throat of the permeable formation and decrease filtration as much as possible.

water-based fluids containing PHPA.

3.1.1.2 Mechanical Behavior

Fisher-Cripps [17] provided an interesting review of analysis methods for sub-micron indentation testing. The relevance of this work resides on the specificness of sub-micron mechanical tests, with indentations around 1 or 2 μm, where the goal is to obtain hardness and elastic modulus of thin films of materials from experimental data of indenter load versus depth of penetration. Unlike conventional indentation hardness tests, the size (and hence the projected contact area) of residual impression left in the surface of specimen is too small to be measured accurately. Therefore, a detailed analysis is given on semi-empirical methods (Hertz elastic equations of contact combined with raw data) to correctly determine the contact area. Consequently, hardness and extraction of elastic modulus of elasto-plastic materials from load-displacement data can be obtained with spherical and pyramidal indenters. The review provides valuable information on how to conduct the same experiments on more challenging materials such as drilling fluid filtercakes.

Although challenging, experimental path seems the only reasonable way to predicting the mechanical behavior of mudcakes and this was the subject of several authors. Reid et al. [48] offered on of the best reviews on these attempts while adding to the list of apparatus aiming at mechanically testing mudcakes. Table 3.1 brings a list a relevant experimental set up developed for the purpose.

Reid et al. [48] developed the so called "stickance tester" which is an apparatus to measure torque resistance of mudcakes formed from static filtration. A sphere lies on top of a filter medium and torque to free the ball measured as filtration proceeds and mudcake is formed. A parameter called "stickance" is used to compare the mechanical behavior, in this case only torque resistance, of mudcakes formed from filtration of water-based and oil-based drilling fluids. The parameter is the slope of the straight line obtained from a graph of resistive torque versus $\sqrt[4]{t^3}$, with t meaning filtration time, and used as a risk score to assess sticking tendencies. Although no decisive correlation could be established between the parameter and presented field cases, the "stickance tester" was considered appropriate for field use and could provide information on sticking tendencies, especially when using ceramic aloxite disks as the filter medium. The use of lubricants was also found to lower the "stickance" tendency of mudcakes. The authors also derived Eq. 3.3 to estimate the sliding friction force to free stuck drillcollars and considered results in agreement with

Table 3.1: Review on Devices used for Mudcake Mechanical Assessment.

Authors	**Sample**	**Indenter**	**Mudcake Formation**	**Direction of Force**	**Max. Temp. (^0C)**	**Max ΔP (psi)**
Krol [23]	Cylinder	Cylinder	Static or Dynamic	Axial	150	2000
Helmick [30]	Cylinder	Cylinder	Static or Dynamic	Axial or Radial	Ambient	100
Annis [37]	Disk	Disk	Static	Axial	Ambient	500
Clark [5]	Cylinder	Cylinder	Static or Dynamic	Axial	150	2000
Bushnell-Watson [41]	Cylinder	Cylinder	Static or Dynamic	Rotation	65	100
Reid [48]	Disk	Sphere	Static	Rotation	200	1200
Lourenco (this study)	Disk or Cylinder	Sphere	Static	Combined Axial (variable rate up and down) and Rotation (variable speed)	150	1000

field experiences in terms of the order of magnitude of pull forces. Instead of using the "stickance" Chesser et al. [55] demonstrated a valuable correlation between mudcake compressibility and differential sticking occurrences in the field. Mudcake compressibility was defined as in Eq. 3.7 and measured utilizing a dynamic filtration apparatus. Although further investigations are needed, this parameter represents a simple way of tracking differential sticking tendencies in the field.

$$V_{500} = V_{100}\sqrt{\frac{p_{500}}{p_{100}}} \tag{3.7}$$

Where V is the volume of filtrate per unit of time and p is the filtration pressure in pounds per square inches. Therefore a mudcake with no compressibility would present a ratio $\frac{V_{500}}{V_{100}}$ of *2.24*.

Isambourg et al. [32] also developed a small scale simulator for the investigation of differential sticking and lubricity problems under simulated downhole conditions. The wellbore was represented by a simulated downhole cell in which the drilling fluid was circulated under pressure. A porous metal cylinder was installed inside the cell to simulate a permeable formation, allowing flow of filtrate from inside the cell to outside and consequent mudcake build-up. Sensors measured axial and radial forces on the pipe and torque was also measured. Differential pressures up to 580 psi could be simulated and cell pressure (maximum of 1450 psi) and pore pressure (although not clearly specified, presumably back pressure measured within the metallic porous medium), filtrate volume, mudcake thickness and pipe penetration in the mudcake were also monitored. The effects of mudcake thickness, presence of KCl and solids concentration were investigated for bentonitic drilling fluid formulations with polymers for filtration control. Apart from confirming the important role of particle shape and size distribution and the non-uniform mudcake permeability on filtration, an increase in axial pull force was observed with increase in solids concentration and the presence of KCl. The first effect was deemed because of increase in cake hardness and permeability given the reduced water content and the second because of hardening of the bentonitic mudcake given the KCl inhibition swelling effect. An interesting observation was made regarding the mudcake thickness effect: higher pull forces were observed for thinner mudcakes despite of its reduced contact area.

This section is concluded looking back on a series of papers published by Amanullah et al. [50, 7, 8]. The Mudcake Characterization Equipment (MCCE) was developed building upon the previously listed experimental experience on the subject. This bench scale apparatus aimed at expanding the assessment

of mechanical properties of mudcakes. Hardness, adhesion as well as torque experiments were conducted on bentonitic drilling fluid formulations. Except for the work of Isambourg et al.[32], all other experimental attempts to mechanically characterizing the mudcake was either based on torque, the most common one, or hardness, through embedment of an indenter into the mudcake matrix. Amanullah et al. used a hemispherical indenter attached to a torque motor and load frame through a shaft to perform the experiments. A stack of load and torque cell connected to the indenter enabled the assessment of resistance to axial loads, adhesive and cohesive forces and torque resistance of mudcakes. Experiments were conducted at ambient temperature and pressure and a major drawback was the fact the mudcake was formed through filtration in standard low pressure (100 psi) API filter presses prior to being transferred to the MCCE. Amanullah et al. [50] defined a parameter called "Embedment Modulus" (EM) to compare the resistance to the embedment of the indenter in the mudcake matrix. This parameter was obtained from the graph of axial force versus superficial embedded area of the indenter. This experiment was performed by driving the indenter at a constant speed of 0.25 $\frac{mm}{min}$ into the mudcake and recording the resultant axial load. Different bentonitic drilling fluid formulations were tested and the effects of concentration of solids (bentonite and barite), type of salt (NaCl and KCl) and filtration control polymer type (PAC, CMC and Starch) on the EM were investigated. Barite-bentonite systems led to the hardest mudcake with EM around 0.4 $\frac{gf}{mm^2}$ and basic systems presenting only NaCl and bentonite resulted in the most soft mudcake. Polymers tended to increase the EM of mudcakes, especially PAC. Analogously, adhesive and cohesive forces of mudcakes were assessed pulling the indenter out the mudcake. Two parameters were proposed to quantify the adhesive and cohesive tendencies of mudcakes: adhesion-cohesion modulus (ACM) and adhesive-cohesive bond strength (ACBS). The first is the slope of the linear part of the graph between pulling force versus embedded area. As the indenter is pulled out of the mudcake the pulling force increases (from the adhesion of the mudcake to the indenter's surface) linearly up to a certain point before a non-linear transition region is observed. A maximum is then reached. According to the authors, the linear part resembles a Hookean behavior of the mudcake with elastic characteristic and the maximum pull could be compared with the yield stress. The maximum pull was named ACBS. Once more, the barite-bentonite with NaCl drilling fluid presented the highest adhesion to the indenter. The presence of KCl drastically reduced the adhesion in the same system. The presence of PAC increased adhesion potential while Starch seemed not to affect it. The third paper from the same author publishes the results of tor-

sional resistances of mudcakes. In this experiments, the indenter was rotated at a constant angular velocity of 0.5 $\frac{deg}{min}$ at a predetermined embedment depth while torque was monitored. The resultant curves presented a peak torque representing the highest torsional resistant of the bond transmitter elements in the mudcake. After a relatively quick relaxation, the post peak region stabilizes at a plateau indicating the completion of the torsional weakening of the bond transmitters. Results demonstrated the complex nature of intermolecular interaction in the mudcake and torsional resistances were very sensitive to mud additives. Higher maximum torque resistances for salt water-based bentonite fluids were observed when compared to fresh water ones. Non-anionic fluid loss additives, barite and non-floculated bentonite systems increased torsional resistance of mudcakes. Contrarily, the presence of KCl and PAC decreased it.

The development of the MCCE played an important role in this dissertation. This precursor work led to the development of the High Pressure and High Temperature Mudcake Characterization Equipment (HPHT MCCE). The intention was to build upon previous experiences here reported and arrive at an improved design for an apparatus capable of extending the capabilities in investigating mechanical properties of mudcakes. The improvements are detailed in Chapter 5 , but the new configuration enables the mudcake to be formed in the same pressure cell where the mechanical assessment is performed. Differential pressures up to 1000 psi and temperatures up to 150 ^oC can be tested, enabling better simulation of downhole conditions. In addition, in situ combined axial and torsional experiments can be performed and all measurements are made without the effect of friction in bearings and seals of the pressure cell, a critical matter rarely mentioned in previous works on the subject.

3.2 Works on Statistical and Knowledge-based Models

O'Keefe and Preece [44] presented a valuable review on the areas where knowledge-based systems (KBS) have been successful. In addition, the paper review the progress made in understanding and using development methodologies, validation methods and implementation of such systems. The work helps with putting into context its value for current and future applications of KBS in the oil industry.

Fletcher and Davis [14] published an interesting work on decision-making

with incomplete evidence. The methodology behind the "Juniper" approach, a risk assessment model to assist decision makers with complex projects is also presented. During their introductory discussion about the subject, problems or models are classified into four categories and stuck pipe can be considered a "Type 3" problem described as follows: "where the structure is largely complete (although possibly vague in part) and the parameters are known only as relations or limits". The authors mention that techniques such as imprecise probabilities (fuzzy logic and interval probability theory) are the most appropriate to handle these models. In these models it is possible to talk in terms of probabilities of fuzzy events (probability of a field being "big") and of fuzzy probabilities (a "high" probability). The selected works in this section present attempt to solve differential sticking by utilizing a probabilistic approach for those author considering stuck pipe to be "Type 2" [5] problem and others incorporating knowledge management techniques into the arsenal of possible solutions.

Hempkins et al. [19, 39] published two important studies utilizing multivariate statistical analysis to tackle petroleum related problems. The most interesting one from the perspective of this thesis is the second one, where the author was able to classify, a priori, field cases of mechanical, differential sticking and cases where the problem did not occur, with a success rate greater than 81 %. The method was based ultimately in a discriminant function analysis performed in a database containing 20 different types of relevant variables related to the problem that were collected from 131 instances of stuck pipe. A factor analysis was initially performed to draw interrelationships between the variables within the tree groups and than two discriminant functions were derived that were able to differentiate between the three groups. The pioneer study highlights the ability of the method to anticipate the tendency to become stuck by tracking the behavior of the variables used in the analysis within a time frame before the occurrence of the problem. In addition to that, an optimization procedure based on a constrained linear programming method was developed where changes to relevant variables were proposed in the discriminant function in order for the case to pertain to the non-stuck set. In spite of the success, variables such as differential pressure between the wellbore and formation was left out of the analysis. Variables related to wall contact of the drilling assembly, for example inclination angle and hole size, were reported to be of great importance. The fact of excluding the differential pressure reveals one of the great disadvantages of purely statistical models: the inability to be resemble the physical phenomena behind the predicted result. This often is

[5] Where the structure of the model is known but the parameters are known only as distributions.

detrimental to extrapolations to other drilling scenarios.

Further to the work of Hempkins [39] , Biegler et al. [24] published a more recent work based on 157 Gulf of Mexico wells from Exxon. The approach was exactly the same, but with improvements related to the nature of variables, a more clear description on how the likelihood of the problem's occurrence is computed and a differentiated optimization procedure. Canonical discriminant analysis was used to discern the predetermined groups of mechanical, differential and non-sticking condition. The ratio of scatter, measured by a covariance matrix of the relevant variables, between groups to the scatter within groups was maximized to derive the two canonical discriminant functions as in Hempkins [19, 39] works. The difference was that parameters or function values that better represent the phenomena surrounding stuck pipe were used as variables instead of raw data. Likewise, isoprobability curves in the canonical plane formed by the discriminant functions were computed using probability density functions of the data points on those planes. From these probability density curves and Bayes theorem, the likelihood that a point plotted in such plane belonged to a particular group could be computed. Finally, sensitivity analysis was used as the optimization criteria. The order and range of values in which the variables were to be changed, once a case fell in the one of the stuck regions, could be decided upon their relative contribution to the risk score. The model presented good agreement with past data from a particular historical well and overall agreement with cases in the database was mentioned although no statistical results were reported.

Artificial neural networks (ANN) applied to differential sticking have been the subject of some applied researchers. Suruvuri et al. [47] utilized a commercial ANN software to develop a predictive model for differential sticking. Working with a database of 120 cases of stuck pipe instances and 50 cases without the problem, a four-layer generalized feed forward ANN was built and trained. Given its relevance to the problem, the drilling fluid served to separate the database into two classes : water-based and oil-based drilling fluid. Variables such as differential pressure, well depth and drilling fluid properties composed the database and served as the input nodes of the network. A ANN is composed by processing nodes connected to each other and distributed in the form of so called layers, or stages, connecting independent variables affecting the problem, the inputs, with the outputs, in this case the status of drillstring: stuck or free. Eq. 3.8 shows the mathematical form of a processing node and Fig. 3.1 a representation of the network .

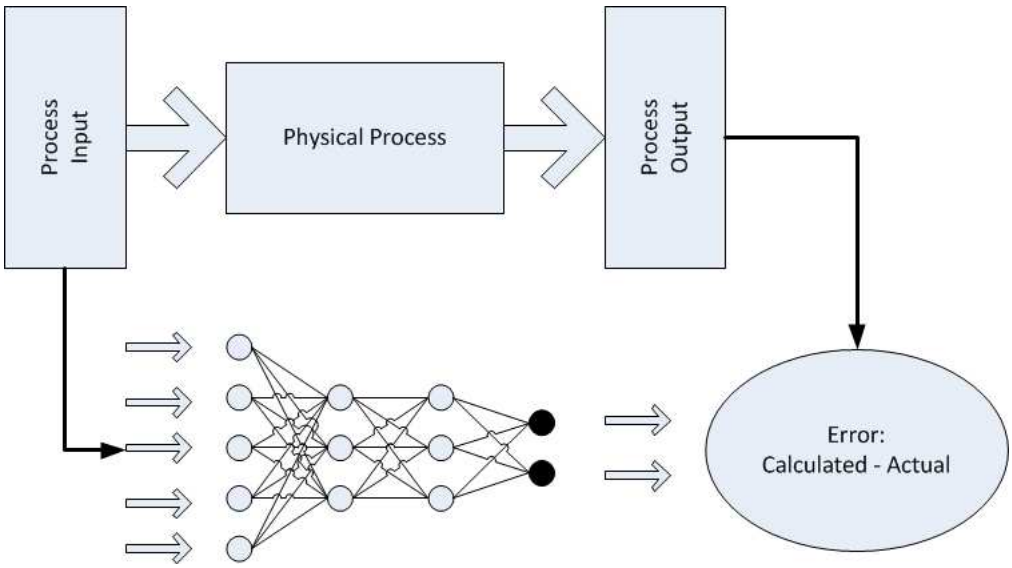

Figure 3.1: Flow of Information in the ANN

$$Y_k = F\left(\sum_{j=1}^{n} W_{kj}x_j + b_k\right) \tag{3.8}$$

The output Y_k of a processing node (neuron) k is calculated through an activation function F. W are the weights to be optimized, x the inputs and b an applied bias.

The weights, or relevance, of each variable in relation to the others are optimized during a training stage with known outputs in order to find the overall interrelation between the nodes. Once this stage is complete, the ANN can be seen as an artificial model of the problem and theoretically able to reason or generate new outputs given different values for the same inputs. The networks are in general as good as their size, quality and relevance of their inputs concerning the pursued answer. Two hidden layers (with a minimum of three nodes each) and two outputs, i.e., stuck or free, concluded the network architecture. A feed forward/back propagation iterative routine was used for training purpose utilizing 90 % of the database. The remaining cases were assigned, equally, for cross validation and testing. Mixed results were reported. Only 10 % of the stuck cases while drilling with oil-based drilling fluids were correctly identified, but two field cases from the Gulf of Mexico were correctly identified regarding not only the outcome, but also depth of sticking occurrence. Miri et al. [31] also utilized ANN to develop a predictive model for differential sticking. The database contained sixty two cases composed by variables similar to Suruvuri et al. [47] coming from wells drilled in the Persian Gulf. Half presented differential sticking. Two types of ANN were proposed, a multilayer perceptron (MLP) and a radial basis function (RBS), both trained with back propagation

Table 3.2: Most Common Hybrid Systems

Model Type	< 1991	92-93	94-95	96-97	98-99	00-01	Total
Neural Networks + Fuzzy Logic	5	6	3	7	-	10	31
Fuzzy Logic + Evolutionary Algorithms	5	7	9	19	1	4	45
Neural Nets + Evolutionary Algorithms	2	3	2	1	2	2	12
Machine Learning + Evolutionary Algorithms	1	1	1	3	2	4	8
Other Hybrids	1	-	-	-	1	6	12
Total	14	17	15	30	6	26	

algorithm. Despite of achieving a 85 % minimum success rate in predicting differential sticking within the testing dataset, it seems there is room for improvements based on results from extrapolations to wells of other fields. Data from three days of drilling of a new well that culminated with an instance of the problem was used to test the model. Although the best performing ANN, the RBS, was able to predict the instance of stuck pipe and an increasing risk tendency during the three days, the work could not clearly define thresholds (risk score from 0 to 1) where action should be taken. The results were very encouraging nonetheless and a sensitivity analysis of input variables on the outcome revealed the complexity of the problem. Although the relative impact of variables such as differential pressure, fluid loss and measured depth was significant, the analysis proved the magnitude of these parameters need not to be high for the problem to occur.

This section is concluded reviewing works that combined different knowledge management techniques, thus developing hybrid intelligent models.

Tsakonas and Dounias [15] published an extended review on hybrid computational intelligence schemes. Detailed statistics about the use of such systems to solve various problems were reported, providing valuable information on research trends in the field of artificial intelligence (AI) and success rates of the deployed techniques. Table 3.2 list the most common types of hybrid systems used up to that moment.

The use of fuzzy logic combined with neural networks is the most common

combination found in modern literature and also the most successful according to the researchers. Their success rate in solving problems with high levels of uncertainty is deemed to the capacity of fuzzy sets in dealing with imperfect data and expert knowledge while ANN provides means of finding answers from unknown functional structure in data. This combination was used by Nikravesh and Aminzadeh [9] to develop a software to map and identify non-linear relationships between well logs and seismic data. A direct application of such software was the calculation of permeability from known rock properties and some well logs such as P-wave velocity and attenuation. Another application was the creation of logs such as gamma ray, density and travel time from spontaneous potential (SP) and resistivity logs. Fuzzy logic was used to extract knowledge from data sets in the form of rules. The ANN was used, based on known input dataset, to adjust the parameters of membership functions describing data in order to better describe their relationship according to desired outputs. Encouraging results concerning the practical use of the methodology was evident through the good correlation between calculated and measured parameters. The work also provides detailed mathematical description of the construction of neuro-fuzzy systems.

Another interesting fact found in Tsakonas and Dounias [15] review is the leadership of fuzzy logic applied to the area of process control, the so called fuzzy controllers, among other AI techniques. Nowadays, practical applications of fuzzy controllers can be found in products such as washing machines and cars. The oil industry did not stay away from developing fuzzy controllers, or use fuzzy sets, for some applications [51, 25, 26, 56] and a few provide valuable insight about using it for prediction of differential sticking. Thonhauser [51] developed a fuzzy controller to model transient cuttings transport in highly inclined wells. Dimensionless numbers were derived describing different aspects relevant to estimating the concentration of solids along the well, such as viscous forces, annular flow velocity, particle's settling forces, inclination, drillstring dynamic forces and erosion forces. A set of rules, utilizing these dimensionless numbers, was created to describe their relationship in regards to predicting the accumulation of solids in the well. Therefore, an attempt to describe the phenomenon based on expert knowledge expressed through the dimensionless numbers, without the need for complex analytical derivations. Two controllers were developed that calculated two outputs, the "cuttings transport efficiency mud" (CTEM) and "cuttings transport efficiency bed" (CTEB). The first for estimating the percentage of cuttings settling in the annulus from poor hydrodynamic carrying capacity and the second to estimate the fraction of cuttings in the cuttings bed eroded and transported out of the well. The author as-

sessed the model comparing simulated results with field data on hole cleaning performance over a seven day drilling of the $12\frac{1}{4}$ inches phase of an extended reach well. Results were considered satisfactory despite of being based on indirect indications of cuttings transport efficiency. Garrouch and Lababidi [25] developed an expert system partially based on fuzzy controllers for screening wells that could be drilled underbalanced and for assisting in selecting the appropriate underbalanced drilling fluid. The expert system framework accounted for estimation of potential for formation damage, lost of circulation, wellbore stability and differential sticking. These factors were estimated from qualitative analysis, such as expert opinion in the case of differential sticking, and quantitative models. Fuzzy logic was used to combine the values of such factors through a set of linguistic rules and propose a confidence level for drilling the candidate well underbalanced. A similar approach, with aid of decision trees, was used to select the best drilling fluid. Results of compared field cases were conformal to field practices and the model seems to be a useful tool for analyzing ambiguous drilling scenarios in the absence of some drilling data.

Machine learning techniques, such as cased-based reasoning, and evolutionary models, such as genetic algorithms, are less used, but nonetheless very useful in modeling drilling related problems. Case-based reasoning is the AI technique dedicated in solving new problems based on the results of similar old ones. Skalle et al. [2] developed a predictive model for differential sticking purely utilizing this approach. The formal steps describing the methodology were followed:

a) Gather data.

b) Detect a possibly approaching problem.

c) Decide if gathered data are sufficient to define the situation as a new problem. If not;

d) Perform additional examinations (i.e. check drag, check circulating pressure etc.).

e) Search the case base for similar past cases.

f) Generate a set of the most likely stuck pipe hypothesis and present a set of possible solutions in descending order to the current problem.

g) Interact with user to select the best hypothesis. Generate a detailed "to do" list.

h) After the case has been solved, the case base can be updated with data from the situation just experienced. The new case will contain information about whether the pipe was successfully freed or not, and depending on this it will be used differently in the future, i.e. to help solving a new problem or avoid repeating previous mistakes respectively.

The methodology relies on a database of historical cases. A case was defined as a set of parameters related to the type of problem (mechanical or differential sticking), operational variables (ROP, WOB, drag, etc, with numeric or linguistic values) , drilling fluid (type, rheology, density and annular velocity), equipment such as length of BHA, wellbore geometry, the solution applied to the problem and the outcome in the form of comments. Only some degree of information was provided about the model, but it was based on a general knowledge model, composed by four modules, dedicated to establish some relations between the involved parameters and verify if their values were abnormal. The first module was named "structural and general inheritance links" dedicated to populate a case and establish primary relations, for example, *"type of operation has subclass (hsc) tripping (the inverse: is subclass of)"*. The second was a module establishing causal relations such as *"water based mud (WBM) enables swelling"*. The third module was composed of some mathematical relationships like Eq.3.9 and the forth module was dedicated to statistical relationships.

$$F_{diff\,sticking} = f \triangle P A \tag{3.9}$$

$$f = \frac{F_{pull} - F_{static}}{F_{static}} \tag{3.10}$$

Where $F_{diff\,sticking}$is the differential sticking force, ΔP is the differential pressure between wellbore and formation, A is the exposed area to differential pressure, F_{pull} is the necessary force to overcome drag and start tripping and F_{static} the slack-off weight of drillstring.

In the fourth module, weights were assigned, based on expert opinion, to relevant variables aiming at strengthening the importance of a particular variable depending on its frequency of occurrence before and after known stuck pipe occurrences. The model was still under development and no verification concerning its efficacy was given. In spite of that, authors conclude that the model is intended to solve the recurrent nature of the problem's incidence over time where peaks of occurrence are observed after a company efforts are phased out and engineers forget to apply learned lessons.

Mendes [35] combined case-based reasoning and genetic algorithms to assist drilling engineers in designing new wells based on information from similar wells already drilled (correlation wells). In summary, the model was composed by a database, a methodology dedicated to find similar wells, an adaptation module based on a genetic algorithm aiming at designing the new well based on parts of similar old wells and a storage methodology able to keep relevant

cases and eliminate others not so important. Several attributes were used to define a case. Some of a general nature were name of the field, water depth, average inclination angle, true vertical depth, departure and azimuth. Others were more specific like formation type and length, time spent with anomalies, rate of penetration and age of the well. Although all attributes were used in the definition a case in the database, the more general attributes were used in a first stage to find similar cases while the more specific ones in a later stage to identify promising cases selected in the first stage. This searching engine was based on a similarity metric that compared the values of attributes of the historical cases with the ones from the target case (new well under design). The attributes were modeled as fuzzy sets to enable translation of numeric values into linguistic statements often used by expert engineers. In a later stage, the set of promising wells, retrieved from the historical database by the searching engine, was divided into depth segments for being processed by the genetic algorithm. The length of each segments was determined by the following attributes: formation type, drilled phase (nominal diameter of the phase), type of drill bit and drilling fluid type. Each segment held the values of those attributes constant and, in theory, can then hold any type of relevant information the engineer may need to design the new well. Utilizing a genetic algorithm described by Goldberg [18], composed by three basic operators (selection, crossover and substitution), so called "Frankstein" wells were automatically built by combining the segments from old wells according to criteria based on relevance of the new well in regards to desired characteristic of the target case. The relevance was also based on the concept of similarity, a combined similarity using general and specific attributes called total similarity, and a penalty function. Well segments with high dog leg severity were penalized, thus considered less relevant and avoided. The final "Frankstein" well could then be evaluated by the drilling engineer. The concept of learning curves, graphs showing the total time spent in drilling, was suggested as criterion for storage or elimination of cases from the database.

Lins [27] presents a study on the application of *Support Vector Machines (SVM)* used together with *Particle Swarm Optimization (PSO)* to predict reliability issues such as failure times of diesel engines and miles to failure of car engines. SVM is a supervised learning method used in regression problems and pattern recognition. Like ANN, it is considered a learning method since it proposes a method to find solutions based on the study of input and output examples of a certain phenomenon without knowing the form of their relationship. In other words, there is a nonlinear dependence (mapping, function) $y = f(x)$ between a multidimensional vector x and an output y . The available

information is a dataset $D = (x_1, y_1), (x_2, y_2), \cdots, (x_l, y_l)$ and the problem can be one of classification or regression depending on the nature of y. It will be a classification problem if it assumes only discrete values or a regression if real-valued, i.e., a function. SVM differs from ANN in its more mathematical clear form of the decision or regression function to be minimized (or optimized) and its solution path. ANN utilizes empirical risk minimization, i.e., measure and minimizes the error from the training steps by adjusting the weights in Eq. 3.8 in each layer while SVM works with structural risk minimization that aims at minimizing the upper bound of a generalized error. In general terms, it sets conditions to guarantee that a global minimum is found for the decision function while ANN can be trapped in local minima. A consequence of this fact is that SVM does not need large and complete data sets to yield good results. For binary classification of linearly separable data, the following problem is to be solved. Consider for data set D, $x_i \in \mathbb{R}^n, y_i \in \{-1, 1\}$ and $i = 1, 2, \cdots l$. If the data is linearly separable, there is a number of hyperplanes that can perform the task. The hyperplane equation can be written as follows in matrix form:

$$H = w^T x + b = 0 \tag{3.11}$$

After some manipulation one arrives at the conclusion that the problem to solved is:

$$\underset{w,b}{Min} \quad \frac{1}{2} w^T w \tag{3.12}$$

$$subject\ to \quad y_i \left(w^T x_i + b \right) \geq 1,\ i = 1\ to\ l \tag{3.13}$$

And it can be solved using Lagrange Multipliers with certain mathematical conditions. Hence, the following Lagrangian equation to be optimized can be derived:

$$\mathcal{L}(w, b, \alpha) = \frac{1}{2} w^T w - \sum_{i=1}^{l} \alpha_i \left[y_i \left(w^T x_i + b \right) - 1 \right] \tag{3.14}$$

Where w, b, α should be selected in order to determine the best decision plane. w is the normal vector to the hyperplane H, x is the input vector and b is the linear coefficient of the hyperplane. α is the l-dimensional vector of Lagrange Multipliers.

Although SVM defines the training algorithm[6] it is still influenced by a set of parameters, leading to a model selection problem to properly select these parameters in the minimization scheme. Lins [27] proposed *PSO,* which is a

[6] A quadratic optimization problem where the objective function entails a generalized error

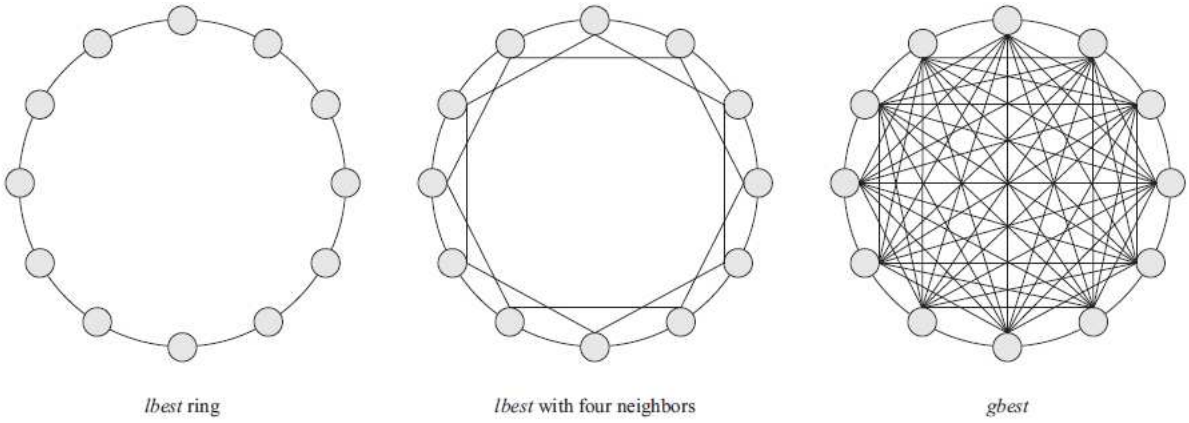

Figure 3.2: Different Swarm Communication Networks. After Lins [27].

optimization probabilistic heuristic optimization approach inspired on the behavior of some biological groups that moves in groups, such as fishes and birds. The concept of cognition and socialization within these groups are translated into mathematical formula for updating relative position x and velocities v of particles (inputs) i, within a search space towards an optimum position concerning the observed output. Relative position is calculated through euclidean distance and velocities from a recursive update equation function of the difference between the actual and best position of the particle, p, until present iteration step. Variable t is time and j are the dimensions of the input vector. P_g is the j-dimensioned vector formed by the best position encountered so far by any neighbor of particle i. Additionally, $c_1$and c_2 is a constant and u_1 and $u_2$uniform random numbers generated at every update for each individual dimension j.

$$v_{ij}\left(t+1\right) = v_{ij}\left(t\right) + c_1 u_1 \left(p_{ij}\left(t\right) - x_{ij}\left(t\right)\right) + c_2 u_2 \left(p_{gj}\left(t\right) - x_{ij}\left(t\right)\right) + \cdots \quad (3.15)$$

$$\cdots \quad , j = 1, 2, \ldots, n \quad (3.16)$$

Two communication network models are used, one where all particles are interconnected (*gbest)* and another where particles are only connected with some of them in the set (*lbest)*. Fig. 3.2 shows these concepts.

Results were evaluated in terms of mean square error between calculated and observed outcomes with the hybrid system *SVM+PSO* outperforming others in regards to forecast of the investigated problem. In spite of that, the relevance of this work comes from the good literature review on the various methods to solve SVM selection problems and the way it resembles part of

the approach proposed in this dissertation. In this study, as far as the soft computing module is concerned, a learning method based on a data set of input/output of unknown dependence is also deployed. The difference is in the form of the data set. It was constructed via several mathematical manipulations or experimentally derived to entail the most important physical aspects affecting the problem, instead of using lose drilling parameters as inputs. This facilitates the phenomenological assessment or traceability of the causes of differential sticking. The analogy can be extended if Eq. 3.14 is replaced by a similarity metric computing distance between data points in a normalized fuzzy space. In addition, parameters present in similarity metric are also optimized in order to use it as the means to differentiate between stuck and free cases, but using a non-linear curve fit analysis different from the *PSO*.

Finally, it is worthy mentioning the importance of this last section since the essence of the model described in this dissertation is hybrid in nature. Some of the aforementioned techniques, such as case-based reasoning and fuzzy logic, are further explained in subsequent chapters as they are used together with analytical models and experimental data in an attempt to build upon the previous works here reviewed and contribute towards a more robust, explicit and reliable predictive software tool to avoid differential sticking.

Chapter 4

The Risk Model

Risk derives from uncertainty. Our inability to foresee all possible outcomes of a given action while solving a problem depends on the amount of uncertainties and the degree of them. As previously explained differential sticking presents many sources of elevated degrees of uncertainty. Only this particular form of stuck pipe is related to three major disciplines in drilling: drilling fluids and hydraulics, directional drilling and drillstring mechanics. Considering the level of complexity of the problem we may classify the risk for the occurrence of differential sticking as subjective, because the odds are not well known. It is different from flipping a coin, for example, where although the outcome is uncertain, the odds are well known. Probabilistic methods, like Bayesian networks, are not always the best approach when subjective risk is concerned. Computation of conditional probabilities becomes considerably cumbersome for relatively small amount of variables and the methods to express interdependence of involved variables are non trivial and often not satisfactory. A different approach is proposed here.

A hybrid engineering model is proposed to quantify the risk for differential sticking. Hybrid for two reasons. Firstly because it is composed by two modules based on distinct approaches to predict the same problem. The first is a knowledge-based model that manipulates data from historical wells (also called correlations wells), where the problem has and has not occurred, to infer a likelihood for occurrence based on similarities of values of parameters calculated from drilling data between the well to be drilled (here called target case) and the outcome of wells already drilled. The second module is a physically-based exact analytical model that estimates the magnitude of the differential sticking force at a given depth and set of drilling conditions. Secondly, the hybrid terminology is justified from the fact that data utilized by the first module are structured on physically based criteria and the analytical model partially rely on experimental data, field data and expert knowledge to compute terms

of the force balance equation.

Risk can finally be interpreted based on the combination between the likelihood for the event to occur and its consequence or severity if it was to occur. Based on the characteristics of the two previously explained modules it can be anticipated that a likelihood score is evaluated by the knowledge-base model, as described in Chapter 6, and the consequence of the event from the magnitude of the required overpull as explained in Chapter 7. This risk definition reflects the way the driller approaches the problem since a drilling scenario would only be considered risky, and therefore worth changing the drilling plan, if the effort to resolve the problem was to be significant.

Based on the previous reasoning a risk table can be proposed:

Table 4.1: Risk Table

Consequence Score (Overpull as % of DP Yield Point)	Likelihood from Similarity Score					
	0.1	0.2	0.4	0.6	0.8	0.95
0 to 20 % Insignificant	Negligible	Negligible	Negligible	Negligible	Negligible to Low	Low
21 to 40 % Minor	Negligible	Negligible	Negligible to Low	Low	Low	Moderate
41 to 50 % Moderate	Negligible	Low	Low	Moderate	Moderate	Moderate to High
51 to 70 % Major	Low	Moderate	Moderate	Moderate to High	High	High to Extreme
71 to 95 % Catastrophic	Moderate	Moderate to High	High	High to Extreme	Extreme	Extreme

The risk level for a particular well segment[1] can be computed based on this table once the average similarity score between the target well segment and segments where the problem occurred and the required overpull is calculated. The measured depth (MD) at the bottom of segment is used as reference for calculation the pull force. Usually, the magnitude of practiced overpull is dictated be the yield strength of drillpipes or the weakest link in the drillstring. Drill-

[1] the criteria defining a well segment is explained in Chapter6

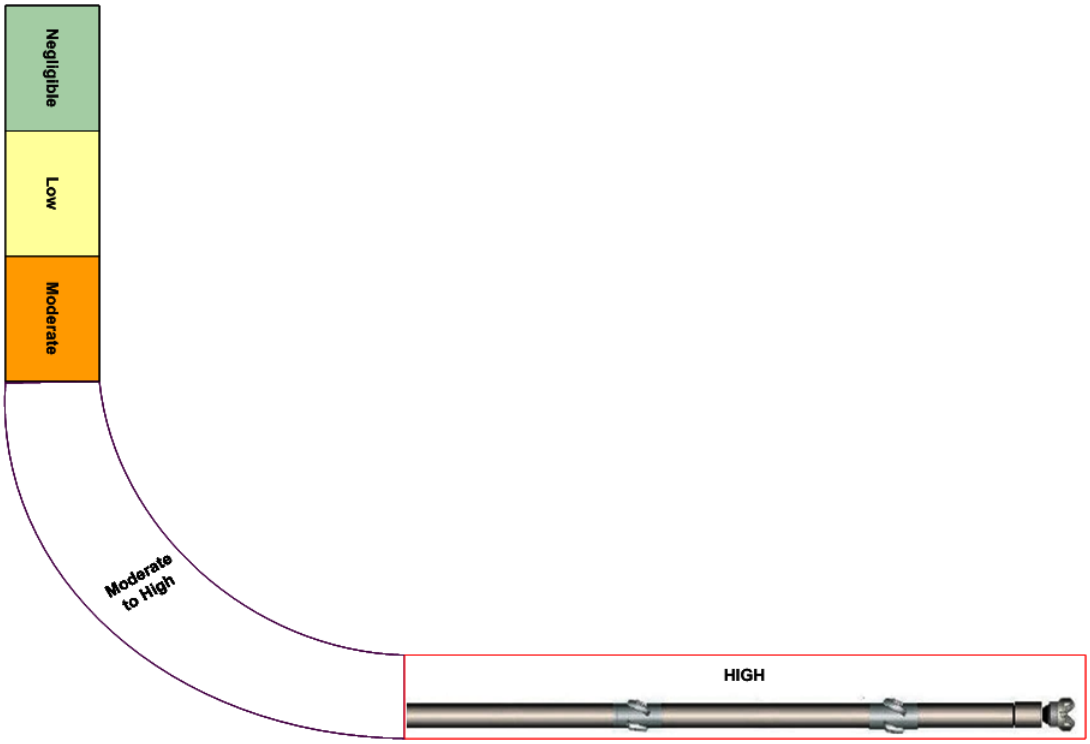

Figure 4.1: Hypothetical Well.

string failure (or plastic deformation) due to excessive overpull[2] once a stuck pipe event occurs is not uncommon and extremely undesirable. The level of risk taken in regards to practiced limits depends on the driller. Therefore, the numbers on Table 4.1 should be ultimately determined by the drilling engineer based on experience and reliability studies of the similarity scores here investigated, and serves here to explain the proposed approach. Fig. 4.1 shows the risk assessment concept transferred to a hypothetical well. The risk analysis can be performed during well design or while drilling, and the risk calculated to the particular well segment should be interpreted as a result of the drilling conditions at a certain point in time, a snapshot as drilling progresses.

[2]net pull force applied, i.e., subtracting the weight of the drillstring and drag forces. It is the differential sticking force in the stuck pipe instances investigated in this dissertation

Chapter 5

Experimental Assessment of Mechanical Properties of Mudcakes

5.1 High Pressure and High Temperature Mudcake Characterization Equipment

Experiments to assess certain mechanical properties of mudcakes were conducted using the high pressure and high temperature mudcake characterization equipment (HPHT MCCE). As explained while stating the problem, this unique equipment was developed during the course of this research project after identifying the reduced amount of studies conducted about the subject and the lack of data. The mechanical behavior of mudcakes affects the degree of contact between the drillstring and the mudcake, having impact on the magnitude of differential sticking force and mechanisms aggravating the problem.

The Mudcake Characterization Equipment (MCCE) is designed to measure mudcake mechanical properties under high temperature and pressure (HPHT) conditions. These mechanical properties can be measured while the mudcake is being formed. The following mechanical properties of partially consolidated solids can be measured: resistance to applied torque, embedment resistance (hardness) and adhesion-cohesion strength of the mudcake.

These information are relevant to assess, screen or develop drilling fluid compositions that will present desirable filtration behavior and resultant mudcakes for a particular drilling campaign. The mechanical properties of mudcakes and its interaction with the formation and drillstring are related with numerous drilling problems such as excessive cuttings retention, excessive torque and drag, differential sticking, formation damage, etc. Hence, a reduc-

tion of operational costs due to these problems is likely to occur if its properties are optimized.

The equipment can be described as a HPHT filtration cell coupled with a multipurpose mechanical measurement device. Therefore, the equipment can also be used to assess filtration behavior of drilling fluids through different porous media. The build up of a mudcake can also be followed by measuring its thickness by the use of a L-bar penetrometer and recording of filtrate volume.

In summary, the filtration of the drilling fluid through a porous medium (filter paper, sintered disks or cores) occurs under high pressure (maximum 1000 psi) and temperature (maximum 150$^{\circ}C$). A filtercake is formed and its thickness and previously described mechanical properties measured. Pressurization is achieved using nitrogen and it is regulated using a pressure manifold panel; temperature is achieved through an electric heater with a temperature controller and all relevant data is monitored and stored via a LabView® data acquisition system.

This equipment is the most versatile of its kind and innovates because it offers not only axial movement and rotation, but also independent measurements of axial force (tension or compression) and torque resistances of the mudcakes. One can actually perform torque measurements under load or even penetrate the mudcake while rotating the indenter in a drilling motion. The assessment is made mechanically via a spherical penetrometer connected to a newly designed internal torque and load cells. Having load and torque measured inside the pressure vessel eliminates the effect of friction in pressure seals while design features of the sensor minimize cross-talk between measurements.

5.2 Investigated Effects

The effects of differential pressure, temperature, type and concentration of insoluble solids, rheology, type of viscosity agent (polymer) and presence of barite on the mechanical behavior of drilling fluid mudcakes from in two water-based fluid systems, bentonite-based and polymer-based with calcium carbonate bridging agent, were investigated. The experimental work aimed at raising a database of relevant mechanical properties for simplified drilling fluid formulations that could generally represent common water-based drilling fluids used in the field.

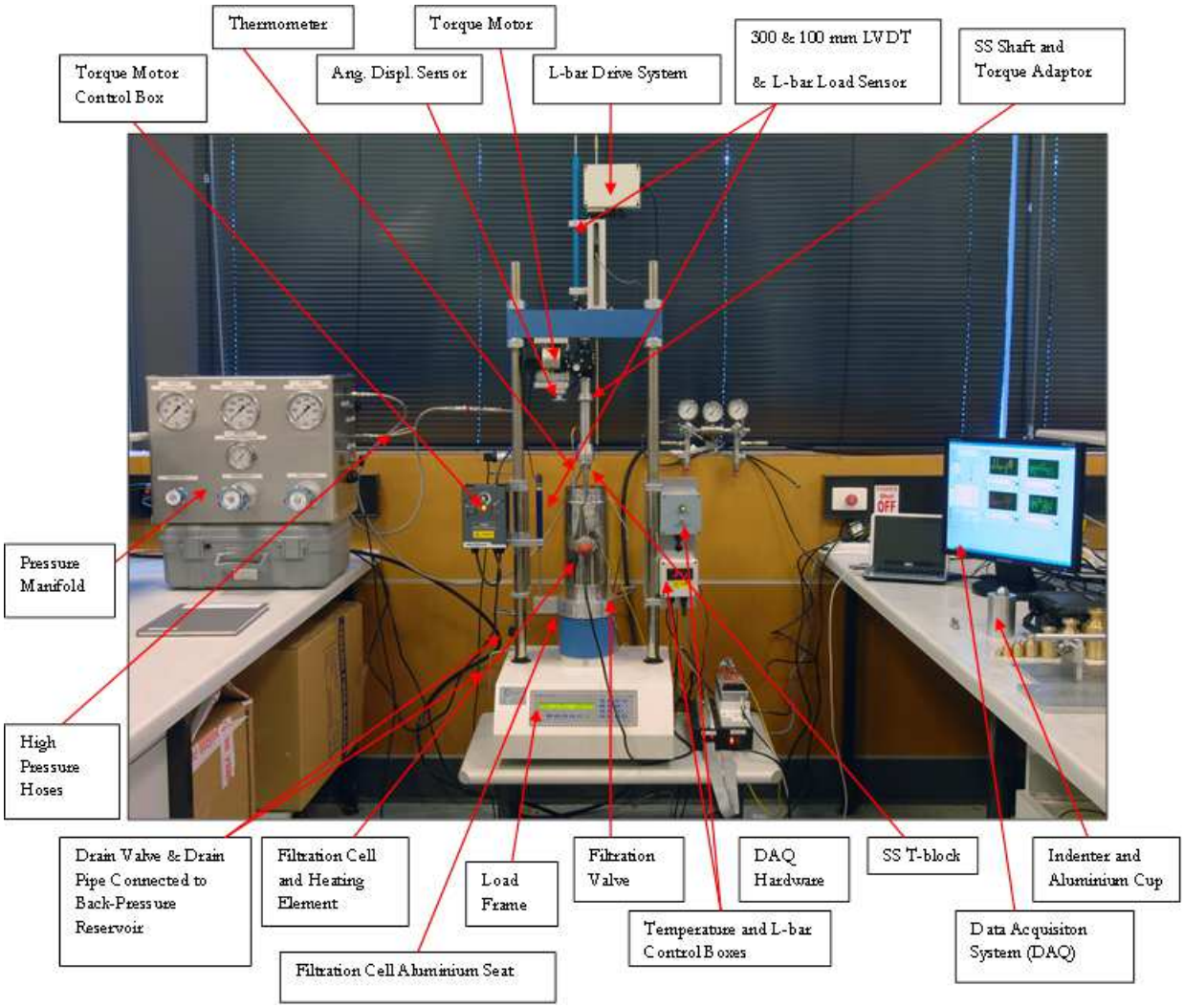

Figure 5.1: HPHT MCCE

5.3 Major Parts

Fig. 5.1 shows the overall view of the equipment set up.

Fig. 5.2 show a detailed view of the pressure vessel with internal parts assembled.

1. High Pressure and High Temperature Filtration Vessel.
2. Back-pressure reservoir. See Fig. 5.1.
3. T-block for shaft rotation and support, nitrogen feed and data acquisition wiring connection.
4. Main shaft.
5. Load (compressive and tensile) and torque sensor.

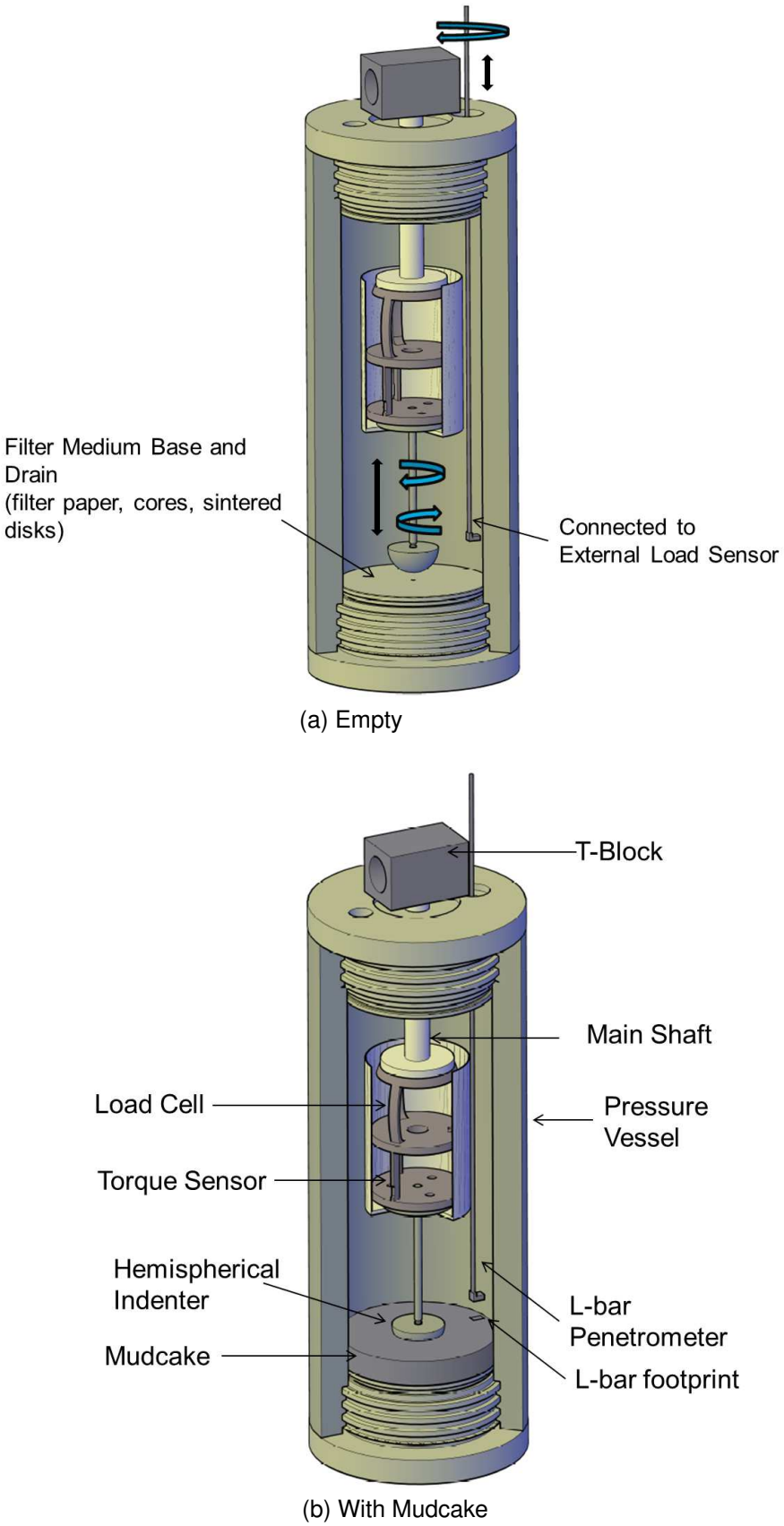

Figure 5.2: Pressure Vessel and Internal Parts.

6. L-bar penetrometer is an independent system to measure mudcake thickness during the experiment. It is composed by a rod with a L-shaped foot and the upper part connected to a 10 lbf load cell. The system is driven up and down by servo electric motor and also connected to a displacement sensor (LVDT). A peak in load is observed whenever the foot touches the top of the mudcake and the thickness can be calculated based on known displacements from the bottom of the filtration vessel. Measurement is made far from center of the mudcake with a small penetrometer to avoid interference with indenter's mechanical assessment.

7. Filter medium: Whatmann API filter papers or sintered disks .

8. Drilling fluid filtercake (mudcake).

9. A 50 KN load frame is used to drive the filtration vessel up and down, i.e., towards the indenter (embedment tests) or away from it (adhesion tests). In other words, the filtration vessel moves axially while the indenter remain stationary. An second electric motor (torque motor) with variable speed drive rotates the main shaft for torque tests. See Fig. 5.1.

10. An electric heating jacket connected to a thermocouple controls the temperature inside the filtration vessel. See Fig. 5.1.

Table 5.1 shows the range of relevant variables concerning the equipment.

5.4 Simplified Experimental Procedure

The equipment's versatility allows for different tests to be run depending on the area of investigation. In addition this section describes only the experimental procedures developed to assess the three relevant parameters used in the predictive model of differential sticking: hardness, torque resistance and adhesion-cohesion strength.

5.4.1 General Steps

1. Prepare target water-based drilling fluid.

2. Pour the drilling fluid into the filtration cell.

3. Close filtration cell and and zero the positions of indenter and L-bar penetrometer. Known dimensions and displacement sensors (LVDT) permit tracking the distances of indenter and L-bar penetrometer to the bottom

Table 5.1: Range of Relevant Variables.

Variable	**Range of Measurement**
Filtration Vessel Pressure (psi)	0 to 1000
Back Pressure – Filtrate Vessel Pressure (psi)	0 to 1000
Temperature ($^{\circ}C$)	0 to 150
Torque ($N.m$)	0 to 1.4
Compressive Load (N) (i)	Cell H - 0 to 50 Cell L – 0 to 20
Tensile Load (N) (i)	Cell H - 0 to 10 Cell L – 0 to 0.7
T-bar Displacement (mm)	0 to 300
Displacement (mm)	0 to 48
Angular Displacement ($degrees$)	0 to 180

(i) Recommended maximum load. Cell H Calibrated for 50 N and Cell L calibrated for 20 N.

of the filtration vessel and the relative position to each other as the filtration vessel moves.

4. Heat the fluid to desired temperature.

5. Pressurize filtration vessel and back-pressure reservoir to establish desired differential pressure.

6. Open filtration valve and start filtration. Mudcake formation starts and mudcake build was measured via the L-bar penetrometer and

7. Perform desired experiment:

   (a) Hardness. Indenter was driven into the mudcake at a velocity of 0.25 $\frac{mm}{min}$ and axial force recorded until either maximum displacement or load cell limit was reached.

   (b) Torque. Mudcake was left to form around indenter that was initially positioned at a known distance from the bottom. Torque required to start indenter rotation was recorded via internal torque sensor and angular displacement sensor attached to main shaft.

   (c) Adhesion-Cohesion Strength. Maximum tensile force observed while pulling the indenter out of a known position inside the mudcake at a velocity of 0.25 $\frac{mm}{min}$ was recorded.

Appendix A describes more detailed experimental procedures.

5.5 Relevance and Use of Data

Hardness provides information about the degree of embedment (penetration) of the drillstring into the mudcake matrix. Torque resistance and adhesion provides a way of comparing the necessary levels of torque and pull to free the drillstring once it is embedded in the mudcake.

Fig. 5.3 illustrates typical raw results of the experiments.

These data are used in two different ways in the risk model. Firstly, the values of the three aforementioned parameters are part of the set of parameters composing a case (well segments where certain drilling data are kept constant) and used by the case-based reasoning module to discriminate between cases where the differential sticking occurred and otherwise. Secondly, the analytical module uses the hardness curve, Fig. 7.4, to estimate the embedment of the drillstring in the mudcake depending on the operational conditions of the same

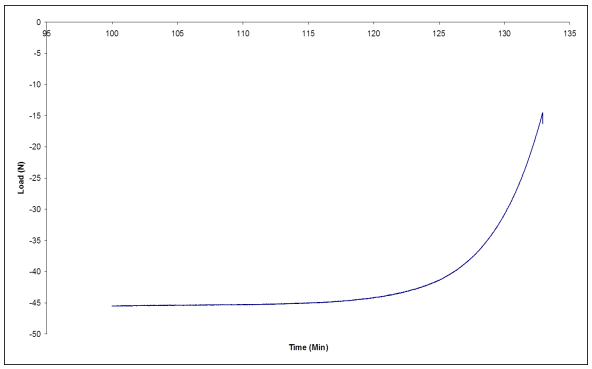

(a) Hardness

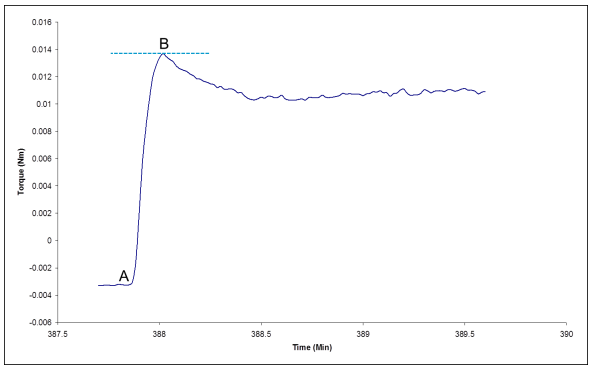

(b) Torque

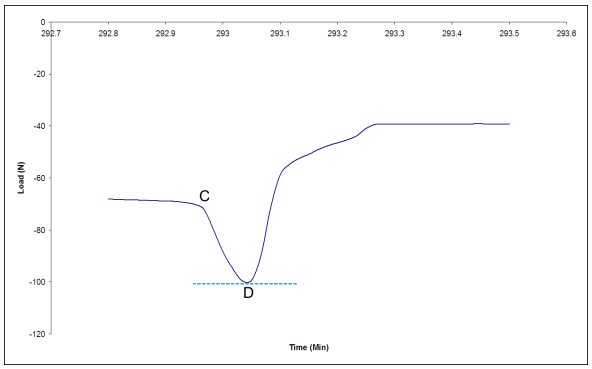

(c) Adhesion

Figure 5.3: Typical Results

case. Details are given in the respective chapters about the two modules. The three measured parameters are defined below:

1. Hardness in this context is assessed by an behavioral index, s, of an experimental mechanical constitutive curve of compressive force versus embedment (penetration depth). This curve can also be expressed in terms of pressure versus embedment. The concept proposed in this study better describes the stress vs strain behavior of the complex structure of mudcakes and differs from traditional measurements of hardness.

2. Torque Resistance is the minimum torque required to rotate the indenter. The Torque Modulus is utilized as normalized measurement and is defined as the maximum value of torque divided by the superficial area of the indenter at the depth where the experiment was conducted.

3. Adhesion is the maximum tensile force (pull force) registered while pulling the indenter out the mudcake. The Adhesive Strength is used as normalized measurement and is defined as the maximum tensile force divided by the superficial area at the depth where the experiment started.

The complete drilling fluid formulation for the cases were not available and the experiments were designed in order to represent common types of water-based drilling fluids used in field as well as the operational conditions in which the mudcake is formed. Table A.1 shows the fluids tested, investigated operational conditions and results concerning the parameters used to assess the mechanical properties of mudcakes. The equipment also provides filtration properties such as filtrate volume curve for the experiment. The API filtrate volume, i.e., the filtrate volume at 30 minutes of filtration, was also recorded. Table A.1 also shows these values and the ratio of these filtrates at different pressures. The so called API filtrate ratio is used to estimate the compressibility of mudcakes and is one of the parameters utilized in the case-based reasoning model.

These parameters are cross-referenced with the cases composing the drilling database according to information about the drilling fluid available from the drilling report for that segment. The following criteria is used to determine which experiment result is the most appropriate to represent the drilling fluid used in that particular well segment:

1. Differential pressure.
2. Type of drilling fluid (water-based, oil-based or synthetic-based mud).
3. Concentration of Insoluble Solids.
4. Volume of API filtrate.
5. Rheology.
6. Mud weight to conclude about the presence of barite whenever not explicitly stated.

It is important to mention, as far as validation with field data is concerned, that the parameters raised during experiments with analog drilling fluids were only used as representative of the drilling fluid used in the well segments whenever not available from the drilling reports, such as missing API filtrate, API filtrate ratios and mechanical properties of mudcake.

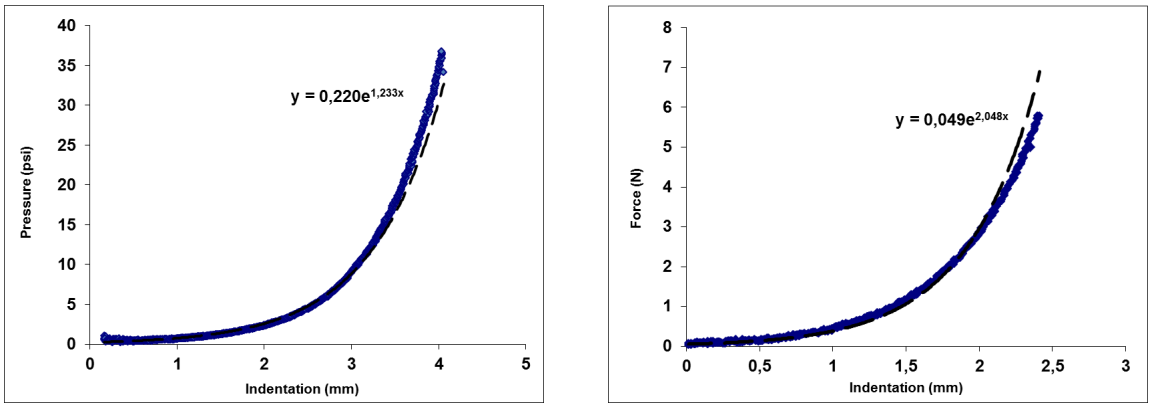

Figure 5.4: Hardness Profile - Bentonite

5.6 Mechanical Behavior of Mudcakes under Compressive Loads.

Drilling fluid mudcake is formed by deposition of solids in suspension during filtration through the permeable formation. This results in an heterogeneous material presenting a density gradient throughout its thickness. Often a layered structure is observed. The gradient points to the interface with the permeable medium and density decreases towards surface. Thickness depends on the magnitude of filtration's driving force, differential pressure throughout the mudcake, and packing mechanisms of suspended particles. Size, physicochemical properties (such as the presence of electrically charged particles or clays) and shape dominates the phenomenon that affects permeability and consequently thickness. Clearly, it also affects its mechanical properties and these properties vary throughout its thickness, i.e., are depth dependent.

Traditional hardness tests, such as Vickers [1] , are adequate for quasi-uniform solid materials and performed at a certain depth of indentation. As far as differential sticking is concerned, the equilibrium depth of embedment into the mudcake is determined by the balance between the forces driving the drillstring into the mudcake and its hardness. Since the material is anisotropic an entire hardness profile is necessary.

Experiments revealed that an exponential curve approximates reasonably well the relationship between compressive force and depth of penetration for the vast majority of tested mudcakes over a wide range of compressive forces. Fig. 5.4 and 5.5 are examples. A power-law relationship presented a better fit only in exceptional cases.

$$F = H \cdot \delta^{\exp s} \tag{5.1}$$

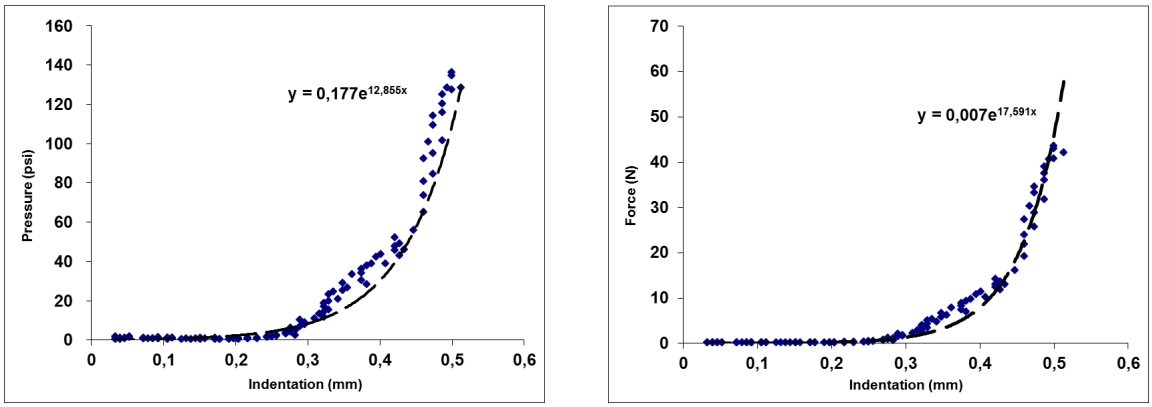

Figure 5.5: Hardness Profile - Carbonate

In fact, the same relationship holds for pressure (or normal stress σ_{xx}) versus penetration depth. Here, pressure was calculated based on the projected area of the indenter at a particular penetration depth, contrary to Vickers hardness, for example, which uses the surface area of the indenter.

The approach proposed here was inspired in works from the field of fluid mechanics. Rabinowitsch [45] and Mooney [38] derived a constitutive equation for non-Newtonian pipe flow. The general model relates the shear rate and shear stress at the pipe wall:

$$\gamma_w = 3\left(\frac{8\,.\,Q}{\pi\,.\,D^3}\right) + \frac{D\,.\,\Delta P}{4\,.\,L}\left(\frac{d\left(\frac{8.Q}{\pi.D^3}\right)}{d\left(\frac{D.\Delta P}{4.L}\right)}\right) \tag{5.2}$$

where γ_w is the shear rate at the wall, D is the pipe diameter, Q is the average flow rate, L is the pipe length and d stands for derivative.

Metzner and Reed [46] simplified Eq. 5.2 by introducing the following parameter:

$$\frac{1}{n'} = \frac{d\left(\frac{8.Q}{\pi.D^3}\right)}{d\left(\frac{D.\Delta P}{4.L}\right)} \tag{5.3}$$

Therefore:

$$\gamma_w = \frac{8\,.\,v}{D}\left(\frac{3\,.\,n'+1}{4\,.\,n'}\right) \tag{5.4}$$

And experimentally observed that Eq. 5.4 holds for a large variety of non-Newtonian fluids and the parameter n' remains constant over a wide range of shear rates and shear stresses.

Parameters H and s are the equivalent of Metzner and Reed [46] K' and n' and may serve as the base to derive a general model for the mechanical behavior of mudcakes in the same sense as Rabinowitsch did for non-Newtonian

fluid flow. The first step would be converting penetration into strain rate.

Based on the previous explanation, it was assumed that the determination of parameter s is all that is needed to characterize the mechanical behavior of mudcakes under compressive load. In fact, this was the parameter chosen to express hardness. Large value of s mean an averaged hard mudcake and a sharp transition from the soft surface to the compact core, while low value of s indicate a gradual increase of pressure at the indenter with penetration, indicating an average soft mudcake.

5.7 Resistive Torque and Adhesion and Cohesion of Mudcakes

Torque and adhesion experiments are important since they measure the magnitude of surface forces acting on the drillstring. These forces are summed to the differential sticking force, which acts normal to the borehole wall, and need to be overcome in order to free a stuck pipe through rotation or pulling actions. In addition, it helps to mechanically characterize the mudcake contributing towards a general phenomenological mechanical model for drilling fluid filtercakes.

Because of the previously explained structure of mudcakes, a full analysis of the curves of resistive torque and tensile strength should be performed to properly characterize the torsional response and adhesive-cohesive properties of mudcakes. Segments A-B and C-D in Fig. 5.3b and 5.3c are of particular interest. In both curves, the rate of increase in over those segments are relevant to assess the viscoelastic responses of the material. As far as the predictive model is concerned, only the maximum values B and D are used. The reason for this simplification lies on the fact that given the constant angular velocity and pull rate adopted in the experiments, these are reference thresholds to classify mudcakes in terms of these forces regardless of the paths A-B or C-D. In spite of that a discussion takes place in the next section about the importance of these paths and how this might provide insights into the best way to rotate or pull the drillstring in a differential sticking situation.

5.8 Final Comments

5.8.1 Hardness

Although only the loading curve was analyzed during this study, further work should be done concerning the unloading curve. As mentioned in Fisher-Cripps [17], the elastic modulus of the material can be estimated from the unloading curve. In addition, the equipment allows experiments to be performed at different penetration rates and such study should be conducted in order to assess kinematic and dynamic effects on embedment resistance of mudcakes.

5.8.2 Torque and Adhesion and Cohesion

Rate dependence and dynamic effects on the torque resistance and adhesion-cohesion strength of mudcakes should also be studied in order to better understand the mechanical behavior of drilling fluid mudcakes. Moreover, these studies are important to guarantee optimum drilling fluid design and operational guidelines to avoid and treat differential sticking occurrences. These studies should be performed by conducting torque experiments at different angular velocities, including oscillatory angular velocities, and adhesion-cohesion experiments at different indenter pull velocities. (oscillating and rotating at different angular velocities), pulling at different velocities. These experiments would allow the investigation about viscoelastic responses of mudcakes, with possible energy storage and loss moduli. This could lead to improved field practices on how to rotate the drillstring in order to use minimum energy to free it.

5.8.2.1 General Tendencies

Drilling fluid filtercake formation is a complex phenomenon because of filtration-related effects associated with the large amount of different components of the drilling fluid and their physico-chemical interactions. The general tendencies presented here regarding the investigated effects does not intend to stand as precise or conclusive behavioral rules. Results of filtration (visual and L-bar mudcake thicknesses, API filtrate and API filtrate ratios to assess compressibility) and mechanical behavior (torque resistance, adhesive strength and hardness index) for the various experimental conditions detailed in Table A.1 from Appendix A serve as the basis for the analysis.

1. Bentonite-based systems tend to form softer, thicker and more compressible mudcakes than carbonate-based ones. Although less evident, higher torque resistances and adhesion-cohesion strengths were also observed in mudcakes from bentonite drilling fluids. It should be noted that inter-system comparisons are always more difficult to be made for obvious reasons.

2. The presence of barite in both water-based systems apparently led to less compressible (less prone to differential pressure effects) and therefore thicker mud. In general, it also resulted in softer mudcakes with higher torque resistance and adhesion-cohesion string.

3. Higher temperature in polymer-based fluids usually leads to higher filtrate losses, thicker and softer mudcakes. It also resulted in higher torque resistance and adhesion-cohesion strength.

4. The increase in solids concentrations resulted in softer mudcakes and led to a decrease in mudcake compressibility with increase in thickness. A decrease of torque resistance and adhesion-cohesion strength was also observed with the increase in solids concentration.

5. The increase in viscosity of the polymer-based drilling fluids results in softer mudcakes for both Xantham Gum (XC) and PHPA systems with a more pronounced effect in the XC fluid. The same increase in viscosity led to higher torque resistances, but lower adhesion-cohesion strengths and these effects were also more pronounced for the XC systems.

6. The results about the effects on filtration-related properties (thickness, compressibility, filtrate volumes, filter medium, etc) are in agreement with previous works [43, 42, 29, 16].

5.8.3 Additional Capabilities of the HPHT MCCE

The equipment can be used for investigations beyond the scope of differential sticking. The data generated can be applied to the study of frictional forces between the drillstring and mudcake and effects of addition of lubricants to the drilling fluids. Hardness and adhesion data can aid on minimizing cuttings retention in the mudcake matrix as well as improve mudcake clean up operations during cementing and completion of oil and gas wells. In addition, the equipment is a HPHT filtration equipment and can be used for optimizing drilling fluid filtration properties.

Finally, the depth at which the differential force between borehole and formation starts to be applied over the drillstring varies depending on the permeability profile of the mudcake. This effect was observed during certain torque or adhesion experiments and can be further studied using the HPHT MCCE.

Chapter 6

Case-based Reasoning Model: Likelihood from Similarity Score

The likelihood of differential sticking occurrence is quantified using principles of case-based reasoning. This simple artificial intelligence technique is based on one of the most common learning methods: solving new problems based on the solutions of similar known ones. It can be used in the identification, or even prediction, of problems based on certain known relevant characteristics related to it. Medical doctors identify diseases in new patients based on symptoms known from other patients. In this study, data from a set of historical wells was structured and defined as cases. A case is a well segment composed by certain variables or parameters relevant to the physical phenomenon of differential sticking. The resultant database is composed by cases with and without the occurrence of the problem. The likelihood of occurrence of the problem in a well segment that is being designed or drilled is estimated based on comparing its values of relevant variables with those of the historical well segments in which the outcome regarding the problem is known. In other words, the methodology calculates how far current operational conditions are from known critical situations. This is accomplished through a similarity metric that calculates the distance between points in a normalized space. The theory of fuzzy sets and fuzzy logic are used to calculate terms of the similarity metric. In addition, an optimization methodology based on non-linear regression analysis is deployed using the similarity metric as the objective function to differentiate between free and stuck cases in a drilling database of historical cases. The optimized, or trained, similarity metric can finally be used to predict the occurrence of the problem in new drilling scenarios. A test database is used for this purpose.

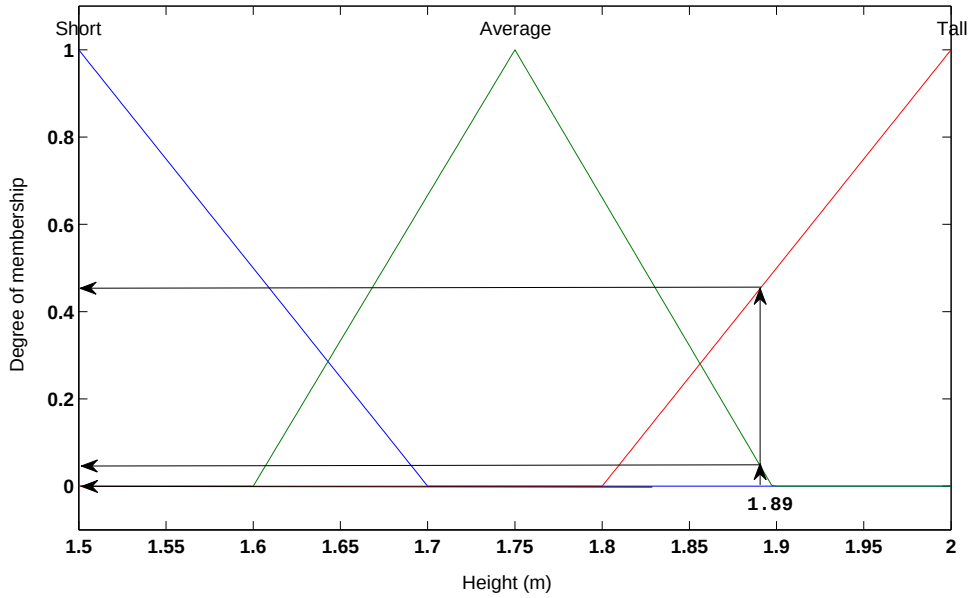

Figure 6.1: Variable "Height" as Linguistic Variable of Three Fuzzy Sets

6.1 Theory of Fuzzy Sets

The theory of fuzzy sets is an extension of the classic set theory, where members to be classified are allowed to partially belong to a certain set. In other words, the concept of partial membership is introduced. An example is the task to classify individuals into "tall", "average" and "short" sets. In classic set theory the establishment of a threshold is required for that, for example, individuals with height above 1.9 m are considered tall. It immediately means that an individual with 1.89 m is considered "average" failing to properly capture the complexity of that transitional range of individuals unless a large amount of sets is created. In a fuzzy set the same individual would belong to both groups, "tall" and "average", but only to a certain degree. It would be "tall", but a "little average". This concept can be mathematically expressed through membership functions such as in Fig. 6.1. If the degree of membership to a certain set is measured between zero (0) and one (1), with one representing total membership, then a man of 1.89 m can be expressed as in Eq. 6.1.

$$H(1.89) = \{short(1.89),\ average(1.89),\ tall(1.8)\} \tag{6.1}$$

If H is a fuzzy set describing a man, with *Height* being one of the attributes or variables used for this purpose, then it can also be expressed as a vector. In addition, Table 6.1 summarizes the notation, where:

mf_{ij}: membership function

v_i: the numeric value of the variable (1.89 m in the previous example)

Table 6.1: Notation for Fuzzy Set H in Figure6.1

Variable	**Terms**	**Membership Functions**
	short	$mf_{11}(v_1)$
Height	average	$mf_{12}(v_1)$
	tall	$mf_{13}(v_1)$

i: indicates the linguistic variable (*height* in the previous example)

j : indicates the term of the linguistic variable (*short*, for example)

The same principle can be applied to variables such as pressure or water depth. This approach utilizes a geometric interpretation of fuzzy sets [22, 21] where a function G maps the numerical attributes of the variables defining a case from a numerical space S into a fuzzy space Ω. In this space, a case can be interpreted as a ordered fuzzy set (vector of degrees of membership) and geometrically represented by a point.

$$G(v_1, v_2, v_3, \ldots, v_n) = (mf_{11}(v_1), mf_{12}(v_1), mf_{13}(v_1), \\ mf_{21}(v_2), mf_{21}(v_2), mf_{21}(v_2), \cdots) \tag{6.2}$$

Or for the previous example:

$$(1.89m) \overset{S}{\underset{\rightarrow}{G}} \overset{\Omega}{(0, 0.06, 0.47)} \tag{6.3}$$

The theory of fuzzy sets is used with two purposes in this study. Firstly, it maps all input variables into a normalized space ranging from zero to one where the distance between cases is calculated. Secondly, it transforms numerical variables into linguistic variables. Engineers, and specialists in general, often reason about a certain problem and make decisions regarding a certain problem using linguistic versions of the attributes listed in Table 6.2. Expressions such as “low" differential pressure, "thick" mudcake or "high" inclination are more subjective, but allow the engineer to interrelate the variables in a simple way and make correct decisions about complex physical systems. Fuzzy logic is the formal technique utilized in this work to perform this task, i.e., combine linguistic variables in order to describe the behavior of complex systems through relatively simple rule-based models built on expert knowledge. This approach is particular interesting in cases where analytical models are

difficult to be derived and variables carry considerable levels of uncertainty. It also attends the initial aspiration of this study in proposing alternative methods to efficiently process available drilling data to assist engineers in anticipating drilling problems.

Hence, if A and B are generic fuzzy sets $A = (a_1, a_2, \ldots, a_n)$ and $B = (b_1, b_2, \ldots, b_n)$ composed by a vector of degrees of membership a_i and b_i, the following equations can be written to describe the distance between these two sets and the concept of similarity between them respectively:

$$d(A,B) = \sqrt[p]{\sum_{1}^{n} |(a_i - b_i)|^p \cdot w_i} \tag{6.4}$$

$$S(A,B) = 1 - \frac{d(A,B)}{d(AUB, \varnothing)} \tag{6.5}$$

Therefore, cases A and B - points in fuzzy space Ω - are considered similar if the distance, $d(A,B)$, between them is small. **Similarity varies between zero (0) and one (1) with one representing total similarity, i.e., equality**. Moreover, $A \cup B = Max(A,B) = (Max(a_1,b_1), Max(a_2,b_2), \ldots, Max(a_n,b_n)$,$\varnothing = (0,0,\ldots,0)$ is the nil set, w is a weight (relative importance) given to a particular variable and p is a integer. The Euclidean distance is obtained by setting $p = 2$ (default) and the Hamming distance is used if $p = 1$, for example.

The well segments are not regular depth intervals. Instead, every time the value of a variable affecting the possible causes of differential sticking changed significantly, a new segment was created. Any of following conditions were used as sufficient criteria for the establishment of the segments:

1. End of phases smaller than 17 $inches$.
2. Inclination variations greater than 15 $degrees$.
3. Change in BHA composition.
4. Drilling Fluid
   (a) Mud weight variation greater than 1 ppg.
   (b) Significant changes in drilling fluid formulation.
   (c) Significant changes in solids concentration.
   (d) Variations greater than 3° in FANN 35 rheometer θ_{100} readings (relevant rheological parameter to flow in porous media such as mudcake).

5. Severe abnormality leading to trouble time.

6. A differential sticking event marks the end of a segment.

This procedure was applied for all the wells in the database. The objective of this procedure is to create cases containing information about relevant drilling parameters before, during and after the occurrence of the problem. In other words, enable Eq. 6.5 to differentiate operational conditions that results in differential sticking from safe operational ones.

Table 6.2 shows the input variables used by the similarity metric.

All variables are averaged for the well segments. The inclination factor is defined as follows.

$$IF = \frac{\theta}{90} \tag{6.6}$$

And θ is the average inclination angle of the well segment. The clearance factor is defined below.

$$CF = \frac{D_w - D_{oavg}}{D_w} \tag{6.7}$$

Where D_w is the internal diameter of the well and D_{oavg} is the average external diameter of the BHA component (drillcollar for example) for that well segment:

$$D_{oavg} = \frac{\sum D_o \cdot L_{Tool}}{\sum L_{Tool}} \tag{6.8}$$

D_o is the external diameter of a particular component of the BHA, L_{Tool} is the length of a component of the BHA and L_{BHA} is the total length of the BHA. L_{crit} is defined as follows:

$$L_{crit} = \sqrt[3]{\frac{E \cdot I}{w_{seg} \cdot \sin\theta}} \tag{6.9}$$

w_{seg} is the weight in fluid of the BHA segment **(single or multiple components connected together)** under consideration, E is the Young's Modulus of the material and I is the area moment of inertia calculated as follows:

$$I = \frac{\pi\left(D_{oseg}^4 - D_{iseg}^4\right)}{64} \tag{6.10}$$

Where

$$D_{oseg} = \sum D_o \cdot \frac{L_{Tool}}{L_{seg}} \tag{6.11}$$

Table 6.2: Input Variables for Calculating the Similarity Score

Variable	Relevance	Terms	No. of Membership Functions
Measured Depth	Drillstring weight	MD Curve	1
Maximum Dog Leg	Drag / Wall Contact	Max Dog Leg Curve	1
Open Hole Time	Mudcake / Wall Contact	Open Hole Time Curve	1
Differential Pressure	Force Modulus / Mudcake	DP Curve	1
Filtrate Volume	Mudcake	Small, Medium, High	3
Solids Concentration	Mudcake	Small, Medium, High	3
Inclination Factor	Wall Contact	Small, Medium, High	3
$L_{BHA} - L_{Crit}$	Wall Contact	Small, Medium, High	3
Clearance Factor	Wall Contact	Small, Medium, High	3
API Filtrate Ratio (500/100 or 1000/500 psi)	Mudcake	Small, Medium, High	3
Hardness Index	Mudcake	Small, Medium, High	3
Torque Resistance	Mudcake	Small, Medium, High	3
Adhesion Strength	Mudcake	Small, Medium, High	3

Notes: Time of BHA exposed to open hole and it may include downhole time related to other drilling problems. All membership functions are trapezoidal.

and

$$D_{iseg} = \sum D_i \cdot \frac{L_{Tool}}{L_{seg}} \tag{6.12}$$

D_i is the internal diameter of the BHA component and L_{seg} is the length of the BHA segment. The parameter L_{crit} measures the tendency of beam or pipe to deflect under its own weight and the smaller the value, the more prone to deflect or less stiff it is. This parameter was calculated to each segment (marked by stabilizers) of the BHA and its value subtracted from it. The entire segment would be removed if its length was smaller than L_{crit}. The difference $L_{BHA} - L_{Crit}$ was used as one of the parameters to assess wall contact as shown in Table 6.2 and the greater the value the more contact is expected.

Tool shape factor is defined as follows:

$$TSF_{Tool} = \frac{\sum_{1}^{n} p_g}{\pi \cdot D_{TN}} \tag{6.13}$$

Where D_{TN} is the nominal diameter of the tool and p_g is the circumferential perimeter of groove as shown in Fig.6.2. Likewise L_{crit}, this parameter was also calculated for each component in the BHA according to its shape whenever its geometrical details were available, like drill collars in Fig. 6.2, otherwise a value of 1 (full contact) was assumed. A value of 0.2 was used for stabilizers without available information. An average TSF was calculated for the BHA for each well segment according to Eq. 6.14.

$$TSF_{avg} = \sum TSF_{Tool} \cdot \frac{L_{Tool}}{L_{BHA}} \tag{6.14}$$

The parameter ranges between 0 and 1 and measures how close the BHA component is of a smooth cylinder. The greater the number, the closest to a cylinder it is and higher wall contact is expected.

The fuzzy sets describing each variable is listed in Appendix G.

6.2 Fuzzy Logic

Fuzzy logic is used to interrelate the aforementioned variables and construct simplified phenomenological models relevant to the problem through approximate reasoning. These models are proposed in replacement of analytical ones that would need to be too complex in order to account for the innate uncertainty of certain phenomena and variables without guaranteeing exactness.

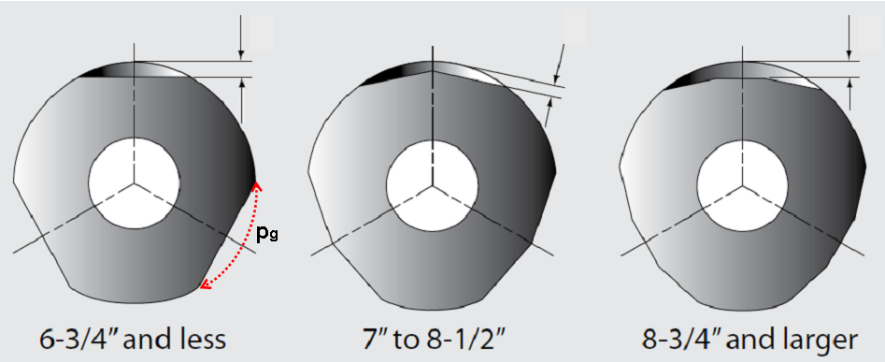

Figure 6.2: Tool Shape Factor

These models are entailed in the so called fuzzy controllers.

Fuzzy controller is the mathematical frame or inference engine that allows a logical statement about a subject to be built and processed in order to generate a meaningful output. A fuzzy controller is comprised by the input variables in the form of fuzzy sets, the rules establishing the interrelation between them - the logic -, the details about how logical connectors ("and", "or", "not") are mathematically interpreted and combined in the antecedent part of a rule to compute the consequent part of the same rule, how the result - consequent part - of these rules are combined and how a crispy deffuzified value - meaningful output - is computed. Each step is further explained in Appendix G.

Three controllers were proposed. The first, called wall contact, computes or estimates the level of contact between the drillstring and the borehole wall. The second, called cake quality, calculates a quality score for a certain mudcake based on its mechanical properties measured by the HPHT MCCE. Finally, a controller called cake thickness computes a thickness score for the mudcake based on variables affecting filtration properties of the drilling fluid. Note that the output of these controllers are values between 0 and 1, called scores, and they are the inputs, together with the other variables listed in Table 6.2, for the similarity metric that performs the comparison between well segments. Therefore, Table 6.4 shows the variables and parameters that compose one case.

A full behavioral analysis of the developed fuzzy controllers is omitted for briefness, but Appendix G brings detailed information about them and demonstrate some of its functionality.

Table 6.4: Variables Composing the Case Structure

Raw Input Variable	**Input for Fuzzy Logic Controller ?**	**Case Structure**	**Normalized Output Variables (Input for Eq. 6.5)**
Measured Depth (m)	No	Measured Depth	0 to 1
Maximum Dog Leg $(^{\circ})$	No	Maximum Dog Leg	0 to 1
Open Hole Time (h)	No	Open Hole Time	0 to 1
Differential Pressure (psi)	No	Differential Pressure	0 to 1
Filtrate Volume (ml)	Mudcake Thickness	Mudcake Thickness	0 to 1
Solids Concentration (ppm)			
API Filtrate Ratio (500/100 or 1000/500psi)			
Clearance Factor	Wall Contact	Wall Contact	0 to 1
Inclination Factor			
$L_{BHA} - L_{Crit}$ (m)			
Hardness Index	Mudcake Quality	Mudcake Quality	0 to 1
Torque Resistance (N/m)			
Adhesion (N/m^2)			

6.3 Optimization of Weights in the Similarity Metric: Classification through History Match.

It is interesting to note, at this point, that the only term left to be resolved in Eq. 6.5 is the set of weights w_i. According to Table 6.4 there are seven weights corresponding to the seven parameters to be used for comparing cases. The weights are responsible the overall importance of the variables in regards to their impact in the occurrence of differential sticking. The weights are also the elements of the model enabling the artificial learning.

Instead of assigning values based on expert's advice, as it is often done, a minimization scheme is proposed for this task. The rigorous approach to set the weights attempts to unveil the detailed relation between variables hidden in the database - consequence of the complex nature of the problem - which is the aid engineers ultimately expects from a method to anticipate the problem. The experts contribution rely only in identifying the variables to be used and general description of their behavior through the rules in the fuzzy controllers.

A data-fitting algorithm uses the similarity metric as objective function and is executed by comparing all cases in the training database. The training database contains cases where the problem occurred and otherwise, and these conditions are identified by the algorithm. The data-fitting is the search for the optimum set of weights to drive the similarity to be **one (1, total similarity)** whenever two cases being compared present the same outcome (free or stuck), and **zero (0)** otherwise. The data-fitting is performed by the function *lsqcurvefit* from MATLAB® optimization toolbox (see Appendix B). It performs the non-linear data-fitting problem in the least-square sense. After a successful minimization procedure, Eq. 6.5 should work as a discriminant function between similar and dissimilar cases. Fig. 6.3 illustrates the idea.

Where S stands for similarity score and the subscripts s and f for *stuck* and *free* respectively. The greater the distinction between the two groups in Fig. 6.3, the better the efficiency of Eq. 6.5 to anticipate the problem.

6.4 Analysis of Results

Therefore, if a new case - segment of a well to be drilled or being drilled - is compared with every historical case in the database of correlation wells through Eq. 6.5, an assessment in regards to the likelihood of occurrence of differential sticking can be made based, for example, on the average value of similarities between the new case and the cases where the problem did, and did not occur. It is important to remember that the outcome of each case in the

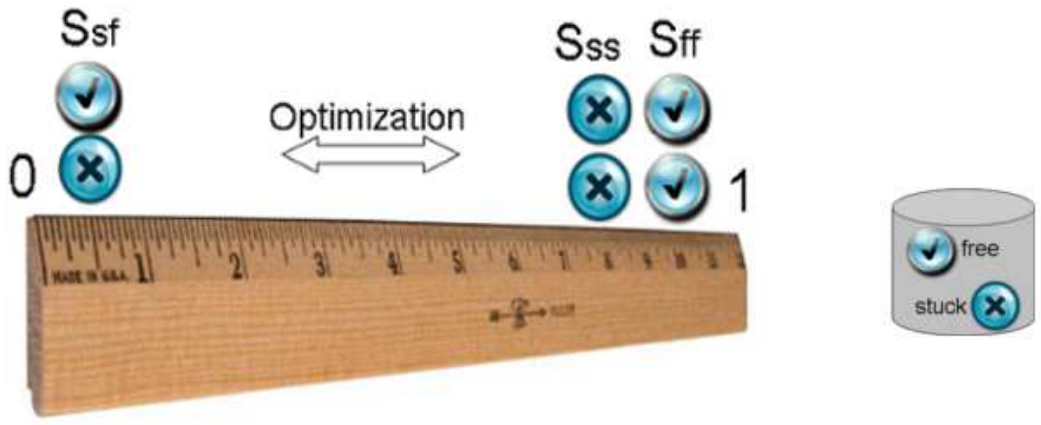

Figure 6.3: Objective of Weight's Optimization in the Similarity Metric

database is known a priori in this study unlike in a real well planning or drilling situation.

Having said that, the database of historical cases was firstly divided into a training and a testing database. **The training database is used to find the optimum set of weights** and the test database used to test the effectiveness of Eq. 6.5.

The results can be interpreted in several ways and the following concepts are suggested here to test the effectiveness of the proposed model in terms of the outcome (free or stuck) and its likelihood of occurrence:

6.4.1 Testing the Model

The model was tested against 127 cases from 44 wells of different fields selected from several operators. Table B.1 in Appendix B shows the raw drilling data database while Table D.1 shows the processed or actual input cases database for calculating the similarity score. The database was divided into a training and a test database, and columns in Table B.1shows both sets by indicating with "1" the members of each group.

In order to assess the model performance the following steps were followed:

1. Optimization of variables weights is performed and optimum weights calculated.

2. The similarity between each case in the test database (here called target cases) and all the cases in the training database was calculated using Eq. 6.5 with the optimum set of weights from step 1.

3. The average of similarity scores between each test case and all the cases

with the same known outcome (test cases free and training cases free, or test cases stuck and training cases stuck was calculated). Eq. 6.15 and Fig. 6.4 further explain the method.

$$Avg\,Similar = \frac{\sum_{i=1}^{n} S_{Ti}}{n} \tag{6.15}$$

4. Analogously, the average of similarity scores between each test case and all the training cases with opposite (dissimilar) known outcome was also calculated.

5. Percentage efficiency in regards to the ability of correctly identifying the outcome of the cases in the test databases was then assessed by comparing the number of cases where the average of similarity of cases with same outcome was greater than the average of similarity of cases with opposite known outcomes.

Optimization efficiency, i.e., ability to separate similar and dissimilar cases *in the training database*, is assessed by comparing the overall average similarity scores of similar and dissimilar cases; the greater the separation the greater the efficiency. In a ideal set, the separation should be one (1) [1], i.e., all similar cases with similarity score equals to one (1) and all dissimilar with score equals to zero (0).

Other comparative methods could have been used, such as computing the Maximum and Minimum similarity scores found when comparing similar and dissimilar cases. The average similarity score was chosen as the default method of risk analysis and is proportional to the likelihood of the problems occurrence [49].

Various scenarios can be run depending on the number of selected cases for the training and testing database, and result analysis can quickly become a cumbersome task. More than a complete efficiency analysis, this study aims at proving the potential of the proposed method to be applied in field applications. One challenging scenario was then proposed for this purpose where a reduced training dataset is used and tested against a larger testing dataset. The training dataset was selected from wells of different fields and operators

[1] A theoretical concept since total similarity only exists between equal points (cases) and total dissimilarity between symmetric points.

with the objective of capturing as much variety as possible in regards to differential sticking occurrence.

Detailed results are shown in Tables E.1 and E.2 of Appendix Band the method achieved **68 %** of success in predicting the correct outcome of all cases in the testing database.

Further analysis can be performed with other scenarios. Dummy wells were proposed to highlight the technical coherence of the proposed method and demonstrate the potential of the proposed variables or parameters to capture the problem's essence. Tables E.5 and E.6 shows the dummy cases and result analysis. Note that the dummy cases were intentionally designed with data that clearly leads to the intended outcome. For example, stuck cases presents data of high differential pressure, high wall contact, thick mudcake, etc. Therefore, the differences between the average similarity scores of similar and dissimilar cases proves that the model is able to interpret these tendencies and differentiate between a clearly favorable operational condition for differential sticking and clearly safe one. Since all dummy cases were used in the optimization step, there is no need to report results in terms of percentage efficiency in identifying the correct outcome. Naturally, it would be very high.

6.4.2 Proposed Analog Method for Field Applications

The exact same analysis should be performed while designing or drilling a well segment to assess the risk for differential sticking. The analog of the previously explained method is as follows.

1. The average similarity is calculated between the target case (unknown outcome) and all cases of the two groups in historical database: free and stuck.

2. The greatest average similarity relative to each group determines the outcome tendency to be free or stuck while its magnitude quantifies the likelihood with one (1) indicating maximum risk. Eq. 6.16 and Fig. 6.4 further explain the method.

$$Avg\,Free = \frac{\sum_{i=1}^{n} S_{Ti}}{n} \tag{6.16}$$

Where n is the number of cases in the historical database without the occurrence of the problem and T refers to target case. An analog equation

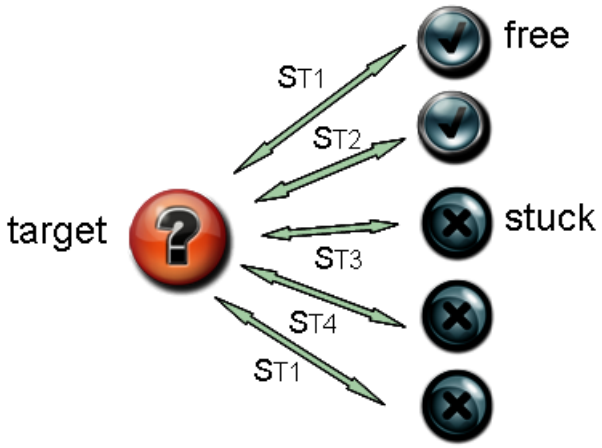

Figure 6.4: Risk from Average Similarity Scores

can also be written for the stuck cases.

3. A more complete analysis can be performed observing the difference between the average similarities to each group: free and stuck. The greater the difference the more clear the tendency. In other words, a well segment is more prone to present differential sticking if it presents high average similarity with the group of cases that presented the problem *and* low average similarity with the group with no instances of the problem. The bi-dimensional analysis is illustrated in Table 6.5.

Three different wells from a particular field presenting four cases of differential sticking were selected from the database to demonstrate the analysis. Table E.7 shows that, with exception of the stuck case *1*06, the average similarities of all other cases where the problem occurred presented greater similarity scores relative to the stuck group than to the free group. Moreover, it is interesting to note, for the exceptional case, the sharp decrease in the difference between similarities to free and stuck group. In other words, the clear decrease in similarity with free cases when compared to its neighboring cases. Therefore, in addition to the magnitude of the average similarity score, an important secondary analysis aspect is revealed, i.e., the ability of the model in capturing shifts in tendencies regarding the occurrence of the problem from one case to another within a particular well. These results are encouraging from the point of view of using the model to assess the risk while drilling is concerned (real-time risk analysis).

Except for three cases, the model was also consistent in regards to predicting the cases without the problem. Within the three exceptions, the scenario

Table 6.5: Bi-dimensional Risk Analysis via Similarity Score - Arbitrary Rank

Average Similarity Score to Stuck Cases	**Average Similarity Score to Free Cases**					
	0.95	0.8	0.6	0.4	0.2	0.1
0.1	Insignificant	Negligible	Negligible	Negligible to low	Undetermined	Undetermined
0.2	Negligible	Negligible	Negligible to Low	Low	Undetermined	Undetermined
0.4	Negligible	Low	Low to Moderate	Undetermined	Moderate	Moderate to High
0.6	Low	Moderate	Undetermined	Moderate to High	High	High to Extreme
0.95	Undetermined	Undetermined	Moderate to High	High to Extreme	Extreme	Extreme

is somehow undefined for case *100*, i.e., close average similarity scores to both groups: stuck and free. Based on the same reasoning, the model suggests that particular attention should be given to the free cases where small differences between the average similarities to free and stuck situations are present. Finally, the severity of the problem assessed based on the criterion of the difference between the average similarity scores to each group presented reasonably good agreement with net time to free the pipe reported for each case where the problem occurred. Results show that the time to free the pipe was longer for those cases where the average similarity to stuck cases was high while presenting low similarity to free cases, i.e., greater difference between average similarities.

The results presented here were derived from the analysis of a few wells and does not pretend to be conclusive, but instead it supports the proposed analysis methodology and serves as the basis for further studies.

6.4.2.1 Further Comments

The method is able to learn through regular optimization rounds of weight factors relative to each relevant variable as new cases are incorporated into the database.

1. The same analysis can be made, but only considering those wells in the historical database with certain characteristic: same field, differential pressure above certain level, etc.

2. Or determine the outcome tendency to be free or stuck based on the percentage of cases in the two groups (free or stuck) that present similarity scores greater than a certain value or, for example, the top quartile.

3. A more comprehensive analysis regarding the critical values of average similarities and their differences should be performed to reveal practical variance levels of the proposed metric and enhance exactness of the model.

4. An extended study about predictions of the model within a particular field should be conducted. An increase accuracy performance is expected since operational particularities of that field could be better encapsulated into the model.

Chapter 7

Consequence Analysis: Approximate Unidimensional Mechanistic Model

The method and equations composing the analytical part of the risk assessment model are detailed here. Based on the statement of the problem (see Fig. 2.1) the following equation can be used to compute the necessary tensile force to be applied at surface in order to keep the drillstring free:

$$F = \beta w \left(L \cos\theta + h_{drag} \mu \sin\theta\right) + \mu d h \Delta P \tag{7.1}$$

whereβ is the buoyancy factor defined as

$$\beta = 1 - \frac{\rho_{fluid}}{\rho_{ds}} \tag{7.2}$$

and where w is the linear weight of the drillstring component, L is the total length of the drillstring, h_{drag} is the length of the drillstring in contact with the borehole and casing walls, h is the length of the drillstring in contact with the borehole wall only, θ is the inclination angle from vertical, μ is the friction coefficient, d is the chord on the drillstring cross sectional delimited by surface area covered by mudcake, ρ_{fluid} is the drilling fluid density, ρ_{ds} is the density of drillstring and ΔP is the differential pressure between the borehole and formation. This unidimensional equation is valid for straight sections of the well and assumes that differential sticking is the only problem occurring in the well. The first and second terms are the weight of the drillstring and the drag force between the drillstring and the well respectively. The last term is the differential sticking force itself and its magnitude is directly proportional to the differential pressure and the area define by the product of d and h. Whenever the magni-

tude of F is larger than the yield point of the drillpipe or the pull capacity of the drilling rig, the drillstring is stuck.

The difficulties in evaluating this apparently simple equation are many and the drag term alone has been the subject of investigation of several researchers. In spite of the importance of the drag force, the differential sticking term of Eq. 7.1 is the focus of this work and this chapter is dedicated to detail the proposed models to compute its variables. The proposed approach combines the results of the mechanical assessment of drilling fluid mudcakes obtained from the experiments conducted in the HPHT MCCE with mechanistic models describing the phenomenon. The method is validated based on field data where instances of the problem are carefully analyzed and the reported magnitude of differential sticking force are compared with model predictions.

7.1 Calculating Wall Contact, h

The question about how much of the drillstring touches the borehole wall has been asked many times in the oil industry. The reason is that the answer directly impacts the accuracy of estimating the magnitude of forces such as torque and drag, the occurrence of problems such as buckling of the drillstring, undesired well trajectory and our target problem: differential sticking. Despite of many years since the first well drilled and efforts from both industry and academia, an accurate answer to this question remains to be given. The methods range from simplified analytical methods to robust numerical methods. The first presents the disadvantages of lying on too many assumptions and the later frequently suffer from problems of numerical instabilities and are time consuming. The importance of parameter h in Eq. 7.1 is evident and the uncertainty in calculating it is proportional to the complexity of the kinematics and dynamics of drilling. In other words, a drillstring composed by pipes of different sizes and shapes connected to a drill bit and several accessories rotating from surface[1], in a long well, often with complex trajectories, filled with a flowing drilling fluid and with one segment under tension and another under compression.

Given the complexity of involved physics and characteristics of existing methods, it is prudent to choose an approach that provides an answer that is accurate enough to allow a satisfactory prediction of the target problem without requiring excessive computational resources and time. Therefore, a method providing a good estimation of h that enables the computation of F in order to differentiate between a stuck and a non-stuck pipe situation is the

[1] True for conventional drilling without the use of downhole motors and turbines. In this case, the drillstring segment downstream of the motor may be the only part being rotated.

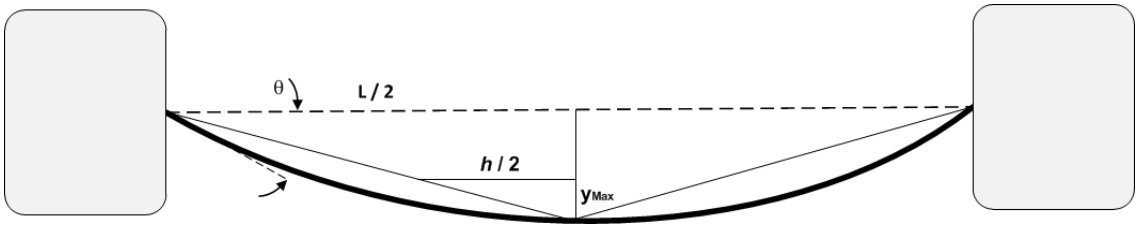

Figure 7.1: BHA Deflection Curve

aim of this study. Existing methods based on finite elements [53, 11] are not only complex, often unstable and time consuming, but defy the purpose of this work in proposing relatively simple analytical methods in conjunction of novel use of common drilling data in order to anticipate the problem. Classic iterative methods are often used to define optimum distances between stabilizers [57] and for computation of side forces in the bit, but solution is only available in the absence of tangency points between stabilizers and with the BHA under compression. This is a problem because despite of design efforts there is no guarantee that this is in fact the case at all times. Moreover, depending on the drilling scenario, the optimum design spacing of stabilizers can be disregarded to accommodate a more important component or to achieve a certain purpose. The bending properties of drillcollars and other BHA components are of major interest of this work because it is exactly in the BHA that the smallest clearance between the drillstring and the borehole wall exists, thus increasing the likelihood of contact with the mudcake and consequently generating differential sticking. Because of these reasons, simplicity and adequacy to the problem of interest, a new model has been proposed here.

7.1.1 Contact Between BHA and Borehole Wall.

7.1.1.1 In Between Stabilizers

The model treats segments of the BHA (single or multiple drillcollars or components or downhole tools connected to each other) in between stabilizers[2] as beams supported by fixed ends [58]. Fig. 7.1 shows a segment of the BHA and Eq. 7.3 describes the deflection of this segment as a function of the distance from the supports and material stiffness. This equation also assumes that the weight of the component is uniformly distributed and no moment exists at the supported ends, i.e., it is alien to effects coming from the characteristics or forces acting on adjacent segments. A reasonable assumption for the case of stabilizers separating segments since they are quite large, short and stiff.

[2]only collars and major components are considered while float subs, drill bit, etc, are not.

$$y = \frac{-w_{seg} \sin \alpha x^2}{24EI} \left(L_{seg}^2 + x^2 - 2xL_{seg} \right) \tag{7.3}$$

where y is the vertical deflection, x is a particular length of interest, L_{seg} is the total length of the segment, w_{seg} is the weight, α is the angle from the horizontal at the length of interest, E is the Young's Modulus of the material, I is the area moment of inertia defined as a function of the outer diameter of the BHA component D_o and inner diameter D_i, according to Eq. 7.4 for cylinders.

$$I = \frac{\pi \left(D_o^4 - D_i^4 \right)}{64} \tag{7.4}$$

A segment is often composed by more than one component and in that case the average I as in Eq. 6.10 is used.

In order to calculate the percentage of contact length between a BHA segment and the mudcake, the concept of proportionality between triangles is used as in Eq. 7.5. Fig. 7.1 illustrates the geometrical relation.

$$\frac{h/2}{L_{seg}/2} = \frac{y_{MAX} - Cl}{y_{MAX}} \tag{7.5}$$

where y_{MAX} is the maximum deflection of the beam given by Eq. 7.6 and is derived from Eq. 7.3 where $x = L/2$ and Cl is the clearance defined according to Eq. 7.7.

$$y_{MAX} = \frac{-w_{seg} L_{seg}^4}{384EI} \tag{7.6}$$

$$Cl = \frac{(D_w - 2m) - D_o}{2} \tag{7.7}$$

The numerator is the hydraulic diameter and m is the mudcake thickness, D_w is the internal diameter of the well and D_o is the external diameter of the BHA component. The proposed method also accounts for the fact that Eq. 7.3 only holds if no contact is made between the drillcollar and the mudcake or borehole wall. As soon as first point of contact happens it tends to deflect less. Using Eq. 7.5 whenever y_{MAX} is greater than the clearance compensates for this fact in a simple and effective manner. Naturally, no contact and thus a nil contact length is computed for a segment where clearance is greater than y_{MAX}.

It is important to mention that most of differential sticking events occur while the drillstring is static, often during connections or interruptions because of various reasons. In these circumstances the drillstring is usually suspended, off the bottom with no weight on bit, what favors the model's assumptions.

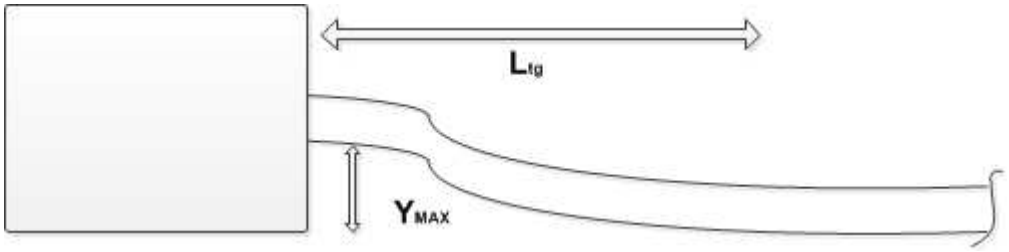

Figure 7.2: Drillpipe Point of Tangency.

7.1.1.2 Point of Tangency

Point of tangency here is defined as the distance between the last stabilizer in the BHA and the point where the BHA segment after it touches the borehole wall. Fig. 7.2 illustrates this downhole configuration. The point of tangency is calculated from the theory of mechanical behavior of cantilevers loaded uniformly with its own weight. Eq. 7.8 describes the interrelation between relevant variables.

$$y = \frac{w_{seg}x^2}{124EI}\left(x^2 + 6L_{seg}^2 - 4L_{seg}x\right) \tag{7.8}$$

$$y_{MAX} = \frac{w_{seg}L_{seg}^4}{8EI} \tag{7.9}$$

Therefore, the length before the point of tangency is subtracted and the remaining length of the BHA is considered to touch the borehole wall. [3]

The analysis is performed only in the BHA and contact between drillpipe and borehole is neglected given that a big clearance exists between the drillpipe and the mudcake. This simplification is also used for curved wellbores although contact is expected in build up or drop off sections of deviated wells. This assumption may impact significantly the results in wells with highly complex trajectories.

7.1.1.3 Tool Shape Effect

As mentioned in chapter 6, several tools have spiraled shapes in order to reduce the contact area with the borehole wall (See Fig. 6.2). The proposed dimensionless tool shape factor described in Eq. 6.13is used once more here to account for that effect whenever spiraled drillcollars or components (MWD, LWD, subs,etc...) are present. An average value of the TSF is calculated for each segment and multiplied to the *contact* length calculated for that particular

[3] The same equation is used for extremely long BHA segments in between stabilizers where deflection would be too big if considered as a structured beam with fixed supports. In that case, the length to point of tangency is subtracted from both ends.

segment in order to compute a shorter effective contact length [4].

7.1.1.4 Summarized Computation Procedure

The following calculation routine was applied to all cases in the historical database:

1. A detailed BHA description was obtained for each case: components list, order, detailed geometrical and material description (length, diameters, linear weight and shape).
2. The position of stabilizers are identified and the following calculation performed for each segment, s, composed by components between stabilizers:
   (a) contact length h from Eq. 7.5.
   (b) TSF from Eq. 6.14.
   (c) compute effective contact length.

$$h_{eff} = \sum TSF \cdot h \tag{7.10}$$

3. The last stabilizer is identified and the following procedure executed:
   (a) Point of tangency L_{tg} calculated from Eq. 7.9 and Eq. 7.7 by using $y_{MAX} = Cl$

$$L_{tg} = \left(\frac{8 \cdot E \cdot I \cdot Cl}{w_{seg}} \right)^{\frac{1}{4}} \tag{7.11}$$

   (b) TSF from Eq. 6.14.
   (c) compute effective contact length after the last stabilizer; where $L_{as}$is the remaining length of the BHA after the last stabilizer:

$$h_{as} = (L_{as} - L_{tg}) \cdot TSF$$

4. Compute total effective contact length of the BHA:

$$h_{total} = h_{eff} + h_{as} \tag{7.12}$$

7.2 Calculating d

The parameter d is defined in Fig. 2.1. It is the chord across the cross section of the outer diameter of the drillstring defined by the embedment depth

[4] it is in fact a reduction in the area $h \times d$

in the drilling fluid filtercake. This is another parameter carrying enormous uncertainty and one of the reasons for the difficulty in predicting differential sticking. The first difficult in predicting d is the effect of the dynamic characteristics of the operation before connections and other idle times on the embedment depth. While drilling ahead, filtration through permeable formation constantly happens and so does the formation of the mudcake. This mudcake is partially eroded by shear force or turbulence eddies of drilling fluid flow and by the rotary action (often not aligned) of parts of the drillstring in contact with it. Another possible operational scenario is a reentry after a trip out operation[5], where static filtration occurs for as long as the operation takes and the reentry happens without rotation. In the first case, the mudcake grows around the drillstring that is probably resting on the borehole wall with a thin and soft layer of mudcake. The second situation suggests that a thicker and harder (at least near the borehole wall) mudcake exists and a completely free drillstring comes in contact with it.

The other difficulty in predicting d concerns the mechanical properties of the mudcake, more particularly its hardness, and consequently the degree of resistance to the embedment of the drillstring. Although the kinematics and dynamics of drilling operations are difficult to reproduce in laboratory conditions, a significant effort was made in assessing the mechanical properties of mudcakes. This section describes how these experimental results together with exact analytical models are used to model the interaction of drillstring and mudcake and consequently calculate a value for parameter d.

7.2.1 Geometrical Relation between Mudcake Embedment Depth and Parameter d

Fig. 7.3 demonstrates how the chord d is a function of the extension of drillstring embedment in the mudcake matrix, while Eq. 7.14 was derived to explicit the interrelationship between the two.

$$d^2 = \frac{Do^2 Di^2 - Z^2}{Do^2 + Di^2 + 2Z} \tag{7.13}$$

where Z is defined below.

$$Z = 2\left(Di - Do + \delta\right)\delta - DoDi \tag{7.14}$$

It is clear that a model is needed to estimate the embedment of the drillstring in the mudcake in order to solve Eq. 7.13. The next section explains the challenges and the proposed solution to resolve the problem.

[5]Trip out: removing the drillstring, running out of hole.

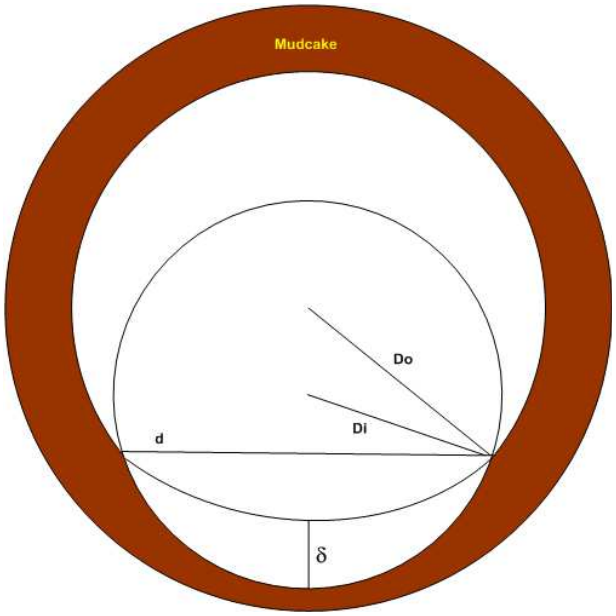

Figure 7.3: Geometry of Embedment

7.2.2 Algorithm for Calculating Parameter d

The difficulties in calculating the embedment depth of drillstring in the mudcake at a certain drilling depth are many. The immense variety of drilling fluid compositions, the anisotropic nature of geological formations, the complexity of filtration phenomena, mudcake formation under cross-flow and the absence of consistent studies about the mechanical properties of mudcakes are some of them. In addition, the interaction between the downhole tools and the mudcake needs to be established.

The approach proposed here utilizes the experimental results from embedment tests (hardness) as basis. They are then combined with a physically-based method to correlate the characteristics of the laboratory test procedure with the real drilling phenomenon in order to estimate the in situ embedment depth in the well.

The variable chosen to establish the correlation between the laboratory results and the field is pressure. The output of the hardness tests conducted for several drilling fluids under various drilling conditions are curves of axial resistive force versus embedment depth. These results were raised by indenting a hemispherical penetrometer into the mudcake, but the drillstring is a cylindrical object with different dimensions. Pressure, instead of force, can relate the two physical scenarios if one consider that a certain embedment depth measured in the lab is likely to be observed in the well if the same pressure is applied by the drillstring on a similar mudcake. It is also assumed that geometrical dis-

similarity or geometrical scale up effect is negligible or compensated by using pressure as the correlation variable. The model also disregards any difference in kinematics and dynamics of embedment (equivalent to the embedment velocity and its variations) between the two scenarios, which was not investigated during the experimental program. Having said that, the following algorithm can be written:

Where d is calculated from Eq. 7.13, pressure on the drillstring is calculated by Eq. 7.15 and δ_{new} by Eq. 7.16 .

$$P_{Tool} = \Delta P + \frac{w}{d} \tag{7.15}$$

$$\delta_{new} = \frac{\delta_{exp} + \delta_{guess}}{2} \tag{7.16}$$

7.3 Validation Method

The models enabling the calculation of the differential sticking force in Eq. 7.1 have been derived and its magnitude can be compared with field data if the overpull in instances of problem is reported. The driller often keeps track of the weight of the drillstring and drag forces, especially while drilling highly inclined wells. If such pull test is performed, the driller may record the tensile force with and without rotation. Therefore, the overpull is the net downhole tensile force and corresponds to the differential sticking force whenever this is the only problem occurring in the well.

Three field cases of differential sticking were selected where the overpull was correctly reported together with stuck depths. Whenever the drillstring is stuck several actions are taken in order to free it, ranging from simply pulling or slacking off the drillstring to circulating spotting fluids followed by new pull sections and deployment of specialized tools run on cables or coiled tubing. Sidetrack is the last option adopted if the drillstring is lost and unable to be recovered or milled. The overpull not always is reported in the drilling report after each trial. These three cases not only bring the overpull observed after each action taken, but more importantly, it provides the overpull at the moment when the drillstring was liberated. The analytical model was fed with the required operational inputs and results compared with the overpull observed before freeing the drillstring.

The model satisfactorily predicted overpulls of the same order of magnitude as those observed in the field. Appendix F provides details of each case and related calculation.

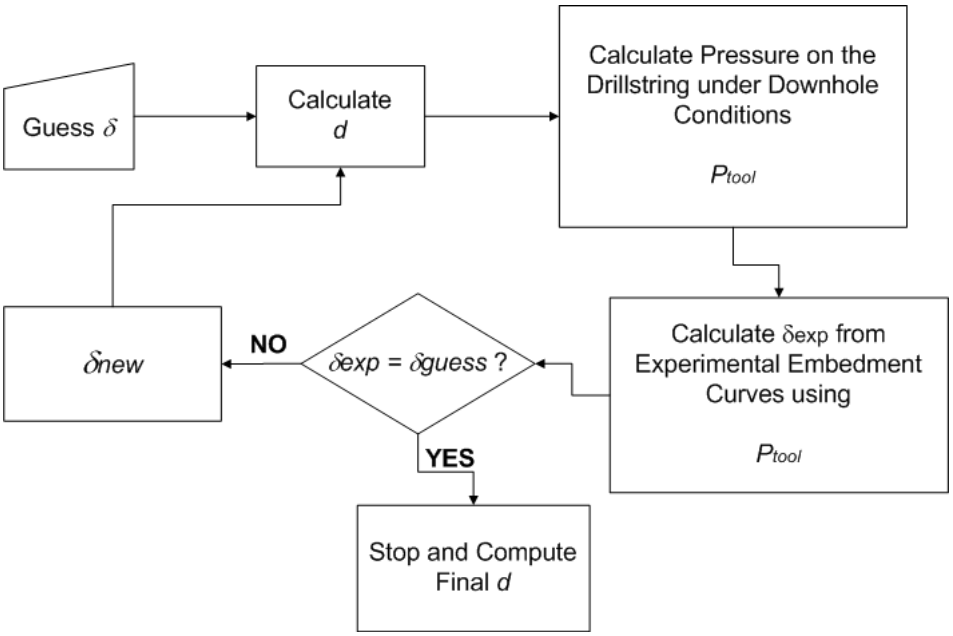

(a) Algorithm

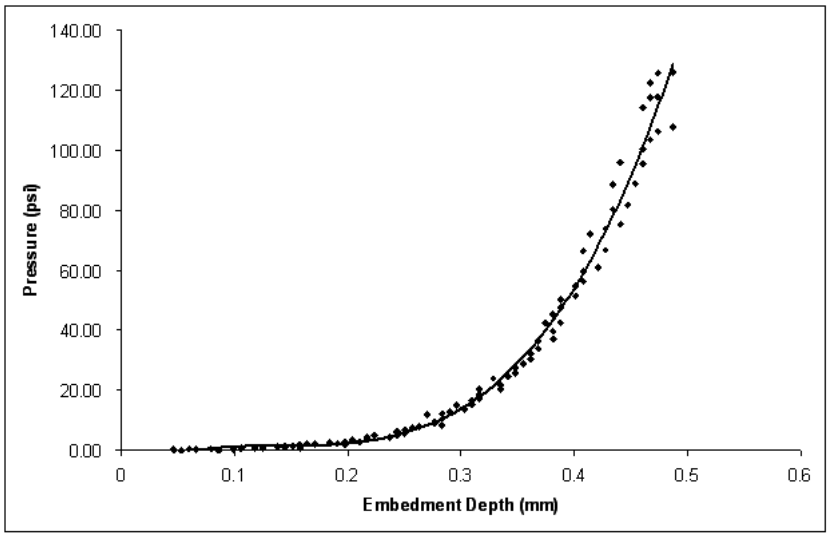

(b) Embedment Experiment - Pressure on Penetrometer

Figure 7.4: Algorithm to Calculate Parameter *d*.

It is relevant to say that a friction factor of 0.1 was used for cases *112* and *130* and 0.15 for the highly inclined case *105*. Friction factors are usually in the range of 0.05 to 0.22. The value of 0.1 was selected based on values reported on the work of Aadnoy [3] where averaged friction factors of 0.12 were observed in pull tests conducted at inclined wells.

Finally, the presence of a downhole overpull force may affect drag through changing the lateral forces applied on contact points of deviated wells, and hence, the overall pull force reported may contain an additional drag component not accounted for at the primary pull test analysis. However, this effect will only be pronounced in highly deviated wells with complex trajectories. The utilized approximate model was derived for straight sections and results reported here apparently demonstrate its good performance even slightly beyond the assumed optimum trajectory and does not reveal significant inter-coupling between overpull and drag for the observed cases.

Chapter 8

Combined Results of Risk Analysis

The risk analysis described at Chapter 4 is illustrated here.

The ultimate result of a combined analysis involving both the similarity score (to free and stuck cases in the historic database and calculated as in Chapter 6) and the analytical model (overpull calculated from equation 7.1 in Chapter) is a tree-dimensional graph that enables tracking the risk of a particular casein regards to differential sticking. This graph is an extended version of Table 6.5, but its essence is preserved. The similarity score analysis (likelihood-related) is bi-dimensional, i.e., conducted on the "x" and "y" axes while the consequence analysis involving the estimated differential sticking force (overpull) is done in the "z" axis.

The average similarity of a particular target case to free and stuck cases in the database is plotted on the x and y axes respectivelyThe likelihood of differential sticking occurrence increases with the increase of the average similarity to stuck cases and the decrease to free cases. The relative magnitude of the downhole overpull to the drillpipe yield point was the suggested parameter in Chapter 4 to assess the consequence or criticality of a certain drilling scenario in regards to the problem. This property was not evaluated here given the difficulties to precisely determine the grade and material properties of all drillpipes for all cases or to identify the weakest link in the drillstring. The absolute value of overpull is used instead. Regardless of that, the risk increases with the increase of the overpull for a particular drilling scenario.

Previously analyzed stuck cases are plotted in Fig. 8.1. The graph serves as a decision support tool enabling an overall risk analysis through the visualization of the position of the point (case) in regards to likelihood of occurrence, i.e., board of average similarities ("x" and "y" axes), and consequence through the magnitude of the calculated overpull. Traditional approach such as com-

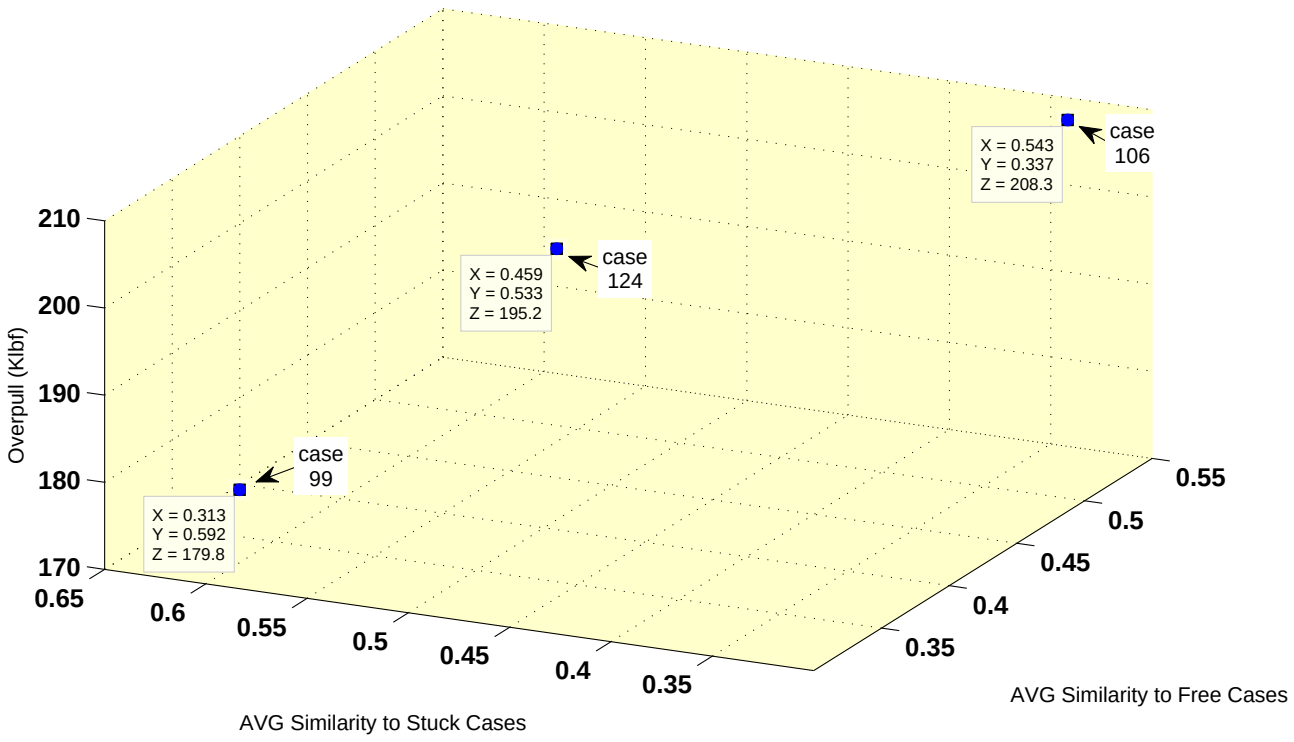

Figure 8.1: 3D Risk Analysis

puting risk as the product between likelihood and consequence can also be implemented. The average similarity to stuck cases can be used as the likelihood score for example. If this criteria is used and the absolute value of overpull is taken as the consequence score, then the following order of risk for the selected cases of differential sticking would have been obtained: case *99* > case *124* > case *1*06. Other risk criteria can be established, but the important fact is that the above 3D risk graph provides the essential elements for the decision maker to assess a certain drilling condition (case in the form of a point in the graph) as risky or not according to its chance to become stuck ("x"and "y" axes) and its severity in case it occurs ("z" axes).

A final analysis is presented in Fig. 8.2using different cases from the same well. The graph shows the higher calculated overpull for the case where the problem occurred. In addition, another important aspect of the proposed risk analysis was revealed: the change in average similarity scores (decrease of average similarity to free cases and increase to stuck cases) for case 106 demonstrated the tendency for differential sticking despite of still presenting a higher absolute average similarity to stuck cases. This example demonstrates a way of tracking the risk while drilling by plotting each case (drilling scenario) as frequently as desired and including them into the historic database as drilling progresses.

It is important to mention that the model predicting overpull does not capture the dynamics of the system, i.e., it is a static model describing part of the system kinematics. Therefore, predicting a certain overpull for a case does not necessarily means that the problem will occur and it should be used as a measure of severity if the problem materializes. Differential sticking is a complex problem and some dynamic factors, like keeping the the drillstring in motion may avoid the problem even in unfavorable operational conditions. Hence, the good estimation of the modulus of the differential sticking force shows its accuracy in predicting the severity of the problem whenever it materializes.

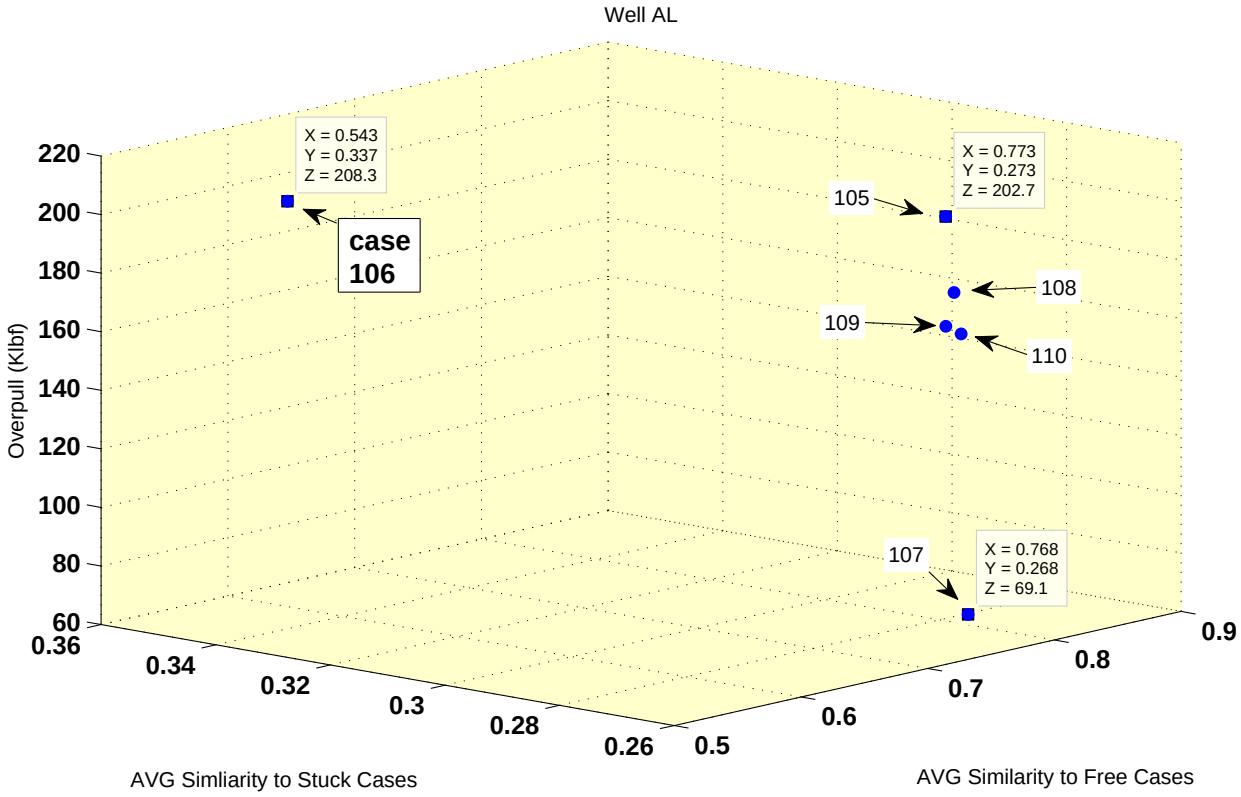

Figure 8.2: 3D Risk Analysis - Well AL

Chapter 9

Conclusions, Observations and Recommendations

1. An innovative theoretical model to quantify the risk of differential sticking was presented and a prototype software designed to execute the model developed. The proposed risk assessment is based on the concept of likelihood versus consequence. The likelihood of the problem's occurrence in a given well segment (case) is evaluated from a knowledge-based model and translated by a similarity score with cases with known outcomes from a historical database. The stand alone module performed satisfactorily and predicts the likelihood of occurrence by more than a chance probability, demonstrated by a successful percentage of 67% of correct predictions against field data from sixty wells drilled from different operators in several fields. The consequence assessment is performed through an unidimensional mechanistic model that predicts the downhole overpull (differential sticking force) and performed well while estimating reported overpulls from known field cases. Together, the models serve as a risk assessment tool able to correctly describe risk operational trends with critical situations being defined as high likelihood plus high potential overpulls. Both models utilizes unique experimental data about mechanical properties of drilling fluids filtercakes under simulated downhole conditions, raised through the HTHP Mudcake Characterization Equipment developed during the course of this research work. The proposed methodology, including models and experimental data, can be adapted to be used in predictions of other drilling problems such as cuttings transport, loss of circulation, torque and drag. Moreover, the study contributes towards the development of modern predictive models aiming at combining large amount of available operational drilling data (LWD,

PWD, mudlogging, survey, drilling reports, etc), expert's knowledge, laboratory data and phenomenological models in order to optimize drilling operations. In fact, the proposed methodology is not only attained to the field of drilling and can be used as a general problem solving scheme.

2. The model is data intensive and its performance directly depends on the availability and quality of data. Particular attention should be paid to the establishment of the historical database of cases. Correlation wells should be converted into cases according to the proposed format and the quality check should start from correctly identifying differential sticking instances and properly documenting its circumstances; a non-trivial task. Standardization and quality check of drilling reports continues to be major hurdles in the path to effective utilization of collected drilling data.

3. A review of the data utilized together with refinements in the configuration of the fuzzy controllers (fuzzy sets, rules and inference methods) and improvement of the analytical module are needed for the present model to become a reliable predictive tool.

4. The presented model is quasi-static, it predicts the risk of differential sticking whenever the drillstring is stopped based on the state of the system derived from past interaction between the drillstring, mudcake and borehole wall.

5. Variables or parameters describing the dynamics of the system should be incorporated into the model.

   (a) Flow rate is an important variable affecting mudcake thickness and quality (mudcake mechanical properties), and to a less extent, the dynamic behavior of the drillstring (vibrations for example). The variable was not used in the model because it was not reliably available nor easily retrievable from the source drilling reports. Moreover, it is fair to state the static growth of mudcakes, for example, provides a conservative approach to risk despite of not correctly reproducing the downhole filtration phenomena. The axial flow erodes the mudcake and an equilibrium thickness, smaller than when formed under static condition, is reached from the so called cross-flow filtration phenomena. Therefore, filtration experiments should be conducted under dynamic conditions (tangential flow to mudcake) and parameters with in situ flow rates incorporated into the estimation of mudcake thickness (the higher the flow rate, the lower the thickness) and

mudcake quality. Thinner mudcakes leading to less interaction with the drillstring or less exposed area would probably result in lower calculated likelihood of occurrence.

(b) The introduction of rotation of the drillstring and parameters reflecting lateral, torsional and axial vibrations of the BHA to the estimate wall contact while drilling could be investigated. Similarly, buckling of the drillstring could also be investigated. This type of study would be relevant in estimating the risk for differential sticking while drilling or to infer about the state of mudcake and wall contact just before connections or other stops. The use of dimension analysis, such as in the work of Tonhauser, coupled with the model presented herein (cased-based reasoning plus fuzzy logic) seems a reasonable starting point.

6. The use of modern Logging While Drilling (LWD) data such as resistivity and Pressure While Drilling (PWD) can be extremely useful to identify high equivalent circulating densities (ECD), i.e., high pressure losses and high bottom hole pressures, tight holes, permeable formations and unusually thick mudcakes or invaded zones. Hence, relevant inputs for estimating mudcake thickness, differential pressure, wall contact and consequently identifying risky zones prior to stops.

7. The identification of depths of overpull while tripping out can certainly aid in improving the accuracy of predictions and further studies should be conducted on how to properly incorporate into the model. The introduction of simple penalty function increasing the likelihood at those depths can be implemented.

8. The ability to learn from past cases and deal with uncertainties of the case-based reasoning module depends on the correct choice of relevant variables (or parameters and sub-models) describing the target phenomenon and correct settings of weights translating their relative importance in the similarity metric. This work went beyond practices of establishing these weights purely on expert's opinion and proposed a rigid mathematical method instead. However, further studies should be performed on how often the weights in Eq. 6.5 should be optimized and how to improve the proposed mathematical technique. Techniques such as support vector machines appears as promising platforms of improvements.

9. Studies to develop relevance criteria in regards to the use of data in the case-based reasoning module, such as age of wells and field, in order to update the historical database of cases should be conducted.

10. Information about the actions taken to free stuck pipe could be incorporated to the database as a first stage to turn the model into a case-based reasoning advisory system.

11. Further studies about the precision, accuracy and resolution of the model should be conducted while planning development wells within a mature field. Moreover, the same study should be performed while drilling. Such studies would expose limiting factors for the use of the method as a real-time model.

12. The knowledge-based (case-based reasoning) model requires to be expanded in regards to number and nature of variables in order to improve its rate of successful predictions. This includes a better and more comprehensive analysis of the mechanical behavior of mudcakes. Ideally, the experiments should be incorporated into routine field tests.

13. The proposed hardness index from the curve of axial force versus penetration depth proved to be a more adequate parameter to express hardness of complex layered materials such as mudcakes when compared to traditional Vickers hardness definition that is taken at a given penetration depth. The index is equivalent to the non-Newtonian behavior index of pseudo-plastic drilling fluids. Further studies should be conducted

14. Further studies should be conducted in order fully utilize the loading and unloading parts of the curve to extract relevant average mechanical properties such as Young's Modulus. Such parameters are vital for numerical simulations on the mechanical behavior of mudcakes in contact with the drillstrings.

15. While the maximum observed reactive torque in the experiments was used as the relevant variable to assess the quality of the mudcake in regards to differential sticking, the post-peak plateau is associated with sliding torsional friction and is relevant to torque and drag studies.

16. Further studies should be performed at different angular velocities and oscillatory mode. These experiments will reveal different failure modes of the torsional strength of mudcakes, possibly leading to improved field procedures to free the drillstring. The HPHT MCCE is already capable of

performing these tests. These studies are also important for a more comprehensive understanding of the viscoelastic properties of mudcakes.

17. Similarly, additional aspects of the adhesion-cohesion curve (pull experiments) the slopes of the pull and relaxation curves at different pull rates should be better investigated.

18. Although pressure was successfully used as the correlation variable between bench-scale experiments and field, factors related to the different geometries and end effects should be further investigated.

19. Variations in friction factor significantly affect the magnitude of the overpull and data from field pull tests should be used whenever available. In addition it should be used to better evaluate the model.

20. Further studies should be conducted to better investigate the range of critical values of average similarity score. Such studies are necessary to establish more realistic risk thresholds for average similarities to free and stuck cases in a particular historical database and consequently improve the use of the 3D risk analysis graphs. Further studies could also lead to improved alternatives to express risk as the product of likelihood and consequence.

Chapter 10

Nomenclature

Roman Letter

A: area $[L^2]$

- A: generic fuzzy set $[-]$
- a: degree of membership function $[-]$
- b: degree of membership function $[-]$
- B: generic fuzzy set $[-]$
- CF: clearance factor $[-]$
- Cl: clearance $[L]$
- D: diameter $[L]$
- d: chord on the drillstring cross sectional area $[L]$
- E: Young's Modulus $[M \cdot L^{-1} \cdot T^{-2}]$
- F: force $[M \cdot L \cdot T^{-2}]$
- G: generic function $[-]$
- g: gravity acceleration $[L \cdot T^{-2}]$
- H: generic fuzzy set $[-]$
- h: length of the drillstring in contact with the borehole wall $[L]$
- I: area moment of inertia $[L^4]$
- IF: inclination factor $[-]$
- L: length $[L]$
- m: mudcake thickness $[L]$
- n: counter $[-]$
- P: pressure $[M \cdot L^{-1} \cdot T^{-2}]$
- p: integer $[-]$
- S: similarity $[-]$
- S: generic space $[-]$
- TSF: tool shape factor $[-]$

w: unit weight $[M \cdot T^{-2}]$
w: weight $[M \cdot L \cdot T^{-2}]$
w: weights of variables in the similarity metric []
x: generic length $[L]$
y: deflection $[L]$
Z: auxiliary parameter $[L]$

Greek Letters

α: angle $[rad]$
β: buoyancy factor $[-]$
Δ: difference or variation $[-]$
μ: friction factor $[-]$
δ: indenter or drillstring penetration depth $[L]$
θ: angle $[\mathrm{deg}]$
ϕ: nil set $[-]$
Ω: generic space $[-]$
ρ: density $[M \cdot L^{-3}]$

Subscripts

avg: average
as: after stabilizer
o: outer
i: inner
BHA: BHA
$crit$: critical
$drag$: drag
ds: drillstring
eff: effective
exp: experimental
$fluid$: fluid
g: groove
$guess$: guess
i: indicates the linguistic variable
j : indicates the term of the linguistic variable

mf: membership function
MAX: maxim
new: new
seg: segment (set of components connected together)
$tool$: tool or component of BHA
tg: tangency
$total$: total
w: well
v: the numeric value of the variable

Bibliography

[1] Vickers hardness test. worldwide web, December 2011.

[2] Skalle, P. ; Aamodt, A. ; Sveen, J. Case-based reasoning, a method for gaining experience and giving advise on how to avoid and how to free stuck drill strings. In *IADC Middle East Drilling Conference*, Dubai, UAE, November 1998.

[3] Berg, K. Aadnoy, P.C. , Larsen, B. S. . Analysis of stuck pipe in deviated boreholes. *Journal of Petroleum Science and Engineering*, 37:195–212, 2003.

[4] Visconti, F.; Allen, T. Gulf of mexico trouble time creates major drilling expenses. Offshore Magazine, January 2004. vol.64, issue 1.

[5] Clark; R.K.; Almiquist; S.G. Evaluation of spotting fluids in a full-scale differential sticking apparatus. In *SPE Annual Technical Conference and Exhibition, Dallas*, number SPE 22550, October 1991.

[6] Amanullah, Md. Experimental determination of adhesive-cohesive bond strengh (acbs) and adhesion-cohesion modulus (acm) of mudcakes. In *IADC/SPE Asia Pacific Drilling Technology*, number SPE 77198, Jakarta, September 2002.

[7] Amanullah, Md. Experimental determination of adhesive-cohesive bond strengh (acbs) and adhesion-cohesion modulus (acm) of mudcakes. In *IADC/SPE Asia Pacific Drilling Technology*, number AADE 01-NC-HO-52, Houston, USA, March 2002.

[8] Amanullah, Md. Experimental determination of the variation of torsional resistance of mudcakes with the variation of mud and mudcake composition. In *SPE Asia Pacific Oil and Gas Conference and Exhibition*, number SPE 88450, October 2004.

[9] Nikravesh, M. ; Aminzaadeh, F. . Mining and fusion of petroleum data with fuzzy logic and neural nework agents. *Journal of Petroleum Science and Engineering*, 29:221–238, 2001.

[10] Aadnoy, B. S. ; Andersen, K. Friction analysis for long-reach wells. In *IADC/SPE Drilling Conference*, number IADC/SPE 39391, Dallas, USA, March 1998.

[11] Millheim, K. K.; Apostal, M. C. The effect of bottomhole assembly dynamics on the trajectory of a bit. *Journal of Petroleum Technology*, pages 2323–38, December 1981.

[12] Barree, R.D. ; Conway, M.W. . Beyond beta factors: A complete model for darcy, forchheimer and trans-forchheimer flow in porous media. In *SPE Annual Technical Conference and Exhibition*, number SPE 89325, Houston, USA, September 2004.

[13] Martins, A. L. ; Massarani, G. ; Waldmann, A.T.A. ; Costa, F.G. . On the rheological mechanisms governing drill-in fluid invasion into reservoir rocks. In *SPE European Formation Damage Conference*, number SPE 82275, The Hague, The Netherlands, May 2003.

[14] Fletcher, A. ; Davis, P.J. Decision-making with incomplete evidence. In *SPE Asia Pacific Oil and Gas Conference and Exhibition*, number SPE 77914, Melbourne, October 2002.

[15] Tsakonas, A. ; Dounias, G. Hybrid computational intelligence schemes in complex domains: An extended review. In *SETN '02 Second Hellenic Conference on AI: Methods and Applications of Artificial Intelligence: Methods and Applications of Artificial Intelligence*, number ISBN:3-540-43472-0, pages 325–334, 2002.

[16] Lomba, R. F. T.; Martins, A. L.; Soares, C. M.; Brandão E. M.; Magalhães, J. V. M.; Ferreira, M. V. D. Drill-in fluids: Identifying invasion mechanisms. In *SPE International Symposium and Exhibition on Formation Damage Control*, number SPE 73714, Lafayette, Louisiana, February 2002.

[17] Fisher-Cripps, A.C. A review of analysis methods for sub-micron indentation testing. *Vacuum*, 58:569–585, April 2000.

[18] Goldberg, D.E. *Genetic Algorithms in Search. Optimisation, and Machine Learning.* Addison-Wesley, 1989.

[19] Hempkins, W.B. Multivariate statistical analysis in formation evaluation. In *48th Annual California Regional Meeting of the SPE of AIME*, number SPE 7144, San Francisco, USA, April 1978.

[20] Durst F. ; Haas, R. ; Interthal, W. . The nature of flows through porous media. *Jornal of Non-Newtonian Fluid Mechanics*, 22:169–189, 1987.

[21] Kosko, B. *Neural networks and fuzzy systems. A dynamical approach to machine intelligence*. Prentice Hall, New Jersey, 1992.

[22] Kosko, B. *Fuzzy Engineering*. Prentice Hall, New Jersey, 1997.

[23] Krol, D.A. Addtives cut differential pipe sticking of drillpipes. *Oil and Gas Journal*, 55, 1984.

[24] Biegler, M.W.; Kuhn, G.R. Advances in prediction of stuck pipe using multivariate statistical analysis. In *IADC/SPE Drilling Conference*, number IADC/SPE 27529, Dallas, USA, February 1994.

[25] Garrouch, A.A. ; Labadidi, H.M.S. Development of an expert system for underbalanced drilling using fuzzy logic. *Journal of Petroleum Science and Engineering*, 31:23–39, July 2001.

[26] Lee, T. ; Cao, Y. ; Lin, Y. . The applications of a time-domain fuzzy logic controller for dynamic positioning of floating structures. *Tamkang Journal of Science and Engineering*, 5(3):137–150, 2002.

[27] Lins, I. D. *Support Vector Machines and Particle Swarm Optimization Applied to Reliability Prediction*. PhD thesis, Universidade Federal de Pernambuco, 2009.

[28] Nascimento, R. C. A. M.; Amorim, L. V.; Lira, D. S.; Lira, H. L. O fenômeno de prisão diferencial: Uma revisão da literatura (in portuguese). *Revista Eletrônica de Materiais e Processos, REMAP*, v.5.2(ISSN 1809-8797):76–87, 2010. free access on www.dema.ufcg.edu.br/revista.

[29] Martins, A. L. ; Waldmann, A.T.A. ; Aragao, A.F.L. ; Lomba, R.F.T. Predicting and monitoring fluid invasion in exploratory drilling. In *SPE International Symposium and Exhibition on Formation Damage Control*, number SPE 86497, Lafayette, USA, February 2004.

[30] Helmick, W.E; Longley, A.J. Pressure differential sticking of drill pipe and how it can be avoided or relieved. *Oil and Gas Journal*, 132, 1957.

[31] Miri, R. ; Sampaio, J. ; Lourenco, A. Development of artificial neural networks to predict differential sticking in iranian offshore oil fields. In *International Oil Conference and Exhibition in Mexico*, number SPE 108500, Veracruz, Mexico, June 2007.

[32] Isambourg, P. ; Ottensen, S. ; Benaissa, S. ; Marti, J. Down-hole simulation cell for measurement of lubricity and differential pressure sticking. In *SPE/IADC Drilling Conference*, number 52816, Amsterdam, Holland, March 1999.

[33] De Souza, D. A. F.; Elias, R. N. ; Alves, J. L. D.; Landau, L.; Coutinho, A. L. G. A.; Lomba, R. F. T.; Martins, A. L. Modelagem computacional da prisão diferencial da coluna de perfuração em poços não convencionais (in portuguese). In *4º Seminário Brasileiro de Simulação Computacional na Engenharia/SOFTEC*, November 2003.

[34] Underhill, W.B.; Moore, L.; Meeten, G.H. Model-based sticking risk assessment for wireline formation testing tools in the u.s. gulf coast. In *SPE Annual Technical Conference and Exhibition*, number SPE 48963, September 1998.

[35] Mendes, J.R.P. *Raciocínio Baseado em Casos Aplicado ao Projeto de Poços de Petróleo*. PhD thesis, Universidade de Campinas, 2001. in Portuguese.

[36] Fisher K.A.; Wakeman, R.J.; Chiu, T.W.; Meuric, O.F.J. Numerical modeling of cake formation and fluid loss from non-newtonian muds during drilling using eccentric/concentric drill strings with/without rotation. *Trans IchemE*, 78(A):707–714, July 2000.

[37] Annis, M.R.; Monaghan, P.H. Differential pressure sticking - laboratory studies of friction between steel and mud filter cake. *Journal of Petroleum Technology; Trans. AIME*, 537:225, May 1962.

[38] Mooney, M. "explicit formulas for slip and fluidity". *Journal of Rheology*, pages 210–222, 1931.

[39] Hempkins, W.B.; Kingsborough, R.H.; Lohec, W.E.; Nini, C.J. . Multivariate statistical analysis of stuck drillpipe situations. *SPE Drilling and Completion*, pages 237–244, September 1987.

[40] Magaji, M. A.; Amoo, A. O.; Owoeye, O. O.;. An innovative approach to stuckpipe reduction in the niger delta. In *IADC/SPE Drilling Conference*, number IADC/SPE 74523, February 2002.

[41] Bushnell-Watson; Y.M.; Panesar; S.S. Differential sticking laboratory tests can improve mud design. In *SPE Annual Technical Conference and Exhibition, Dallas*, number SPE 22549, October 1991.

[42] Peng, S.J. ; Peden, J. . Prediction of filtration under dynamic conditions. In *Symposium on Formation Damage Control*, number SPE 23824, Lafayette, USA, February 1992.

[43] Arthur, K.G. ; Peden, J. M. The evaluation of drilling fluid filter cake properties and their influence on fluid loss. In *SPE International Meeting of Petroleum Engineering*, number SPE 17617, Tianjin, China, November 1988.

[44] O'Keefe, R.M. ; Preece, A.D. The development, validation and implementation of knowledge-based systems. *European Journal of Operational Research*, 92, 1996.

[45] Rabinowitsch, B. Z. *Physik. Chem.*, 1(145A), 1929.

[46] Metzner, A. B. ; Reed, J. C. "flow of non-newtonian fluids: Correlation of the laminar, transition, and turbulent-flow regions". *A.I.Ch.E. J.*, 1955.

[47] Siruvuri, C ; Nagarakanti, S ; Samuel, R. Stuck pipe prediction and avoidance: A convolutional neural network approach. In *IADC/SPE Drilling Conference*, volume IADC/SPE 98378, Miami, USA, February 2006.

[48] Reid, P.I.; Meeten, G.H; Way, P.W.; Clark, P.,; Chambers, B.D.; Gilmour, A.; Sanders, M.W.;. Differential-sticking mechanisms and a simple wellsite test for monitoring and optimizing drilling mud properties. *SPE Drilling and Completion*, 15(2):189–192, June 2000.

[49] STATSOFT. Statistica electronic textbook. world wide web by STATSOFT Inc., February 2006.

[50] Amanullah, Md. ; Tan, C. P. Embedment modulus of mudcakes: Its drilling engineering significance. In *AADE 2001 National Drilling Conference Drilling Technology: The Next 100 years*, number AADE 01-NC-HO-52, Houston, USA, March 2001.

[51] Thonhauser, G. *Cuttings Transport Simulation and Monitoring for Extended Reach Wells*. PhD thesis, University of Leoben, 1998.

[52] Stamatakis, K.; Tien, C. A simple model of cross-flow filtration based on particle adhesion. *AIChe*, 39(8), August 1993.

[53] Walker, H. B. Downhole assembly design increases rop. *World Oil*, pages 59–65, June 1977.

[54] Jones, D.M. ; Walters, K. . The behavior of polymer solutions in extension-dominated flows, with applications to enhanced oil recovery. *Rheologica Acta*, 28:482–498, 1989.

[55] Chesser, B.G.; Clark, D.E.; Wise, W.V. Dynamic and static filtrate-loss techniques for monitoring filter-cake quality improves drilling-fluid performance. *SPE Drilling and Completion*, pages 189–192, September 1994.

[56] Prassl, W.F. ; Peden J.M. ; Wong, K.W. . A process-knowledge management approach for assessment and mitigation of drilling risks. *Journal of Petroleum Science and Engineering*, 49:142 –161, 2005.

[57] Bourgoyne, Jr. A.; Millheim, K. K.; Chenevert, M. E.; Young, Jr. F.S. *Applied Drilling Engineering*, volume 2 of *SPE Textbook*. Society of Petroleum Engineers, Richardson, TX, 1986.

[58] Roark, R. J.; Young, W. C. *Formulaes for Stress and Strain*. McGraw-Hill, 5th edition, 1975.

Every reasonable effort has been made to acknowledge the owners of copyright material. I would be pleased to hear from any copyright owner who has been omitted or incorrectly acknowledged.

Appendix A

HPHT MCCE

A.1 General Experimental Stages

1. Prepare a maximum of 500 ml of a water-based drilling fluid.
2. Pour the drilling fluid into the filtration cell.
3. Place the L-bar penetrometer's L-shape foot facing inwards.
4. Place and secure the top cap onto the filtration cell.
5. Start Data Acquisition System (hardware and software).
6. Drive the load frame base downwards to zero position, i.e., bottom.[1]
7. Pull the T-block to fully extend the shaft and hold it. Drive the load frame upward until it connects the top cap shaft (T-block) with the rotating steel shaft. It should read 24mm on the load frame's base rule and the base's handle should touch the end of the LVDT. This is the Zero Filtration Vessel position.
8. Connect top cap DAQ plug with the DAQ board via the pin connection.
9. Insert thermometer in the top cap thermometer casing.
10. Slot the L-bar rod into the L-bar driving copper rod. Use the driving system to bring the cooper rod down. Secure it in place via the two provided screws. Mind the position of the L-bar foot and avoid bending the rod.
11. Drive the L-bar until the bottom of the Filtration Vessel. This reading is the Zero L-bar position.

[1] **Note that it is the pressure vessel that moves during the test and not the indenter.**

12. Position the L-bar penetrometer within the safe zone between the bottom and load/torque cell cup (use the indenter's spreadsheet).

13. Pressurize the filtration cell to the desired test pressure and measure the maximum traveling distance for the hemispherical indenter. This step is performed due to possible minor deformations of the mesh-filter paper stack that may occur under elevated pressures. See Table C-1 as reference.

A.1.1 Hardness

1. Go through the common steps section.

2. Pressurize the filtration cell to the desired test pressure, (while performing experiments at elevated temperatures, it is recommended to initially set the filtration cell pressure to 50 psi lower than the desired pressure. Adjust the pressure after heating is complete.

3. Increase the filtration cell temperature to the desired set point.

4. Wait 10-15 minutes until steady state.

5. Start filtration via opening filtration valve.

6. Wait for desired time or filtration volume or mudcake thickness.

7. Drive the L-bar penetrometer and monitor load to estimate mudcake thickness. Do not exceed the load capacity of the L-bar while moving the L-bar. In addition, maintain low speeds to avoid overload of the same load cell whenever the mudcake surface is reached.

8. Calculate hemispherical foot distance from the bottom using the indenter's spreadsheet. Drive the filtration cell towards the hemispherical indenter under a desired speed and monitor closely the load profile versus cell displacement.

9. Mind maximum load and cell displacement.

10. Pull out of the drilling fluid mudcake and/or perform a torque test before pulling out. Note: If excessive load or torque is observed during the test, remove the indenter slowly from the mudcake until the abnormal reading ceases. If the abnormal reading continues and it is severe - sudden increase of pull for example -, close the filtration valve. The filtration pressure can also be decreased to stop this behavior. It is common

to experience a tensile force if the indenter is too close to the porous medium. It is actually due to the occurrence of the differential sticking force or phenomenon. This is valuable data and this step can be considered an experiment itself to measure the magnitude of the differential sticking force and its rate of growth as a function of the distance to the bottom (permeable medium).

11. Perform steps 1 to 11 as many times as desired and under any desired embedment velocities.
12. Close the filtration valve.
13. Stop logging and save data. Keep reading, i.e., displaying data.
14. Wait for the system to cool down.
15. Depressurize and disassemble the MCCE.

A.1.2 Torque

1. Go through the common steps section.
2. Place the indenter within the expected mudcake formation zone. A minimum gap of 1mm from the bottom should be respected.
3. The torque motor should be OFF and initially set to Brake/BRK. The Reverse/REV switch rotates the system anti clockwise and the Forward/ FWD clockwise.
4. Rotate the stainless steel shaft anticlockwise by using the rotation speed control knob until the T-junction reaches a minimum distance from the thermometer's well assembly.
5. Pressurize the filtration cell to the desired test pressure, (while performing experiments at elevated temperatures, it is recommended to initially set the filtration cell pressure to 50 psi lower than the desired pressure. Adjust the pressure after heating is complete.)
6. Increase the filtration cell temperature to the desired set point.
7. Wait 10-15 minutes until steady state.
8. Start filtration via opening filtration valve.
9. Wait for desired time or filtration volume or mudcake thickness.

10. Drive the L-bar penetrometer and monitor load to estimate mudcake thickness. Do not exceed the load capacity of the L-bar while moving the L-bar. In addition, maintain low speeds to avoid overload of the same load cell whenever the mudcake surface is reached.

11. Preset the rotation speed to zero in the torque motor speed controller. Slowly increase the rotation speed knob until a torque and/or angular speed reading is detected. Note: If excessive load or torque is observed during the test, remove the indenter slowly from the mudcake until the abnormal reading ceases. If the abnormal reading continues and it is severe - sudden increase of pull for example -, close the filtration valve. The filtration pressure can also be decreased to stop this behavior. It is common to experience a tensile force if the indenter is too close to the porous medium. It is actually due to the occurrence of the differential sticking force. This is valuable data and this step can be considered an experiment itself to measure the magnitude of the differential sticking force and its rate of growth as a function of the distance to the bottom (permeable medium).

12. Stop rotation once the T-junction block reaches its maximum traveling distance and always mind the torque limit of the sensor.

13. Repeat steps 8 to 10 as many times as desired minding the initial position of the T-junction block (it defines the direction of rotation) and the filtrate volume. Note: The experiment can be conducted at any desired angular velocity and not necessarily as described in step 11. Experiments with oscillatory motion can also be performed.

14. Close the filtration valve.

15. Stop logging and save data. Keep reading, i.e., displaying data.

16. Wait for the system to cool down.

17. Depressurize and disassemble the MCCE.

A.1.3 Adhesion-Cohesion

1. Go through the common steps section.

2. Place the indenter within the expected mudcake formation zone. A minimum gap of $1mm$ from the bottom should be respected.

3. Pressurize the filtration cell to the desired test pressure. While performing experiments at elevated temperatures, it is recommended to initially set the filtration cell pressure to 50 psi lower than the desired pressure. Adjust the pressure after heating is complete.
4. Increase the filtration cell temperature to the desired set point.
5. Wait 10-15 minutes until steady state.
6. Start filtration via opening filtration valve.
7. Wait for desired time or filtration volume or mudcake thickness.
8. Drive the L-bar penetrometer and monitor load to estimate mudcake thickness. Do not exceed the load capacity of the L-bar while moving the L-bar. In addition, maintain low speeds to avoid overload of the same load cell whenever the mudcake surface is reached.
9. Drive the filtration cell away from the indenter by using the load frame until a maximum tensile force is observed or load cell limit is reached. Same note about excessive load or torque readings as in step 11 of torque test should be observed.
10. Mind maximum pull load.
11. Close the filtration valve.
12. Stop logging and save data. Keep reading, i.e., displaying data.
13. Wait for the system to cool down.
14. Depressurize and disassemble the MCCE.

The above experiments enable the assessment of mechanical properties of mudcakes under elevated temperature and pressure conditions. In addition, the experiments described above can be combined, i.e., performed sequentially. The operator can establish any desired sequence to simulate a particular operational scenario or downhole condition. Figures A.1a to A.1d illustrates the main steps of a possible experimental run composed by the following sequence: torque test, followed by a adhesion-cohesion test and finalized by a hardness test.

It is important to say that the above sequence is one of many possible experimental sequences, including, obviously, the possibility of running each test separately. During experiments, the hardness tests were conducted separately. Torque and pull experiments were conducted sequentially.

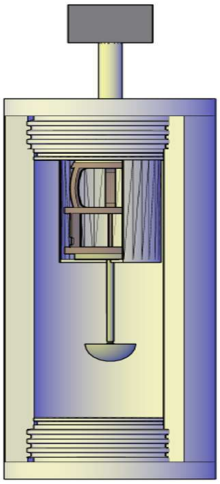

(a) Step 1 - Start

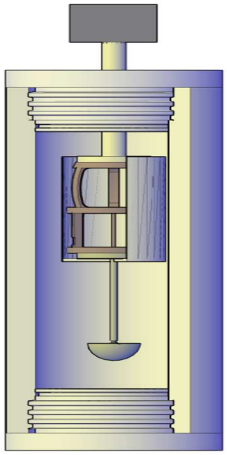

(b) Step 2 - Lowering Indenter.

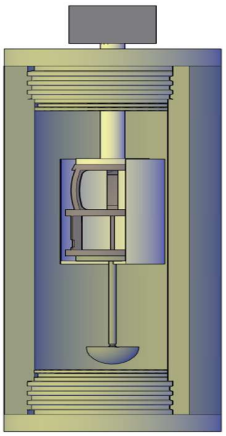

(c) Step 3 - Near Bottom Position.

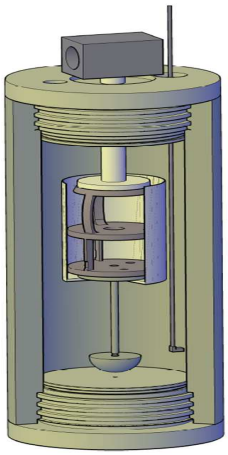

(d) Step 4 - L-bar Positioned Above Mudcake Maximum Thickness.

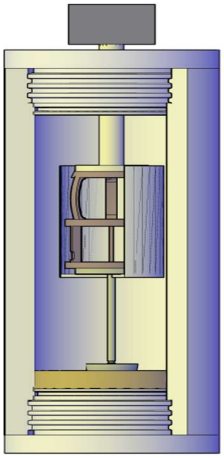

(e) Step 5 - Mudcake Growth.

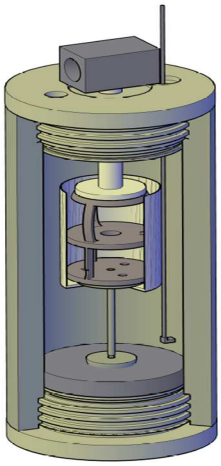

(f) Step 6 - Measure Mudcake Thickness Prior to Torque Test.

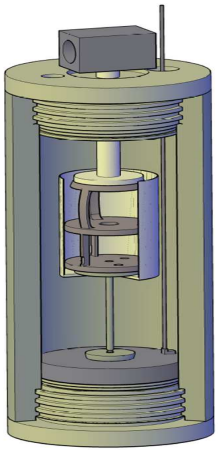

(g) Step 7 - L-bar on Top of Mudcake.

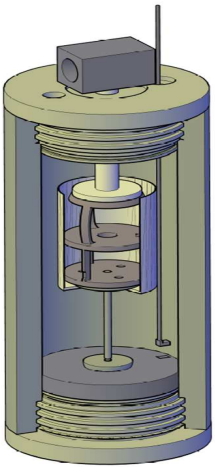

(h) Step 8 - L-bar Lifted.

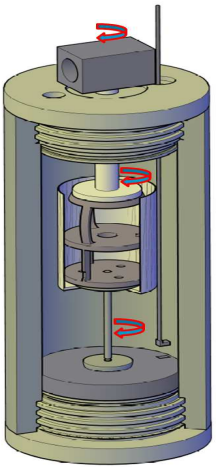

(i) Step 9 - Torque Test.

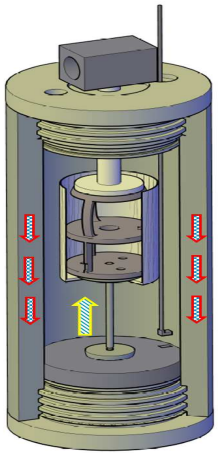

(a) Step 10 - Pull Test.

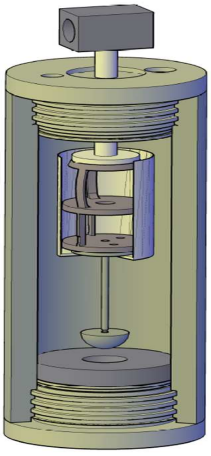

(b) Step 11 - Configuration after Pull Test .

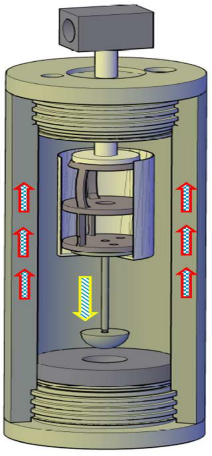

(c) Step 12 - Hardness Test; Embedment.

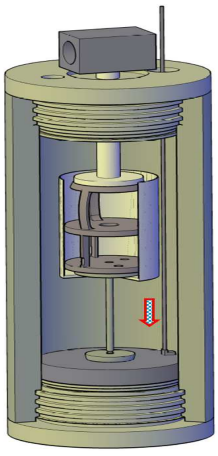

(d) Step 13 - End of Run with Final Thickness Measurement.

A.2 Experimental Matrix and Results

Table A.1: Mudcake Experiments

Experiment	**Test Pressure** (psi)	**Bentonite** (ppb)	**Viscosity Agent**	**Polymer** (ppb)	**Carbonate** (ppb)	**Barite** (ppb)	**Solids** (ppm)
Bentonite 01	1000	23	BENT	NA	NA	NA	64.286
Bentonite 01b	500	23	BENT	NA	NA	NA	64.286
Bentonite-Barite	500	23	BENT	NA	NA	200	637.143
Bentonite-Barite 01	1000	23	BENT	NA	NA	200	637.143
Carbonate 01	1000	NA	PHPA	4.0	30	NA	97.142
Carbonate 01b	500	NA	PHPA	4.0	30	NA	97.142
Carbonate 02	1000	NA	PHPA	4.0	50	NA	154.286
Carbonate 02b	500	NA	PHPA	4.0	50	NA	154.286
Carbonate 04	500	NA	XC	2.6	50	NA	150.286
Carbonate 05	1000	NA	XC	1.2	50	NA	146.285
Carbonate 06	500	NA	PHPA	5.6	50	NA	158.857
Carbonate-Barite 01-3	500	NA	PHPA	4	30	200	668.571

NA: Not Applicable, NR: Not Raised.

* All Polymer-Carbonate Drilling Fluids were prepared in a 20 ppb KCl solution and all Bentonite Drilling Fluids in a 35 ppb NaCl solution.

* Ratio calculated from non-reported tests at 1000 psi. Only filtration data were used for the non-reported tests.

** Estimated, embedment was not performed.

Experiment	**Test Pressure** (psi)	**Bentonite** (ppb)	**Viscosity** Agent	**Polymer** (ppb)	**Carbonate** (ppb)	**Barite** (ppb)	**Solids** (ppm)
AVGLP1	100	NA	PHPA	5.6	50	NA	142,857
AVGLP2	100	NA	PHPA	4.0	30	NA	85,714
AVGLP3	100	NA	PHPA	4.0	50	NA	142,857
LP4	100	NA	PHPA	4.0	60	NA	171,428
LP5	100	NA	XC	1.9	50	NA	142,857
AVGLP6	100	NA	XC	4.0	50	NA	142,857
LP7	100	NA	PHPA	4.0	60	200	742,856
AVGLP8	100	NA	PHPA	4.0	30	200	657,142
AVGF	100	NA	**XC (STARCH+CMC)**	NA	30	NA	85,714

Experiment	**Density** (ppg)	**Mudcake Thick-ness (L-bar)** (mm)	**L3** RPM	**L6** RPM	**L100** RPM	**L200** RPM	**L300** RPM	**L600** RPM
Bentonite 01	8.52	6.40	13	14	18	20	22	27
Bentonite 01b	9.05	2.40	30	34	40	50	52	58
Bentonite-Barite	11.5	7.00	30	32	37	40	43	52
Bentonite-Barite 01	10.38	7.40	25	30	37	40	41	47
Carbonate 01	9.10	3.00	5	7	22	31	38	54
Carbonate 01b	9.00	5.50	3	4	21	30	36	52
Carbonate 02	9.30	2.00	3	4	22	31	38	54
Carbonate 02b	9.30	6.00	3	5	24	34	40	53
Carbonate 04	9.25	2.80	18	20	32	38	44	54
Carbonate 05	9.20	4.56	5	6	12	15	18	24
Carbonate 06	9.28	2.98	5	8	32	44	53	73
Carbonate-Barite 01-3	11.79	6.20	5	7	33	45	55	78

Experiment	**Density** (ppg)	**Mudcake Thick-ness (L-bar)** (mm)	**L3** RPM	**L6** RPM	**L100** RPM	**L200** RPM	**L300** RPM	**L600** RPM
AVGLP1	9.00	NA	5	8	33	47	57	80
AVGLP2	9.00	NA	3	4	20	29	37	53
AVGLP3	9.00	NA	3	4	20	29	37	53
LP4	9.00	NA	3	4	20	29	37	53
LP5	9.00	NA	10	11	20	25	28	37
AVGLP6	9.00	NA	33	36	53	61	67	81
LP7	9.00	NA	3	4	20	29	37	53
AVGLP8	9.00	NA	3	4	20	29	37	53
AVGF	9.00	NA	4	5	18	25	31	46

Experiment	Visual Mudcake Thickness (mm)	API Filtrate (30 min) (ml)	API 1000/API 500	Torque Resistance (Max Torque / Indenter Superf. Area) (N/m)	Adhesive Strength (Max Pull / Indenter Superf. Area) (N/m^2)	Hardness Index s	Pressure Index H_p $(\frac{psi}{\exp^{spmm}})$	Pressure Index s_p
Bentonite 01	11.9	62	0.72	4	2,876	0.56	0.183	0.356
Bentonite 01b	9.3	45	0.72	200	257,210	2.24**	NR	NR
Bentonite-Barite	12.5	57	1.78	219	85,499	1.85	0.217	1.230
Bentonite-Barite 01	14.4	102	1.78	52	56,017	0.75	0.038	0.747
Carbonate 01	4.0	344	2.58	402	67,563	48.86	229	23.470
Carbonate 01b	3.7	134	2.58	2	866	14.58	$5E-9$	13.800
Carbonate 02	7.7	233	1.25	137	30,937	36.65**	NR	NR
Carbonate 02b	6.9	186	1.25	177	33,433	10.94**	NR	NR
Carbonate 04	2.0	8	4.67	1.018	192,478	17.59	0.177	12.850
Carbonate 05	3.2	35	NA	16	27,788	61.27	0.141	51.800
Carbonate 06	2.3	3	0.20*	28	45,690	18.32	0.0004	16.420
Carbonate-Barite 01-3	7.6	3	1.33*	27	24,843	7.89	0.471	5.710

Experiment	Visual Mudcake Thickness (mm)	API Filtrate (30 min) (ml)	API 500/API 100	Torque Resistance (Max Torque / Indenter Superficial Area) (N/m)	Adhesive Strength (Max Pull / Indenter Superficial Area) (N/m^2)	Hardness Index s	Pressure Index H	Pressure Index s
AVGLP1	7.0	71	0.04	46.9	1,300	1.26	0.30	0.57
AVGLP2	4.0	49	2.72	158.0	1,278	3.69	0.27	2.30
AVGLP3	6.4	88	2.11	45.1	1,463	1.95	0.21	1.00
LP4	8.7	110	1.69	37.5	1,610	1.55	0.70	0.65
LP5	4.0	27		54.6	4,931	4.02	0.52	1.16
AVGLP6	4.0	13	0.58	22.5	2,123	1.53	0.09	0.90
LP7	5.0	15	0.20	21.7	700	0.36	0.09	0.19
AVGLP8	10.0	23	0.13	2.2	345	0.78	0.09	0.17
AVGF	3.5	10	0.35	2.1	1,049	2.21	0.35	0.64

Appendix B

Tables of Results - Raw Drilling Input Data

B.1 Input Data

The following tables summarize the raw drilling database. Blank cells are missing or not raised information. In those cases, variables were not directly used by the model or simply served as guidance or base for establishing range of variables for the experimental program.

Table B.1: Raw Input Data

Well ID	Case	Status(0 = Stuck)	Training Set	Test Set	Segment Top MD (m)	Segment Bottom MD (m)	Segment Top TVD (m)	Segment Bottom TVD (m)	$D_{well}(m)$
A	1	1	1	0	500	2028	500	1802	17.50
A	2	0	1	0	2028	3638	1802	2934	12.25
B	3	0	1	0	4790	4855	2889	2913	12.25
C	4	0	1	0	3205	3310	2207	2245	6.00
D	5	0	1	0	2707	2720	1938	1940	12.25
E	6	0	1	0	1619	1793	1618	1788	12.25
F	7	0	0	1	2511	2695	2264	2416	12.25
F	8	1	0	1	2695	2709	2416	2427	12.25
F	9	1	0	1	2709	2831	2427	2625	12.25
F	10	1	0	1	2831	3515	2625	3175	12.25
F	11	1	1	0	3515	3546	3175	3206	8.00
F	12	1	0	1	3546	3627	3206	3285	8.50
F	13	1	0	1	3627	4119	3285	3774	8.50
F	14	1	1	0	4119	4250	3774	3905	8.50
G	15	1	0	1	2588	2810	2587	2807	12.25
H	16	0	0	1	1026	2255	1026	2255	12.25

Well ID	Case	$D_{oavg}(in)$	Average Inclination (°)	Mud Density (ppg)	Mud Type	600 RPM (°)	300 RPM (°)	200 RPM (°)	100 RPM (°)	6 RPM (°)	3 RPM (°)
A	1	7.71	25.7	9.1	WBM XC	75	56		37	17	15
A	2	6.53	45.3	9.8	SYNTH	95	63		34	14	13
B	3	6.37	67.7	9.8	SYNTH	125	85		52	21	20
C	4	3.67	69.8	9.6	SYNTH	85	60		39	16	15
D	5	5.65	78.3	10.6	WBM XC	86	61		40	21	18
E	6	7.00	11.5	10.6	WBM PHPA	55	41		26	14	12
F	7	5.94	35.3	10.1	WBM PHPA	68	53			13	10
F	8	6.40	31.3	10.1	WBM PHPA	71	55			13	11
F	9	6.11	28.3	10.1	WBM PHPA	70	53			13	11
F	10	6.40	20.2	10.2	WBM PHPA	71	54			13	11
F	11	6.09	11.9	10.9	WBM PHPA	65	48			13	11
F	12	5.44	10.3	11.6	WBM PHPA	63	45			12	10
F	13	5.44	7.6	14.2	WBM PHPA	69	48			14	11
F	14	5.39	0.0	15.4	WBM PHPA	78	55			22	16
G	15	6.22	6.3	10.0	WBM PHPA	60	43			11	8
H	16	6.27	1.2	9.8	WBM PHPA	39	25			6	5

Well ID	Case	Gel 10s $(lbf/100ft^2)$	Gel 10min $(lbf/100ft^2)$	Solid (ppm)	Total Open Hole Time (h)	Average Differential Pressure (psi)	Mudcake Thickness (mm)	Total Open Hole Time (h)	Trouble Time (h)	MAX dog leg severity $(deg/100ft)$
A	1	18.20	34.17	103875	66	85	4	66.25		0.06
A	2	14.00	21.00	103875	101	396	2.8	100.5	6.25	0.16
B	3	21.00	38.00	103875	462	516	2.8	461.75	88.2	0.35
C	4	18.00	21.00	91000	389	323	2.8	388.5	42	4.23
D	5	16.00	24.50	112500	208	641	2.8	208	21.5	2.24
E	6	14.14	20.77	115000	156	574	6	156		2.55
F	7	11.00	19.45	100000	482	531	6	481.75	9	1.06
F	8	10.85	18.93	100000	578	549	6	577.75		1.40
F	9	9.57	17.95	100000	623	574	6	623.25		1.57
F	10	11.12	20.80	107656	768	679	6	768.25		0.79
F	11	10.76	24.33	139048	816	1107	2	815.75	4	1.68
F	12	11.00	22.50	152500	1106	1494	6.2	1106.25		0.79
F	13	15.21	32.50	243542	1225	3154	6.2	1224.75		0.81
F	14	25.75	47.67	293750	1282	4206	6.2	1281.75	3.5	0.81
G	15	9.50	22.25	92500	264	528	6	263.5		0.27
H	16	5.18	9.18	96000	135	284	6.4	135	2.5	0.09

Well ID	Case	Status(0 = Stuck)	Training Set	Test Set	Segment Top MD (m)	Segment Bottom MD (m)	Segment Top TVD (m)	Segment Bottom TVD (m)	$D_{well}(m)$
I	17	1	0	1	1901	2748	1894	2729	8.50
J	18	1	0	1	530	1500	530	1499	12.25
J	19	1	0	1	1500	2096	1499	2090	8.50
J	20	0	0	1	2096	2413	2090	2402	8.50
J	21	1	0	1	2413	2435	2402	2424	8.50
J	22	1	0	1	2435	2479	2424	2468	8.50
J	23	1	0	1	2479	2617	2468	2606	8.50
J	24	1	0	1	2617	2664	2606	2653	8.50
J	25	0	0	1	2664	2905	2653	2893	8.50
K	26	1	0	1	1901	2748	1894	2729	8.50
L	27	1	0	1	2748	2862	2735	2850	8.50
M	28	1	0	1	1385	2486	1385	2467	12.25
M	29	1	0	1	2486	2901	2467	2880	12.25
M	30	0	0	1	2901	2977	2880	2957	12.25
N	31	1	0	1	2572	2817	2571	2814	8.50

Well ID	Case	$D_{oavg}(in)$	Average Inclination ($^\circ$)	Mud Density (ppg)	Mud Type	600 RPM ($^\circ$)	300 RPM ($^\circ$)	200 RPM ($^\circ$)	100 RPM ($^\circ$)	6 RPM ($^\circ$)	3 RPM ($^\circ$)
I	17	5.46	9.1	10.1	WBM PHPA	38	25			9	7
J	18	6.21	3.0	9.3	WBM PHPA	59	45			11	14
J	19	5.27	7.2	9.8	WBM PHPA	53	40			13	10
J	20	5.27	9.6	10.0	WBM PHPA	48	36			12	9
J	21	5.69	4.8	10.0	WBM PHPA	47	35			11	8
J	22	5.26	4.5	10.0	WBM PHPA	49	37			12	9
J	23	5.43	4.0	10.0	WBM PHPA	52	38			11	9
J	24	5.37	4.6	10.0	WBM PHPA	50	37			10	8
J	25	5.42	4.5	10.1	WBM PHPA	53	40			11	8
K	26	5.46	9.1	10.1	WBM PHPA	38	25			9	7
L	27	5.42	9.1	10.2	WBM PHPA	36	25			8	6
M	28	5.96	7.3	9.3	WBM PHPA	62	47		28	12	9
M	29	5.89	7.3	9.5	WBM PHPA	47	35		22	9	6
M	30	5.85	7.3	9.6	WBM PHPA	46	34		22	10	7
N	31	5.88	6.5	9.6	WBM PHPA	58	42		22	8	6

Well ID	Case	Gel 10s $(lbf/100ft^2)$	Gel 10min $(lbf/100ft^2)$	Solid (ppm)	Total Open Hole Time (h)	Average Differential Pressure (psi)	Mudcake Thickness (mm)	Total Open Hole Time (h)	Trouble Time (h)	MAX dog leg severity $(deg/100ft)$
I	17	7.25	14.00	87500	250	519	6	249.5		3.40
J	18	30.67	41.67	67500	77	123	6.4	77		0.22
J	19	27.96	44.94	78750	156	349	6	156		0.23
J	20	23.61	40.88	83963	179	480	6	178.5	1	1.00
J	21	21.00	35.30	82296	216	511	6	215.5		0.32
J	22	23.00	38.00	85000	240	516	6	240		0.32
J	23	23.67	39.33	85000	292	527	6	292		0.22
J	24	21.00	37.67	86667	393	554	6	392.5		0.89
J	25	21.00	37.83	95000	508	597	6	508.25	2	0.70
K	26	7.25	14.00	87500	250	519	6	249.5		3.40
L	27	7.00	13.67	86667	295	500	2	294.5		0.01
M	28	10.50	17.10	64444	107	187	6.4	106.5		0.10
M	29	7.15	11.46	70000	241	200	2	240.5		0.10
M	30	6.67	10.67	70000	271	200	2	271	2	0.10
N	31	7.75	16.75	75000	162	355	6	162		7.74

Well ID	Case	Status(0 = Stuck)	Training Set	Test Set	Segment Top MD (m)	Segment Bottom MD (m)	Segment Top TVD (m)	Segment Bottom TVD (m)	$D_{well}(m)$
O	32	1	0	1	801	1708	801	1708	12.25
O	33	1	0	1	1708	2775	1708	2738	8.50
O	34	1	0	1	2739	2755	2738	2774	6.00
O	35	0	0	1	2775	2850	2774	2849	6.00
P	36	1	0	1	2815	2927	2794	2905	8.50
Q	37	1	0	1	506	1111	506	1111	12.25
Q	38	0	0	1	1111	2232	1111	2232	8.00
R	39	1	0	1	1342	2586	1342	2585	12.25
S	40	1	0	1	3088	3500	3088	3500	16.00
S	41	0	0	1	3500	4673	3500	4673	12.25
S	42	1	0	1	4673	4777	4673	4777	8.50
S	43	1	1	0	4777	4841	4777	4841	8.50
S	44	1	0	1	4841	4911	4841	4910	8.50
S	45	1	0	1	4911	4913	4910	4912	8.50
S	46	1	0	1	4913	4924	4912	4924	8.50

Well ID	Case	$D_{oavg}(in)$	Average Inclination (°)	Mud Density (ppg)	Mud Type	600 RPM (°)	300 RPM (°)	200 RPM (°)	100 RPM (°)	6 RPM (°)	3 RPM (°)
O	32	6.20	0.4	9.4	WBM PHPA	54	43		18	17	14
O	33	5.81	2.1	10.2	WBM PHPA	50	38		20	10	8
O	34	4.73	4.6	10.4	WBM PHPA	51	39		22	11	8
O	35	4.73	6.5	11.6	WBM PHPA	54	41		25	10	6
P	36	5.76	3.9	11.1	WBM PHPA	53	37		20	10	7
Q	37	6.19	0.2	9.1	WBM PHPA	52	41		21	9	6
Q	38	5.78	1.1	9.5	WBM PHPA	65	48		28	11	9
R	39	6.24	2.3	9.7	WBM PHPA	66	47			17	8
S	40	6.79	1.3	9.4	WBM PHPA	79	56	46	35	13	10
S	41	6.88	0.8	9.8	WBM PHPA	84	59	49	36	14	12
S	42	6.88	1.4	9.9	WBM PHPA	85	58	47	34	12	10
S	43	7.07	1.8	10.0	WBM PHPA	81	56	43	33	12	9
S	44	7.06	2.0	10.1	WBM PHPA	89	61	47	36	13	11
S	45	6.63	2.1	10.1	WBM PHPA	95	65	52	38	13	11
S	46	6.35	2.2	10.4	WBM PHPA	103	69	55	38	12	10

Well ID	Case	Gel 10s $(lbf/100ft^2)$	Gel 10min $(lbf/100ft^2)$	Solid (ppm)	Total Open Hole Time (h)	Average Differential Pressure (psi)	Mudcake Thickness (mm)	Total Open Hole Time (h)	Trouble Time (h)	MAX dog leg severity $(deg/100ft)$
O	32	6.00	10.50	77500	23	168	6.4	23		0.01
O	33	7.00	11.17	95000	109	539	6	109		0.21
O	34	7.33	11.00	100000	673	729	6	672.5		0.83
O	35	6.75	9.88	138750	770	1310	6.2	769.5	104.5	2.04
P	36	7.33	13.33	126905	402	1072	6.2	402		0.08
Q	37	7.00	9.00	50000	20	82	6.4	2		0.02
Q	38	9.00	13.75	70000	68	224	6.4	68	48.5	0.18
R	39	9.75	20.50	90000	145	307	6	145		0.11
S	40			515	143	667	2.98	142.5		0.30
S	41			515	138	650	2.98	137.5	2	0.09
S	42			515	684	251	4	683.5		0.09
S	43			515	684	76	4	683.5		0.20
S	44			515	684	108	7	683.5		0.26
S	45			515	684	229	7	683.5		0.26
S	46			515	684	91	7	683.5		0.22

Well ID	Case	Status(0 = Stuck)	Training Set	Test Set	Segment Top MD (m)	Segment Bottom MD (m)	Segment Top TVD (m)	Segment Bottom TVD (m)	$D_{well}(m)$
S	47	1	0	1	4924	4962	4924	4961	8.50
S	48	1	0	1	4962	4969	4961	4968	8.50
S	49	1	0	1	4969	5235	4968	5234	8.50
S	50	1	0	1	5235	5367	5234	5365	8.50
S	51	1	0	1	5367	5458	5365	5456	8.50
S	52	1	0	1	5458	5463	5456	5461	8.50
S	53	1	0	1	5463	5847	5461	5842	8.50
S	54	1	0	1	5847	6350	5842	6338	8.50
S	55	1	0	1	6350	6406	6338	6388	8.50
S	56	0	0	1	6406	6644	6388	6623	8.50
T	57	1	0	1	4450	5873	4449	4880	12.25
U	58	1	0	1	5873	6289	4870	6289	8.50
V	59	0	0	1	1762	2863	1762	2859	12.25
V	60	1	0	1	2863	3162	2859	3152	12.25
W	61	1	0	1	1975	2273	1974	2272	12.25

Well ID	Case	$D_{oavg}(in)$	Average Inclination (°)	Mud Density (ppg)	Mud Type	600 RPM (°)	300 RPM (°)	200 RPM (°)	100 RPM (°)	6 RPM (°)	3 RPM (°)
S	47	6.34	2.3	10.7	WBM PHPA	107	72	57	38	12	10
S	48	6.33	2.3	10.8	WBM PHPA	105	70	55	38	11	9
S	49	6.36	3.6	10.8	WBM PHPA	99	68	55	37	11	9
S	50	6.30	3.2	10.8	WBM PHPA	98	67	54	38	11	9
S	51	6.37	4.0	10.8	WBM PHPA	105	71	57	39	11	9
S	52	6.19	2.8	10.8	WBM PHPA	111	75	60	41	10	8
S	53	6.37	7.0	10.8	WBM PHPA	106	72	57	40	10	8
S	54	6.77	9.6	11.0	WBM PHPA	121	82	66	45	12	9
S	55	6.60	5.9	11.1	WBM PHPA	131	89	72	49	13	10
S	56	6.60	6.0	11.1	WBM PHPA	118	80	66	46	12	11
T	57	7.46	0.4	10.0	SYNTH	61	39	30	21	11	9
U	58	6.33	0.8	10.2	SYNTH	62	38	28	19	11	10
V	59	6.63	4.4	9.5	WBM PHPA						
V	60	6.74	11.7	9.7	WBM PHPA						
W	61	6.81	0.8	9.2	WBM PHPA						

Well ID	Case	Gel 10s $(lbf/100ft^2)$	Gel 10min $(lbf/100ft^2)$	Solid (ppm)	Total Open Hole Time (h)	Average Differential Pressure (psi)	Mudcake Thickness (mm)	Total Open Hole Time (h)	Trouble Time (h)	MAX dog leg severity $(deg/100ft)$
S	47			515	684	613	2.98	683.5		0.25
S	48			515	684	990	3	683.5		0.25
S	49			515	817	1049	3	816.5		0.39
S	50			515	819	798	3	818.5		2.02
S	51			515	896	488	2.98	895.5		2.71
S	52			515	1020	368	2.98	1019.5		7.94
S	53			515	1153	280	7	1153		1.48
S	54			515	1212	270	7	1211.5		0.87
S	55			515	1236	345	6.2	1235.5		1.23
S	56			515	1593	351	6.2	1593	2	1.00
T	57			98946	1098	514	2.8	1098		0.14
U	58			98946	1286	784	4.56	1285.5		0.11
V	59			515	31	314	5.5	30.5	0.5	0.01
V	60			515	201	511	5.5	201		0.01
W	61			515	200	253	4			0.11

Well ID	Case	Status(0 = Stuck)	Training Set	Test Set	Segment Top MD (m)	Segment Bottom MD (m)	Segment Top TVD (m)	Segment Bottom TVD (m)	$D_{well}(m)$
X	62	1	0	1	2873	4125	2873	4125	12.25
X	63	0	0	1	4125	4432	4125	4432	12.25
X	64	1	0	1	4432	4927	4432	4926	12.25
Y	65	1	0	1	4188	4522	4187	4521	12.25
Y	66	1	0	1	4188	4522	4187	4521	12.25
Y	67	1	0	1	4522	4899	4521	4898	12.25
Y	68	1	0	1	4899	4952	4898	4950	12.25
Y	69	1	0	1	4952	5024	4950	5022	12.25
Y	70	0	0	1	5024	5033	5022	5031	12.25
Y	71	1	0	1	5033	5178	5031	5176	8.50
Y	72	1	0	1	5178	5362	5176	5359	8.50
Y	73	1	0	1	5362	5530	5359	5525	8.50
Y	74	0	0	1	5530	5556	5525	5551	8.50
Y	75	1	0	1	5556	5574	5551	5569	8.50
Y	76	1	0	1	5574	5721	5569	5714	8.50
Y	77	1	0	1	5721	5778	5714	5770	8.50

Well ID	Case	$D_{oavg}(in)$	Average Inclination (°)	Mud Density (ppg)	Mud Type	600 RPM (°)	300 RPM (°)	200 RPM (°)	100 RPM (°)	6 RPM (°)	3 RPM (°)
X	62	8.25	0.1	10.3	WBM PHPA	87	61	48	37	15	13
X	63	8.25	1.4	10.5	WBM PHPA	101	71	58	42	17	14
X	64	8.25	2.0	10.6	WBM PHPA	112	79	64	47	19	17
Y	65	6.50	1.6	9.6	WBM PHPA	86	63	54	41	16	14
Y	66	6.50	1.6	9.6	WBM PHPA	86	63	54	41	16	14
Y	67	7.43	2.6	9.6	WBM PHPA	82	60	51	39	15	13
Y	68	7.10	3.1	9.8	WBM PHPA	94	69	58	44	18	15
Y	69	7.22	2.2	10.2	SYNTH	84	61	49	37	16	14
Y	70	6.09	3.0	10.1	SYNTH	62	43	34	26	13	12
Y	71	6.76	4.4	9.9	SYNTH	61	42	34	27	15	13
Y	72	6.76	6.5	10.2	SYNTH	59	39	31	23	12	11
Y	73	6.76	7.6	11.0	SYNTH	68	45	37	28	13	11
Y	74	6.76	7.5	11.5	SYNTH	76	47	38	27	11	10
Y	75	6.34	7.6	11.3	SYNTH	71	43	35	24	10	8
Y	76	6.76	8.7	11.0	SYNTH	81	50	39	27	10	8
Y	77	6.76	9.8	11.0	SYNTH	83	51	40	28	10	9

Well ID	Case	Gel 10s $(lbf/100ft^2)$	Gel 10min $(lbf/100ft^2)$	Solid (ppm)	Total Open Hole Time (h)	Average Differential Pressure (psi)	Mudcake Thickness (mm)	Total Open Hole Time (h)	Trouble Time (h)	MAX dog leg severity $(deg/100ft)$
X	62			515	111	619	2.98	111		0.15
X	63			515	326	717	2.98	326	1	0.16
X	64			515	532	451	2.98	532		0.17
Y	65			515	745	374	2.98	745		0.07
Y	66			515	745	376	2.98	745		0.07
Y	67			515	913	384	2.98	912.5		0.39
Y	68			515	979	473	2.98	979		1.90
Y	69			98946	1074	853	4.56	1073.5		0.69
Y	70			98946	1235	725	2.8	1235	0.5	0.56
Y	71			98946	1552	383	2.8	1552		0.42
Y	72			98946	1699	192	4	1698.5		0.46
Y	73			98946	1759	501	6.2	1758.5		0.23
Y	74			98946	1838	811	6.2	1837.5	0.5	0.19
Y	75			98946	1895	643	6.2	1894.5		0.18
Y	76			98946	2028	293	5	2028		0.17
Y	77			98946	2111	257	5	2111		0.37

Well ID	Case	Status(0 = Stuck)	Training Set	Test Set	Segment Top MD (m)	Segment Bottom MD (m)	Segment Top TVD (m)	Segment Bottom TVD (m)	$D_{well}(m)$
Y	78	1	0	1	5778	5796	5770	5788	8.50
Y	79	1	0	1	5796	5859	5788	5850	8.50
Z	80	1	0	1	4717	5157	7716	5156	8.50
AA	81	1	0	1	5157	5449	5156	5445	8.50
AB	82	0	0	1	1705	2294	1705	2293	12.25
AB	83	1	0	1	2294	2923	2293	2919	12.25
AB	84	0	0	1	2923	3452	2919	3447	12.25
AB	85	1	0	1	3119	3560	3447	3554	12.25
AB	86	0	0	1	3560	3560	3554	3554	12.25
AC	87	1	0	1	2194	3123	2194	3122	12.25
AD	88	1	0	1	3123	3445	3122	3445	8.50
AE	89	1	0	1	3445	3750	3445	3750	8.50
AF	90	1	0	1	2844	3231	2844	3231	12.25
AF	91	1	0	1	3231	3244	3231	3244	8.50
AF	92	1	0	1	3244	3245	3244	3245	8.50
AF	93	1	0	1	3245	3304	3245	3304	12.25

Well ID	Case	$D_{oavg}(in)$	Average Inclination (°)	Mud Density (ppg)	Mud Type	600 RPM (°)	300 RPM (°)	200 RPM (°)	100 RPM (°)	6 RPM (°)	3 RPM (°)
Y	78	6.34	10.2	11.0	SYNTH	79	49	38	27	11	9
Y	79	6.76	10.5	11.0	SYNTH	75	48	38	27	11	9
Z	80	6.76	3.7	9.8	SYNTH	78	57	47	36	15	13
AA	81	6.76	7.8	10.3	SYNTH	60	40	32	24	12	10
AB	82	7.19	3.9	9.4	WBM PHPA	34	25	21	16	8	7
AB	83	7.27	4.8	9.4	WBM PHPA	68	50	42	33	15	13
AB	84	7.39	4.5	9.6	WBM PHPA	81	59	49	37	15	13
AB	85	7.33	5.9	9.9	WBM PHPA	88	62	51	38	15	13
AB	86	6.41	5.9	10.2	WBM PHPA	100	69	55	40	14	12
AC	87	6.29	0.5	10.1	SYNTH	55	40		25	11	10
AD	88	5.89	1.7	10.6	SYNTH	63	45		28	11	10
AE	89	6.05	2.4	10.7	SYNTH	66	46		30	11	10
AF	90	6.67	1.4	9.3	WBM PHPA	61	42		24	7	5
AF	91	6.42	1.5	9.5	WBM PHPA	59	41		24	7	5
AF	92	5.81	1.5	9.5	WBM PHPA	59	41		24	7	5
AF	93	6.68	1.5	9.5	WBM PHPA	60	42		25	8	6

Well ID	Case	Gel 10s $(lbf/100ft^2)$	Gel 10min $(lbf/100ft^2)$	Solid (ppm)	Total Open Hole Time (h)	Average Differential Pressure (psi)	Mudcake Thickness (mm)	Total Open Hole Time (h)	Trouble Time (h)	MAX dog leg severity $(deg/100ft)$
Y	78			98946	2133	243	5	2132.5		0.32
Y	79			98946	2270	237	5	2269.5		0.20
Z	80			98946	1362	658	2.8	1362		0.20
AA	81			98946	1695	289	4	1694.5		0.20
AB	82			515	65	318	5.5	65	143	0.24
AB	83			515	270	226	4	270		0.17
AB	84			515	395	170	7	395	946.5	0.16
AB	85			515	1357	383	2.98	1357		0.03
AB	86			515	1368	548	2.98	1367.5	254	0.11
AC	87	12.02	15.40	1210	119	853	4.56	118.5		0.22
AD	88	12.13	16.00	1440	393	1349	4.56	393		0.31
AE	89	12.33	17.11	1484	521	1543	4.56	520.5		0.18
AF	90	5.67	9.00	654	25	367	5.5	25		0.09
AF	91	6.09	10.00	803	59	415	5.5	58.5		0.09
AF	92	6.18	10.00	802	63	419	5.5	63		0.09
AF	93	6.73	10.00	801	75	438	5.5	75		0.09

Appendix C

Tables of Results - Raw Drilling Input Data (cont.)

C.1 Input Data

Well ID	Case	Status(0 = Stuck)	Training Set	Test Set	Segment Top MD (m)	Segment Bottom MD (m)	Segment Top TVD (m)	Segment Bottom TVD (m)	$D_{well}(m)$
AF	94	1	0	1	3304	3313	3304	3313	8.47
AF	95	0	0	1	3313	4024	3313	4024	12.25
AG	96	1	0	1	3104	3880	2902	3401	12.25
AH	97	1	0	1	1906	2683	1906	2620	17.50
AH	98	0	0	1	2683	2995	2620	2828	17.50
AH	99	0	0	1	2995	3104	2828	2902	17.50
AH	100	1	0	1	3104	3880	2902	3401	12.25
AI	101	1	1	0	2787	3106	2787	2106	12.25
AJ	102	1	0	1	3310	3752	3187	3508	12.25
AJ	103	0	0	1	3752	4152	3508	3832	12.25
AK	104	1	0	1	3805	4109	3556	3793	12.25
AL	105	1	0	1	2585	3074	2585	3073	8.50
AL	106	0	0	1	3074	3110	3073	3109	8.50
AL	107	1	0	1	3110	3114	3109	3113	8.47
AL	108	1	0	1	3114	3118	3113	3117	8.50
AL	109	1	0	1	3118	3145	3117	3144	8.47

Well ID	Case	$D_{oavg}(in)$	Average Inclination (°)	Mud Density (ppg)	Mud Type	600 RPM (°)	300 RPM (°)	200 RPM (°)	100 RPM (°)	6 RPM (°)	3 RPM (°)
AF	94	6.43	1.5	9.5	WBM PHPA	62	43		26	8	6
AF	95	6.68	1.7	9.6	WBM PHPA	68	47		27	8	6
AG	96	6.48	49.7	9.8	WBM PHPA	108	82		54	20	17
AH	97	6.68	21.5	10.2	WBM PHPA						
AH	98	6.68	46.5	10.2	WBM PHPA	43	30		19	11	9
AH	99	6.56	47.3	10.4	WBM PHPA	70	50		31	15	13
AH	100	6.48	49.7	9.8	WBM PHPA	108	82		54	20	17
AI	101	6.60	0.6	9.4	WBM PHPA	65	47		28	10	7
AJ	102	6.10	43.3	9.6	WBM PHPA	76	49		26	7	5
AJ	103	6.26	36.8	9.6	WBM PHPA	77	50		26	6	4
AK	104	7.07	41.7	9.6	WBM PHPA	74	48		26	6	5
AL	105	5.86	2.6	9.6	SYNTH	64	40		23	11	10
AL	106	5.80	0.9	9.5	SYNTH	64	39		22	11	10
AL	107	5.48	0.8	9.5	SYNTH	63	40		22	11	10
AL	108	5.77	0.8	9.5	SYNTH	63	40		22	11	10
AL	109	5.80	0.8	9.5	SYNTH	63	40		22	11	10

Well ID	Case	Gel 10s $(lbf/100ft^2)$	Gel 10min $(lbf/100ft^2)$	Solid (ppm)	Total Open Hole Time (h)	Average Differential Pressure (psi)	Mudcake Thickness (mm)	Total Open Hole Time (h)	Trouble Time (h)	MAX dog leg severity $(deg/100ft)$
AF	94	7.00	10.00	800	26	450	5.5	25.5		0.09
AF	95	7.11	10.56	823	145	555	5.5	144.5	3.5	0.07
AG	96	16.07	26.09	1402	275	601	2.98	274.5		0.11
AH	97			781	82	500	3	82		0.01
AH	98	6.04	13.39	781	134	790	3	134	10	2.70
AH	99	9.68	19.58	781	231	861	3	231	71.5	2.10
AH	100	16.07	26.09	1402	275	627	2.98	274.5		0.11
AI	101	8.00	12.00	700	200	361	5.5			0.06
AJ	102	4.85	12.69	421	232	501	5.5	232		0.22
AJ	103	3.85	10.17	465	269	572	5.5	268.5	5	0.80
AK	104	4.00	10.00	470	106	563	5.5	106		0.44
AL	105	12.52	14.79	793	32	435	2.8	31.5		0.22
AL	106	12.58	15.00	1000	204	420	2.8	204	38.5	0.76
AL	107	12.42	15.00	1000	1434	423	2.8	1433.5		0.23
AL	108	12.39	15.00	1000	1458	424	2.8	1458		0.24
AL	109	12.27	15.00	1000	1552	426	2.8	1552		0.24

Well ID	Case	Status(0 = Stuck)	Training Set	Test Set	Segment Top MD (m)	Segment Bottom MD (m)	Segment Top TVD (m)	Segment Bottom TVD (m)	$D_{well}(m)$
AL	110	1	0	1	3145	3192	3144	3191	8.50
AL	111	1	0	1	3192	3210	3191	3209	8.47
AL	112	1	0	1	3210	3211	3209	3210	8.50
AL	113	1	0	1	3211	3227	3210	3226	8.47
AL	114	1	0	1	3227	3334	3226	3333	8.50
AL	115	1	0	1	3334	3530	3333	3529	8.50
AM	116	1	0	1	3081	3442	3079	3429	12.25
AN	117	0	0	1	1622	2495	1622	2495	17.50
AO	118	1	1	0	2200	2759	2200	2760	12.25
AP	119	1	0	1	2071	2385	2069	2382	16.00
AP	120	0	0	1	2385	2520	2382	2517	16.00
AP	121	1	1	0	2520	2969	2517	2966	8.50
AP	122	1	0	1	2969	3420	2966	3416	8.50
AQ	123	1	0	1	2200	2759	2200	2760	12.25
AR	124	0	0	1	2689	3568	2681	3425	12.25
AR	125	1	0	1	3568	3794	3425	3616	12.25
AR	126	1	0	1	3794	3867	3616	3678	12.25
AS	127	1	1	0	2862	3056	2861	3055	12.25

Well ID	Case	$D_{oavg}(in)$	Average Inclination (°)	Mud Density (ppg)	Mud Type	600 RPM (°)	300 RPM (°)	200 RPM (°)	100 RPM (°)	6 RPM (°)	3 RPM (°)
AL	110	5.93	0.9	9.5	SYNTH	63	40		22	11	10
AL	111	5.82	0.7	9.5	SYNTH	65	41		23	11	10
AL	112	5.93	0.8	9.5	SYNTH	65	41		23	11	10
AL	113	5.80	0.9	9.5	SYNTH	66	42		23	12	11
AL	114	5.93	1.0	9.5	SYNTH	69	44		25	12	11
AL	115	6.02	1.0	9.5	SYNTH	69	43		24	12	11
AM	116	5.09	0.8	9.6	WBM PHPA	58	38		21	5	4
AN	117	6.45	1.0	8.6	WBM PHPA	47	36		27	23	21
AO	118	6.27	0.4	9.0	WBM PHPA	40	28		18	10	8
AP	119	6.33	2.9	8.9	WBM PHPA	43	33		25	19	18
AP	120	6.81	2.0	9.0	WBM PHPA	29	22		14	7	6
AP	121	6.06	2.3	9.4	WBM PHPA	50	33		18	5	3
AP	122	6.06	2.8	9.7	WBM PHPA	59	38		21	5	4
AQ	123	6.27	0.4	9.0	WBM PHPA	40	28		18	10	8
AR	124	7.56	31.6	9.5	SYNTH	62	44		28	14	13
AR	125	7.43	32.4	9.6	SYNTH	59	44		28	15	13
AR	126	7.67	31.9	9.6	SYNTH	60	45		29	16	14
AS	127	7.55	1.6	9.3	WBM PHPA	70	49		27	9	7

Well ID	Case	Gel 10s $(lbf/100ft^2)$	Gel 10min $(lbf/100ft^2)$	Solid (ppm)	Total Open Hole Time (h)	Average Differential Pressure (psi)	Mudcake Thickness (mm)	Total Open Hole Time (h)	Trouble Time (h)	MAX dog leg severity $(deg/100ft)$
AL	110	12.18	15.12	1000	1578	431	2.8	1577.5		0.23
AL	111	12.51	15.51	1000	1630	435	2.8	1630		0.49
AL	112	12.64	15.64	1000	1650	437	2.8	1650		0.82
AL	113	12.76	15.76	1000	1707	438	2.8	1707		1.14
AL	114	13.69	16.69	1000	136	446	2.8	135.5		1.03
AL	115	14.14	16.67	1000	1788	467	2.8	1788		0.41
AM	116	4.22	4.97	946	67	522	5.5	66.5		0.11
AN	117	11.54	16.13	236	46	35	4	46	3	0.22
AO	118	4.81	7.47	530	57	225	4	57		0.01
AP	119	9.84	13.78	97	66	133	4	66		0.07
AP	120	3.82	5.68	400	165	194	4	164.5	2	0.15
AP	121	3.45	5.26	651	439	382	5.5	439		0.07
AP	122	4.50	5.55	910	537	549	5.5	536.5		0.04
AQ	123	4.81	7.47	530	57	225	4	57		0.01
AR	124	17.43	26.61	96837	902	468	2.8	901.5	3	0.41
AR	125	18.00	24.41	100000	931	504	2.8	931		0.64
AR	126	18.00	23.89	100000	964	543	2.8	963.5		0.49
AS	127	7.09	15.76	385	135	394	5.5	135		0.35

Appendix D

Tables of Results - Processed Input Data

D.1 Input Data

The following tables show the actual input data for the computing the likelihood part of the risk analysis model (similarity score).

Table D.1: Cases - Processed Input Data

Well ID	Case	Status	Training Set	Test Set	Clearence Factor	Inclination Factor	TSF	Differential Pressure (psi)	API Filtrate (cm^3)
A	1	1	1	0	0.560	0.285	0.886	85	11.5
A	2	0	1	0	0.467	0.503	0.878	396	9.0
B	3	0	1	0	0.481	0.753	0.922	516	13.0
C	4	0	1	0	0.388	0.775	0.864	323	5.2
D	5	0	1	0	0.539	0.870	0.995	641	7.7
E	6	0	1	0	0.429	0.127	0.861	574	7.1
F	7	0	0	1	0.515	0.392	0.899	531	5.7
F	8	1	0	1	0.478	0.348	0.867	549	5.6
F	9	1	0	1	0.502	0.314	0.867	574	5.5
F	10	1	0	1	0.478	0.224	0.958	679	5.8
F	11	1	1	0	0.239	0.132	0.958	1107	6.0
F	12	1	0	1	0.360	0.115	0.960	1494	6.5
F	13	1	0	1	0.360	0.084	0.960	3154	6.6
F	14	1	1	0	0.366	0.000	0.902	4206	8.0

Well ID	Case	Filtrate Ratio Corrected (100/500)	$L_{BHA} - L_{crit}(m)$	Hardness Index	Torque Resistance (N/m)	Adhesion Strength (N/m^2)	Solid (ppm)	MAX dog leg severity $(deg/100ft)$	Total Open Hole Time (h)	Segment Bottom MD (m)
A	1	0.58	343.48	1.53	23	2123	103875	0.06	66	2028
A	2	1.75	338.56	17.59	1018	192478	103875	0.16	101	3638
B	3	0.58	324.43	17.59	1018	192478	103875	0.35	462	4855
C	4	3.58	252.00	17.59	1018	192478	91000	4.23	389	3310
D	5	0.58	441.61	17.59	1018	192478	112500	2.24	208	2720
E	6	2.11	211.68	10.94	177	33433	115000	2.55	156	1793
F	7	2.11	196.55	10.94	177	33433	100000	1.06	482	2695
F	8	2.11	182.14	10.94	177	33433	100000	1.40	578	2709
F	9	2.11	300.00	10.94	177	33433	100000	1.57	623	2831
F	10	2.11	252.08	10.94	177	33433	107656	0.79	768	3515
F	11	2.11	300.00	36.65	137	30937	139048	1.68	816	3546
F	12	0.13	253.04	7.89	27	24843	152500	0.79	1106	3627
F	13	5.51	250.22	7.89	27	24843	243542	0.81	1225	4119
F	14	4.83	334.26	7.89	27	24843	293750	0.81	1282	4250

Well ID	Case	Status	Training Set	Test Set	Clearance Factor	Inclination Factor	TSF	Differential Pressure (psi)	API Filtrate (cm^3)
G	15	1	0	1	0.492	0.070	0.800	528	6.8
H	16	0	0	1	0.488	0.013	0.894	284	5.3
I	17	1	0	1	0.358	0.101	0.612	519	6.1
J	18	1	0	1	0.493	0.033	0.926	123	7.0
J	19	1	0	1	0.380	0.080	0.921	349	6.9
J	20	0	0	1	0.380	0.106	0.928	480	6.9
J	21	1	0	1	0.330	0.054	0.830	511	5.7
J	22	1	0	1	0.381	0.050	0.830	516	5.6
J	23	1	0	1	0.361	0.044	0.837	527	5.7
J	24	1	0	1	0.368	0.052	0.645	554	6.2
J	25	0	0	1	0.362	0.050	0.612	597	6.0
K	26	1	0	1	0.358	0.101	0.844	519	6.1
L	27	1	0	1	0.362	0.101	0.744	500	6.0
M	28	1	0	1	0.513	0.081	0.692	187	6.2
M	29	1	0	1	0.519	0.081	0.789	200	6.4
M	30	0	0	1	0.523	0.081	0.807	200	6.1

Well ID	Case	Filtrate Ratio Corrected (100/500)	$L_{BHA} - L_{crit}(m)$	Hardness Index	Torque Resistance (N/m)	Adhesion Strength (N/m^2)	Solid (ppm)	MAX dog leg severity $(deg/100ft)$	Total Open Hole Time (h)	Segment Bottom MD (m)
G	15	2.11	231.17	10.94	177	33433	92500	0.27	264	2810
H	16	2.11	344.19	1.95	45	1463	96000	0.09	135	2255
I	17	2.11	246.69	10.94	177	33433	87500	3.40	250	2748
J	18	2.11	339.82	1.95	45	1463	67500	0.22	77	1500
J	19	2.11	339.81	10.94	177	33433	78750	0.23	156	2096
J	20	2.11	339.93	10.94	177	33433	83963	1.00	179	2413
J	21	2.11	247.89	10.94	177	33433	82296	0.32	216	2435
J	22	2.11	300.00	10.94	177	33433	85000	0.32	240	2479
J	23	2.11	243.30	10.94	177	33433	85000	0.22	292	2617
J	24	2.11	0.00	10.94	177	33433	86667	0.89	393	2664
J	25	2.11	160.76	10.94	177	33433	95000	0.70	508	2905
K	26	2.11	223.15	10.94	177	33433	87500	3.40	250	2748
L	27	2.11	184.92	36.65	137	30937	86667	0.01	295	2862
M	28	2.11	184.73	1.95	45	1463	64444	0.10	107	2486
M	29	2.11	212.08	36.65	137	30937	70000	0.10	241	2901
M	30	2.11	195.08	36.65	137	30937	70000	0.10	271	2977

Well ID	Case	Status	Training Set	Test Set	Clearance Factor	Inclination Factor	TSF	Differential Pressure (psi)	API Filtrate (cm^3)
N	31	1	0	1	0.308	0.072	0.995	355	5.7
O	32	1	0	1	0.494	0.005	0.430	168	7.5
O	33	1	0	1	0.316	0.023	0.430	539	6.2
O	34	1	0	1	0.212	0.052	0.430	729	6.0
O	35	0	0	1	0.212	0.072	0.430	1310	6.6
P	36	1	0	1	0.322	0.044	0.430	1072	6.4
Q	37	1	0	1	0.494	0.002	0.800	82	5.6
Q	38	0	0	1	0.277	0.012	0.846	224	6.4
R	39	1	0	1	0.491	0.026	0.875	307	5.9
S	40	1	0	1	0.576	0.014	0.699	667	4.8
S	41	0	0	1	1.000	0.008	0.699	650	6.3
S	42	1	0	1	0.190	0.015	0.655	251	6.0
S	43	1	1	0	0.169	0.020	0.830	76	6.1
S	44	1	0	1	0.169	0.023	0.830	108	6.5
S	45	1	0	1	0.220	0.023	0.808	229	6.5
S	46	1	0	1	0.253	0.025	0.712	91	5.1

Well ID	Case	Filtrate Ratio Corrected (100/500)	$L_{BHA} - L_{crit}(m)$	Hardness Index	Torque Resistance (N/m)	Adhesion Strength (N/m^2)	Solid (ppm)	MAX dog leg severity $(deg/100ft)$	Total Open Hole Time (h)	Segment Bottom MD (m)
N	31	2.11	441.61	10.94	177	33433	75000	7.74	162	2817
O	32	2.11	318.58	1.95	45	1463	77500	0.01	23	1708
O	33	2.11	300.00	10.94	177	33433	95000	0.21	109	2775
O	34	2.11	300.00	10.94	177	33433	100000	0.83	673	2755
O	35	0.13	300.00	7.89	27	24843	138750	2.04	770	2850
P	36	0.13	300.00	7.89	27	24843	126905	0.08	402	2927
Q	37	2.11	231.17	1.95	45	1463	50000	0.02	20	1111
Q	38	2.11	230.83	1.95	45	1463	70000	0.18	68	2232
R	39	2.11	290.54	10.94	177	33433	90000	0.11	145	2586
S	40	0.04	360.66	18.32	28	45690	515	0.30	143	3500
S	41	0.04	300.00	18.32	28	45690	515	0.09	138	4673
S	42	2.72	275.28	3.69	158	1278	515	0.09	684	4777
S	43	2.72	250.67	3.69	158	1278	515	0.20	684	4841
S	44	0.04	250.67	1.26	47	1300	515	0.26	684	4911
S	45	0.04	282.82	1.26	47	1300	515	0.26	684	4913
S	46	0.04	109.55	1.26	47	1300	515	0.22	684	4924

Well ID	Case	Status	Training Set	Test Set	Clearance Factor	Inclination Factor	TSF	Differential Pressure (psi)	API Filtrate (cm^3)
S	47	1	0	1	0.254	0.026	0.674	613	3.9
S	48	1	0	1	0.255	0.026	0.652	990	3.5
S	49	1	0	1	0.251	0.040	0.853	1049	3.7
S	50	1	0	1	0.259	0.035	0.807	798	3.6
S	51	1	0	1	0.250	0.045	0.735	488	3.7
S	52	1	0	1	0.271	0.031	0.867	368	3.3
S	53	1	0	1	0.250	0.078	0.860	280	3.4
S	54	1	0	1	0.203	0.107	0.688	270	2.9
S	55	1	0	1	0.224	0.066	0.688	345	3.0
S	56	0	0	1	0.224	0.066	0.688	351	3.5
T	57	1	0	1	0.391	0.004	0.688	514	1.4
U	58	1	0	1	0.255	0.009	0.688	784	27.0
V	59	0	0	1	0.459	0.049	0.700	314	49.0
V	60	1	0	1	0.450	0.130	0.689	511	49.0
W	61	1	0	1	0.444	0.008	0.689	253	49.0

Well ID	Case	Filtrate Ratio Corrected (100/500)	$L_{BHA} - L_{crit}(m)$	Hardness Index	Torque Resistance (N/m)	Adhesion Strength (N/m^2)	Solid (ppm)	MAX dog leg severity $(deg/100ft)$	Total Open Hole Time (h)	Segment Bottom MD (m)
S	47	0.04	229.22	18.32	28	45690	515	0.25	684	4962
S	48	0.04	231.72	48.86	402	67563	515	0.25	684	4969
S	49	0.04	200.37	48.86	402	67563	515	0.39	817	5235
S	50	0.04	225.83	48.86	402	67563	515	2.02	819	5367
S	51	0.04	169.83	18.32	28	45690	515	2.71	896	5458
S	52	0.04	427.44	18.32	28	45690	515	7.94	1020	5463
S	53	0.04	405.36	1.26	47	1300	515	1.48	1153	5847
S	54	0.04	348.76	1.26	47	1300	515	0.87	1212	6350
S	55	0.13	335.76	7.89	27	24843	515	1.23	1236	6406
S	56	0.13	300.00	7.89	27	24843	515	1.00	1593	6644
T	57	2.58	300.00	17.59	1018	192478	98946	0.14	1098	5873
U	58	0.58	300.00	61.27	16	27788	98946	0.11	1286	6289
V	59	2.72	322.86	14.58	2	866	515	0.01	31	2863
V	60	2.72	342.27	14.58	2	866	515	0.01	201	3162
W	61	2.72	300.00	3.69	158	1278	515	0.11	200	2273

Well ID	Case	Status	Training Set	Test Set	Clearance Factor	Inclination Factor	TSF	Differential Pressure (psi)	API Filtrate (cm^3)
X	62	1	0	1	0.327	0.001	0.689	619	5.9
X	63	0	0	1	0.327	0.016	0.689	717	5.4
X	64	1	0	1	0.327	0.022	0.688	451	5.3
Y	65	1	0	1	0.470	0.017	0.688	374	5.2
Y	66	1	0	1	0.470	0.017	0.688	376	5.2
Y	67	1	0	1	0.394	0.029	0.756	384	5.6
Y	68	1	0	1	0.420	0.035	0.738	473	5.7
Y	69	1	0	1	0.411	0.025	0.713	853	3.0
Y	70	0	0	1	0.503	0.033	0.705	725	13.0
Y	71	1	0	1	0.205	0.049	0.782	383	13.0
Y	72	1	0	1	0.205	0.072	0.782	192	27.0
Y	73	1	0	1	0.205	0.085	0.745	501	23.0
Y	74	0	0	1	0.205	0.084	0.856	811	23.0
Y	75	1	0	1	0.254	0.085	0.833	643	23.0
Y	76	1	0	1	0.205	0.097	0.875	293	15.0
Y	77	1	0	1	0.205	0.109	0.809	257	15.0

Well ID	Case	Filtrate Ratio Corrected (100/500)	$L_{BHA} - L_{crit}(m)$	Hardness Index	Torque Resistance (N/m)	Adhesion Strength (N/m^2)	Solid (ppm)	MAX dog leg severity $(deg/100ft)$	Total Open Hole Time (h)	Segment Bottom MD (m)
X	62	0.04	478.73	18.32	28	45690	515	0.15	111	4125
X	63	0.04	478.73	18.32	28	45690	515	0.16	326	4432
X	64	0.04	344.55	18.32	28	45690	515	0.17	532	4927
Y	65	0.04	300.00	18.32	28	45690	515	0.07	745	4522
Y	66	0.04	348.84	18.32	28	45690	515	0.07	745	4522
Y	67	0.04	173.80	18.32	28	45690	515	0.39	913	4899
Y	68	0.04	214.62	18.32	28	45690	515	1.90	979	4952
Y	69	0.90	250.38	61.27	16	27788	98946	0.69	1074	5024
Y	70	0.58	259.51	17.59	1018	192478	98946	0.56	1235	5033
Y	71	0.58	172.90	17.59	1018	192478	98946	0.42	1552	5178
Y	72	0.58	300.00	4.02	55	4931	98946	0.46	1699	5362
Y	73	0.13	274.08	7.89	27	24843	98946	0.23	1759	5530
Y	74	0.13	289.56	7.89	27	24843	98946	0.19	1838	5556
Y	75	0.13	317.74	7.89	27	24843	98946	0.18	1895	5574
Y	76	0.20	329.74	0.36	22	700	98946	0.17	2028	5721
Y	77	0.20	185.72	0.36	22	700	98946	0.37	2111	5778

Well ID	Case	Status	Training Set	Test Set	Clearance Factor	Inclination Factor	TSF	Differential Pressure (psi)	API Filtrate (cm^3)
Y	78	1	0	1	0.254	0.114	0.764	243	15.0
Y	79	1	0	1	0.205	0.116	0.764	237	15.0
Z	80	1	0	1	0.205	0.041	0.764	658	4.2
AA	81	1	0	1	0.205	0.087	0.764	289	27.0
AB	82	0	0	1	0.413	0.043	0.764	318	3.8
AB	83	1	0	1	0.407	0.053	0.803	226	5.2
AB	84	0	0	1	0.397	0.050	0.803	170	3.3
AB	85	1	0	1	0.401	0.065	0.818	383	4.8
AB	86	0	0	1	0.477	0.066	0.818	548	4.8
AC	87	1	0	1	0.487	0.006	0.818	853	4.3
AD	88	1	0	1	0.307	0.019	0.821	1349	4.0
AE	89	1	0	1	0.289	0.026	0.825	1543	3.9
AF	90	1	0	1	0.455	0.016	0.841	367	6.9
AF	91	1	0	1	0.245	0.017	0.810	415	6.6
AF	92	1	0	1	0.316	0.017	0.837	419	6.7
AF	93	1	0	1	0.455	0.017	0.810	438	6.9

Well ID	Case	Filtrate Ratio Corrected (100/500)	$L_{BHA} - L_{crit}(m)$	Hardness Index	Torque Resistance (N/m)	Adhesion Strength (N/m^2)	Solid (ppm)	MAX dog leg severity $(deg/100ft)$	Total Open Hole Time (h)	Segment Bottom MD (m)
Y	78	0.20	224.12	0.36	22	700	98946	0.32	2133	5796
Y	79	0.20	224.12	0.36	22	700	98946	0.20	2270	5859
Z	80	0.33	300.00	17.59	1018	192478	98946	0.20	1362	5157
AA	81	0.58	300.00	4.02	55	4931	98946	0.20	1695	5449
AB	82	2.72	224.82	14.58	2	866	515	0.24	65	2294
AB	83	2.72	186.96	3.69	158	1278	515	0.17	270	2923
AB	84	0.04	300.00	1.26	47	1300	515	0.16	395	3452
AB	85	0.04	300.00	18.32	28	45690	515	0.03	1357	3560
AB	86	0.04	300.00	18.32	28	45690	515	0.11	1368	3560
AC	87	0.04	283.76	61.27	16	27788	1210	0.22	119	3123
AD	88	0.04	288.31	61.27	16	27788	1440	0.31	393	3445
AE	89	0.04	271.56	61.27	16	27788	1484	0.18	521	3750
AF	90	2.72	239.24	14.58	2	866	654	0.09	25	3231
AF	91	2.72	176.89	14.58	2	866	803	0.09	59	3244
AF	92	2.72	176.80	14.58	2	866	802	0.09	63	3245
AF	93	2.72	175.69	14.58	2	866	801	0.09	75	3304

Well ID	Case	Status	Training Set	Test Set	Clearance Factor	Inclination Factor	TSF	Differential Pressure (psi)	API Filtrate (cm^3)
AF	94	1	0	1	0.240	0.017	0.810	450	7.1
AF	95	0	0	1	0.454	0.019	0.810	555	7.2
AG	96	1	0	1	0.471	0.553	0.810	601	2.4
AH	97	1	0	1	0.618	0.239	0.810	500	49.0
AH	98	0	0	1	0.618	0.516	0.855	790	5.0
AH	99	0	0	1	0.625	0.526	0.721	861	5.2
AH	100	1	0	1	0.471	0.553	0.810	627	2.4
AI	101	1	1	0	0.461	0.006	0.950	361	6.1
AJ	102	1	0	1	0.502	0.481	0.800	501	6.2
AJ	103	0	0	1	0.489	0.408	0.918	572	5.6
AK	104	1	0	1	0.422	0.463	0.836	563	5.7
AL	105	1	0	1	0.311	0.029	0.800	435	2.4
AL	106	0	0	1	0.318	0.010	0.877	420	13.0
AL	107	1	0	1	0.353	0.009	0.888	423	13.0
AL	108	1	0	1	0.322	0.009	0.888	424	13.0
AL	109	1	0	1	0.315	0.009	0.941	426	13.0

Well ID	Case	Filtrate Ratio Corrected (100/500)	$L_{BHA} - L_{crit}(m)$	Hardness Index	Torque Resistance (N/m)	Adhesion Strength (N/m^2)	Solid (ppm)	MAX dog leg severity $(deg/100ft)$	Total Open Hole Time (h)	Segment Bottom MD (m)
AF	94	2.72	300.00	14.58	2	866	800	0.09	26	3313
AF	95	2.72	300.00	14.58	2	866	823	0.07	145	4024
AG	96	0.04	300.00	18.32	28	45690	1402	0.11	275	3880
AH	97	0.04	300.00	48.86	402	67563	781	0.01	82	2683
AH	98	0.04	231.96	48.86	402	67563	781	2.70	134	2995
AH	99	0.04	194.97	48.86	402	67563	781	2.10	231	3104
AH	100	0.04	211.34	18.32	28	45690	1402	0.11	275	3880
AI	101	2.72	338.63	14.58	2	866	700	0.06	200	3106
AJ	102	2.72	300.00	14.58	2	866	421	0.22	232	3752
AJ	103	2.72	179.25	14.58	2	866	465	0.80	269	4152
AK	104	2.72	177.87	14.58	2	866	470	0.44	106	4109
AL	105	2.30	300.00	17.59	1018	192478	793	0.22	32	3074
AL	106	0.58	227.60	17.59	1018	192478	1000	0.76	204	3110
AL	107	0.58	178.96	17.59	1018	192478	1000	0.23	1434	3114
AL	108	0.58	178.96	17.59	1018	192478	1000	0.24	1458	3118
AL	109	0.58	219.74	17.59	1018	192478	1000	0.24	1552	3145

Well ID	Case	Status	Training Set	Test Set	Clearance Factor	Inclination Factor	TSF	Differential Pressure (psi)	API Filtrate (cm^3)
AL	110	1	0	1	0.302	0.010	0.941	431	13.0
AL	111	1	0	1	0.313	0.008	0.864	435	13.0
AL	112	1	0	1	0.302	0.009	0.839	437	13.0
AL	113	1	0	1	0.315	0.010	0.869	438	13.0
AL	114	1	0	1	0.302	0.011	0.863	446	13.0
AL	115	1	0	1	0.292	0.011	0.866	467	13.0
AM	116	1	0	1	0.584	0.009	0.956	522	4.4
AN	117	0	0	1	0.631	0.011	0.956	35	4.0
AO	118	1	1	0	0.488	0.005	1.000	225	4.9
AP	119	1	0	1	0.604	0.032	0.822	133	5.1
AP	120	0	0	1	0.574	0.022	0.822	194	5.5
AP	121	1	1	0	0.287	0.025	0.812	382	4.7
AP	122	1	0	1	0.287	0.031	0.956	549	4.5
AQ	123	1	0	1	0.488	0.005	1.000	225	4.9
AR	124	0	0	1	0.527	0.352	0.800	468	13.0
AR	125	1	0	1	0.393	0.360	0.855	504	13.0
AR	126	1	0	1	0.374	0.355	0.855	543	13.0
AS	127	1	1	0	0.384	0.017	0.800	394	8.6

Well ID	Case	Filtrate Ratio Corrected (100/500)	$L_{BHA} - L_{crit}(m)$	Hardness Index	Torque Resistance (N/m)	Adhesion Strength (N/m^2)	Solid (ppm)	MAX dog leg severity $(deg/100ft)$	Total Open Hole Time (h)	Segment Bottom MD (m)
AL	110	0.58	219.74	17.59	1018	192478	1000	0.23	1578	3192
AL	111	0.58	252.00	17.59	1018	192478	1000	0.49	1630	3210
AL	112	0.58	210.58	17.59	1018	192478	1000	0.82	1650	3211
AL	113	0.58	202.05	17.59	1018	192478	1000	1.14	1707	3227
AL	114	0.58	192.58	17.59	1018	192478	1000	1.03	136	3334
AL	115	0.58	202.06	17.59	1018	192478	1000	0.41	1788	3530
AM	116	2.72	479.95	14.58	2	866	946	0.11	67	3442
AN	117	2.72	479.95	3.69	158	1278	236	0.22	46	2495
AO	118	2.72	462.71	3.69	158	1278	530	0.01	57	2759
AP	119	2.72	257.12	3.69	158	1278	97	0.07	66	2385
AP	120	2.72	257.12	3.69	158	1278	400	0.15	165	2520
AP	121	2.72	219.38	14.58	2	866	651	0.07	439	2969
AP	122	2.72	473.71	14.58	2	866	910	0.04	537	3420
AQ	123	2.72	462.71	3.69	158	1278	530	0.01	57	2759
AR	124	0.58	300.00	17.59	1018	192478	96837	0.41	902	3568
AR	125	0.58	231.96	17.59	1018	192478	100000	0.64	931	3794
AR	126	0.58	231.96	17.59	1018	192478	100000	0.49	964	3867
AS	127	2.72	300.00	14.58	2	866	385	0.35	135	3056

Appendix E

Risk Analysis Results

E.1 Testing the Model: Success Rate Analysis

The model achieved 68% success rate in identifying the cases correct outcome based on the average similarity score method. In other words, the average similarity between each test cases and all training cases with same outcome was greater than the average similarity between each test cases and all training cases with opposite outcome (called here dissimilarity) in 68% of comparisons performed. Table E.1 shows the results of weights optimization and regression analysis parameters.

The MATLAB lsqrcurvefit function used to perform the non-linear regression is explained below.

The following input settings were used as well as changes from defaults values:

Lower Bound: 0 for all weights
No Upper Bound
MaxIter = 100000
MaxFunEvals = 100000

Transcript of Part of Code of the Differential Sticking Risk Analysis Model

```
% calling LSQRCURVEFIT. Initial guess for % weights was already entered.  See
ydata.
options=optimset('MaxIter',100000,'MaxFunEvals',100000,'Display','final-detailed');
[x,resnorm,residual,exitflag,output]=lsqcurvefit('sim2',w,data,ydata,[0,0,0,
0,0,0,0],[],options);
```

Table E.1: Weights Optimization Statistics

(a) Optimization Efficiency

Overall Average Similarity Score for Cases with Same Outcome (Similar)	**Overall Average Similarity Score for Cases with Different Outcome (Dissimilar)**
0,57	0,28

(b) Optimum Weights

w_1**(Wall Contact)**	w_2**(Mudcake Quality)**	w_3**(Mudcake Thickness)**	w_4**(Differential Pressure)**	w_5**(MAX Dog Leg Severity)**	w_6**(Total Open Hole Time)**	w_7**(Segment Bottom MD)**
12,076	7,061E-08	0,035	2,792	444,757	2,234E-14	7,191E-13

Algorithm E.1 Lsqcurvefit from MATLAB®

Solve nonlinear curve-fitting (data-fitting) problems in least-squares sense Equation

$$\min_x \mid\mid F(x, xdata) - ydata \mid\mid_2^2 = min \sum_x \left(F\left(x, xdata_i\right) - ydata_i\right)^2 \quad \text{(E.1)}$$

Find coefficients x that solve the problem given input data $xdata$, and the observed output $ydata$, where xdata and ydata are matrices or vectors of length m, and$F(x, xdata)$ is a matrix-valued or vector-valued function.

SyntaxTarget Case

x = lsqcurvefit(fun,x0,xdata,ydata)
x = lsqcurvefit(fun,x0,xdata,ydata,lb,ub)
x = lsqcurvefit(fun,x0,xdata,ydata,lb,ub,options)

Description

lsqcurvefit solves nonlinear data-fitting problems. lsqcurvefit requires a user-defined function to compute the vector-valued function F (x, xdata). The size of the vector returned by the user-defined function must be the same as the size of the vectors ydata and xdata.
x = lsqcurvefit(fun,x0,xdata,ydata) starts at x0 and finds coefficients x to best fit the nonlinear function fun(x,xdata) to the data ydata (in the least-squares sense). ydata must be the same size as the vector (or matrix) F returned by fun.
x = lsqcurvefit(fun,x0,xdata,ydata,lb,ub) defines a set of lower and upper bounds on the design variables in x so that the solution is always in the range lb $\leq$ x $\leq$ ub.

Options

Algorithm:

Trust-Region-Reflective Optimization
By default lsqcurvefit chooses the trust-region-reflective algorithm. This algorithm is a subspace trust-region method and is based on the interior-reflective Newton method. Each iteration involves the approximate solution of a large linear system using the method of preconditioned conjugate gradients (PCG).

DiffMaxChange

Maximum change in variables for finite-difference gradients (a positive scalar). The default is 0.1

DiffMinChange

Minimum change in variables for finite-difference gradients (a positive scalar). The default is 1e-8.

Display

Level of display. 'off' displays no output, and 'final' (default) displays just the final output.

FunValCheck

Check whether function values are valid. 'on' displays an error when the function returns a value that is complex, Inf, or NaN. The default 'off' displays no error.

Jacobian

If 'on', lsqcurvefit uses a user-defined Jacobian (defined in fun), or Jacobian information (when using JacobMult), for the objective function. If 'off' (default), lsqcurvefit approximates the Jacobian using finite differences.

MaxFunEvals

Maximum number of function evaluations allowed, a positive integer. The default is 100*numberOfVariables.

MaxIter

Maximum number of iterations allowed, a positive integer. The default is 400.

TolFun

Termination tolerance on the function value, a positive scalar. The default is 1e-6.

TolX

Termination tolerance on x, a positive scalar. The default is 1e-6.

TypicalX

Typical x values. The number of elements in TypicalX is equal to the number of elements in x0, the starting point. The default value is ones(numberofvariables,1). lsqcurvefit uses TypicalX for scaling finite differences for gradient estimation.

Table E.2: Average Similarity Scores Between Each Target Case and All Training Cases

Test Case ID	Average Similarity	Average Dissimilarity	Test Case ID	Average Similarity	Average Dissimilarity
7	0,570	0,405	37	0,753	0,222
8	0,359	0,569	38	0,254	0,779
9	0,355	0,577	39	0,803	0,251
10	0,399	0,564	40	0,707	0,290
12	0,479	0,433	41	0,270	0,744
13	0,264	0,390	42	0,785	0,268
15	0,752	0,295	44	0,741	0,310
16	0,244	0,801	45	0,763	0,268
17	0,139	0,430	46	0,753	0,256
18	0,761	0,260	47	0,735	0,283
19	0,778	0,287	48	0,636	0,297
20	0,422	0,499	49	0,603	0,321
21	0,740	0,297	50	0,231	0,447
22	0,739	0,296	51	0,162	0,434
23	0,762	0,281	52	0,034	0,218
24	0,500	0,369	53	0,339	0,420
25	0,348	0,574	54	0,547	0,405
26	0,136	0,427	55	0,397	0,399
27	0,724	0,287	56	0,247	0,783
28	0,786	0,262	57	0,768	0,259
29	0,771	0,248	58	0,694	0,267
30	0,248	0,771	59	0,241	0,787
31	0,037	0,225	60	0,653	0,332
32	0,772	0,225	61	0,794	0,244
33	0,757	0,274	62	0,727	0,242
34	0,513	0,369	63	0,273	0,717
35	0,463	0,231	64	0,781	0,265
36	0,623	0,280	65	0,806	0,246
			66	0,806	0,246
			67	0,724	0,294

Table E.3: Average Similarity Scores Between Each Target Case and All Training Cases

Test Case ID	Average Similarity	Average Dissimilarity	Test Case ID	Average Similarity	Average Dissimilarity
68	0.248	0.435	97	0.503	0.464
69	0.542	0.350	98	0.566	0.257
70	0.331	0.609	99	0.592	0.313
71	0.715	0.312	100	0.432	0.518
72	0.696	0.316	102	0.438	0.529
73	0.754	0.303	103	0.564	0.405
74	0.308	0.699	104	0.371	0.533
75	0.738	0.298	105	0.773	0.273
76	0.764	0.296	106	0.337	0.543
77	0.702	0.343	107	0.768	0.268
78	0.704	0.341	108	0.766	0.270
79	0.710	0.328	109	0.764	0.271
80	0.729	0.262	110	0.767	0.269
81	0.761	0.260	111	0.663	0.305
82	0.274	0.777	112	0.518	0.344
83	0.789	0.263	113	0.404	0.378
84	0.258	0.783	114	0.439	0.368
85	0.790	0.253	115	0.705	0.295
86	0.271	0.770	116	0.770	0.256
87	0.671	0.284	117	0.250	0.740
88	0.537	0.315	119	0.779	0.239
89	0.501	0.305	120	0.251	0.783
90	0.804	0.248	122	0.762	0.252
91	0.798	0.251	123	0.785	0.228
92	0.797	0.251	124	0.533	0.459
93	0.793	0.252	125	0.358	0.534
94	0.790	0.252	126	0.361	0.528
95	0.253	0.762	68 % Average Similarity >Average Dissimilarity		
96	0.433	0.518			

Table E.4: Example Computation of Average Similarity Score with Similar and Dissimilar Cases

Test Case ID	Training Case	Similarity Score	STATUS Test Case (0 means Stuck)	STATUS Training
83	1	0.419	1	1
83	2	0.331	1	0
83	3	0.342	1	0
83	4	0.163	1	0
83	5	0.277	1	0
83	6	0.223	1	0
83	11	0.345	1	0
83	14	0.161	1	0
83	43	0.829	1	1
83	101	0.884	1	1
83	118	0.865	1	1
83	121	0.892	1	1
83	127	0.844	1	1
Average Score Similar			0.789	
Average Score Dissimilar			0.263	

Table E.5: Dummy Cases Input Data

Dummy Case ID	Status (0 means Stuck)	Training Set	Test Set	Clearance Factor	Inclination Factor	TSF	Differential Pressure (psi)	API Filtrate (cm^3)	Filtrate Ratio Corrected (100/500)
1	1	1	1	0.010	0.100	0.3	120	2.00	0.3
2	0	1	1	0.600	1.000	0.9	1000	8.59	2.72
3	1	1	1	0.200	0.200	0.4	200	3.00	0.5
4	1	1	1	0.300	0.300	0.5	300	6.00	0.6
5	0	1	1	0.580	0.800	0.7	800	7.50	2
6	1	1	1	0.325	0.333	0.55	320	6.20	0.65
7	1	1	1	0.375	0.500	0.6	400	4.00	0.3
8	0	1	1	0.500	1.000	0.85	950	8.00	2.3

Dummy Case ID	$L_{BHA} - L_{Crit}\ (m)$	Hardness Index (s)	Torque Resistance (N/m)	Adhesive Strength (N/m^2)	Solid (ppm)	MAX dog leg severity (deg/100ft)	Total Open Hole Time (h)	Segment Bottom MD(M)
1	177	14.58	2.18	865.9225557	385.00	0.35	135	3056
2	450	0.36	1000.00	190000	75000.00	8	1000	6500
3	200	8	10.00	1000	500.00	2	200	3300
4	250	10	15.00	1500	1000.00	3	300	3500
5	400	1	900.00	150000	70000.00	7	750	5000
6	275	11	20.00	1700	1100.00	3.5	350	3550
7	250	13	15.00	865.9225557	385.00	0.35	135	3056
8	375	1.5	750.00	160000	60000.00	5	600	4800

Table E.6: Dummy Cases Weights Optimization Statistics

(a) Optimization Efficiency

Average Similarity Score for Cases with Same Outcome (Similar)	**Average Similarity Score for Cases with Different Outcome (Dissimilar)**
0.75	0.32

(b) Optimum Weights

w_1**(Wall Contact)**	w_2**(Mudcake Quality)**	w_3**(Mudcake Thickness)**	w_4**(Differential Pressure)**	w_5**(MAX dog leg severity)**	w_6**(Total Open Hole Time)**	w_7**Segment Bottom**
2.220E-14	470	2.231E-14	8487	970	2.070E-11	2.222E-14

E.1.1 Proposed Method for Field Applications: Bi-dimensional Analysis based on Similarity Scores.

Table E.7: Detailed Bi-dimensional Analysis

Well ID	Case ID	Status (0 means Stuck)	Average Similarity to Free	Average Similarity to Stuck	Net Time to Free the Drillstring * (h)
AH	97	1	0.503	0.464	
AH	98	0	0.257	0.566	10
AH	99	0	0.313	0.592	71.5
AH	100	1	0.432	0.518	
AL	105	1	0.773	0.273	
AL	106	0	0.543	0.337	38.5
AL	107	1	0.768	0.268	
AL	108	1	0.766	0.270	
AL	109	1	0.764	0.271	
AL	110	1	0.767	0.269	
AL	111	1	0.663	0.305	
AL	112	1	0.518	0.344	
AL	113	1	0.404	0.378	
AL	114	1	0.439	0.368	
AL	115	1	0.705	0.295	
AR	124	0	0.459	0.533	3
AR	125	1	0.358	0.534	
AR	126	1	0.361	0.528	

* Actions directly related to working drillstring. It discounts assembling and running tools, waiting on weather, etc..

Appendix F

Overpull Reference Data

F.1 CASE I

F.1.1 Input Data

Tables F.1 and F.2 and Fig. F.1 shows input data for Case I.

Note from drilling report before releasing drillstring (See note in Fig. F.1b in Portuguese): *"working upwards stuck drillstring at 2700 m (DJAR is not working downwards) with 70-90 KIPS/ 200 KIPS of overpull and 21 KIPS x ft of torque."*

F.1.2 Output Data

Results for Case I are shown in Table F.3

Table F.1: BHA Data

Description	**Number**	**Outer Diameter**(in)	**Length** (m)	**Cumulative Length** (m)
Drill Bit	1	8.50	0.3	0.3
STB	1	8.50	0.89	1.19
LWD	1	6.75	5.87	7.06
MWD	1	6.75	8.47	15.53
STB	1	8.50	1.54	17.07
Non-Magnetic DC	1	6.75	9.23	26.3
STB	1	8.50	1.52	27.82
DC	6	6.75	55.83	83.65
DJAR	1	6.50	9.36	93.01
DC	2	6.75	18.99	112
HWDP	15	5.00	139.64	251.64

Note: STB (Stabilizer), LWD (Logging While Drilling), MWD (Measurement While Drilling), DC (Drill Collar), DJAR (Drilling Jar), HWDP (Heavy Weight Drill Pipe). HWDP were not considered to significantly touch the wellbore because of the "upsets" in the middle of the tool and small diameter, i.e., big clearance. This applies for all subsequent cases.

Table F.2: Summary of Operational Data for Occurrence

Well Segment ID (case)	Well Diameter (in)	MD (m)	Reported Stuck Depth (m)	$\triangle P\,(psi)$	Pressure Curve Index H $(\frac{psi}{\exp^{sp^{mm}}})$	Pressure Curve Index s_p	Mudcake Thickness (mm)
106	8.5	3110	2700	420	0.47	5.71	2.8

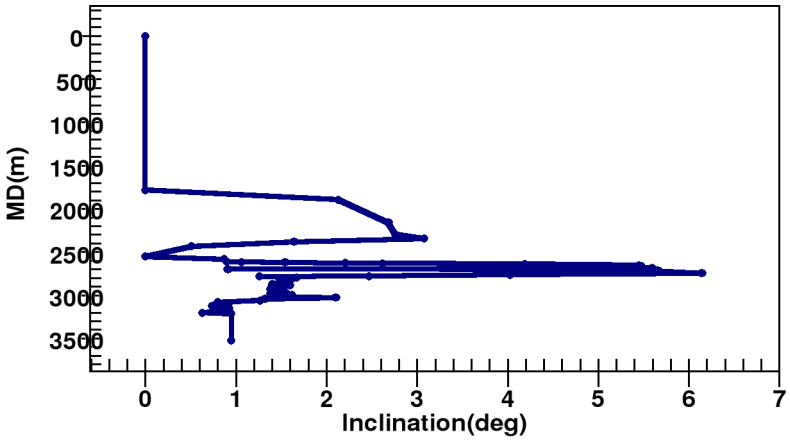

(a) Well Trajectory

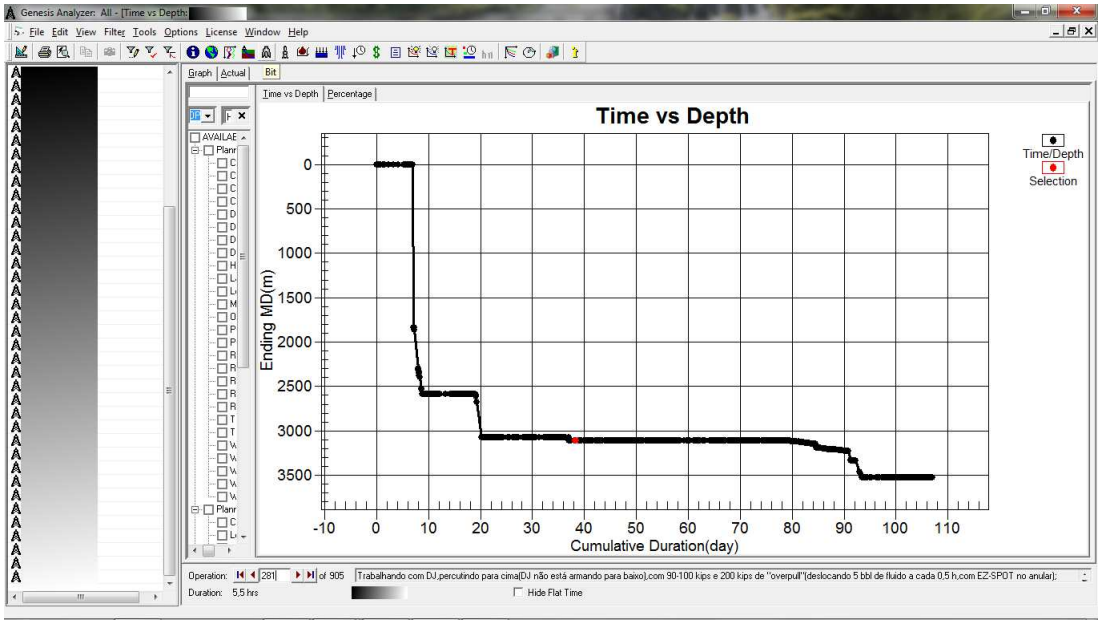

(b) Time versus Depth

Figure F.1: Well Data CASE I

Table F.3: Summary of Results

Overall BHA TSF *	$h_{eff}(m)$	$h_{as}(m)$	$h\ (m)$	$\delta(mm)$	$d(cm)$	Calculated d Overpull $(Klbf)$	Reported Overpull $(Klbf)$
0.63	0	70.5	44.5	1.19	7.17	208.3	200

Table F.4: BHA Data

Description	**Number**	**Outer Diameter**(in)	**Length** (m)	**Cumulative Length** (m)
Drill Bit	1	12.25	0.33	0.33
MOTOR	1	12.25	9.31	9.64
FLOAT SUB	1	12.25	0.76	10.4
STB	1	12.25	1.48	11.88
MWD	1	8.25	8.45	20.33
ADAPTER SUB	1	8.25	0.71	21.04
non-Magnetic DC	1	8.25	8.51	29.55
DC	6	8.25	55.52	85.07
DJAR	1	8.25	9.1	94.17
ADAPTER SUB	1	8.25	0.99	95.16
DC	3	6.75	28.05	123.21
HWDP	9	6.75	84	207.21

F.2 CASE II

F.2.1 Input Data

Tables F.4 and F.5 and Fig. F.2 shows input data for Case II.

Note from drilling report before releasing drillstring (See note in Fig. F.2b in Portuguese): *"working drillstring and releasing with 180 KLB of overpull and 5 KLB of torque."*

F.2.2 Output Data

Results for Case II are shown in Table F.6

Table F.5: Summary of Operational Data for Occurrence

Well Segment ID	Well Diameter (in)	MD (m)	Reported Stuck Depth (m)	$\triangle P\,(psi)$	Pressure Curve Index H $(\frac{psi}{\exp^{sp\,mm}})$	Pressure Curve Index s_p	Mudcake Thickness (mm)
124	12.25	2890	2884	467	0.177	12.85	2.8

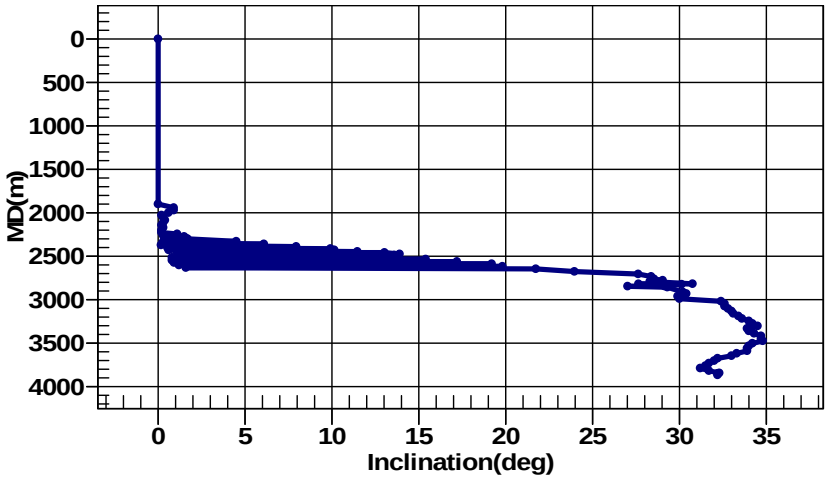

(a) Well Trajectory

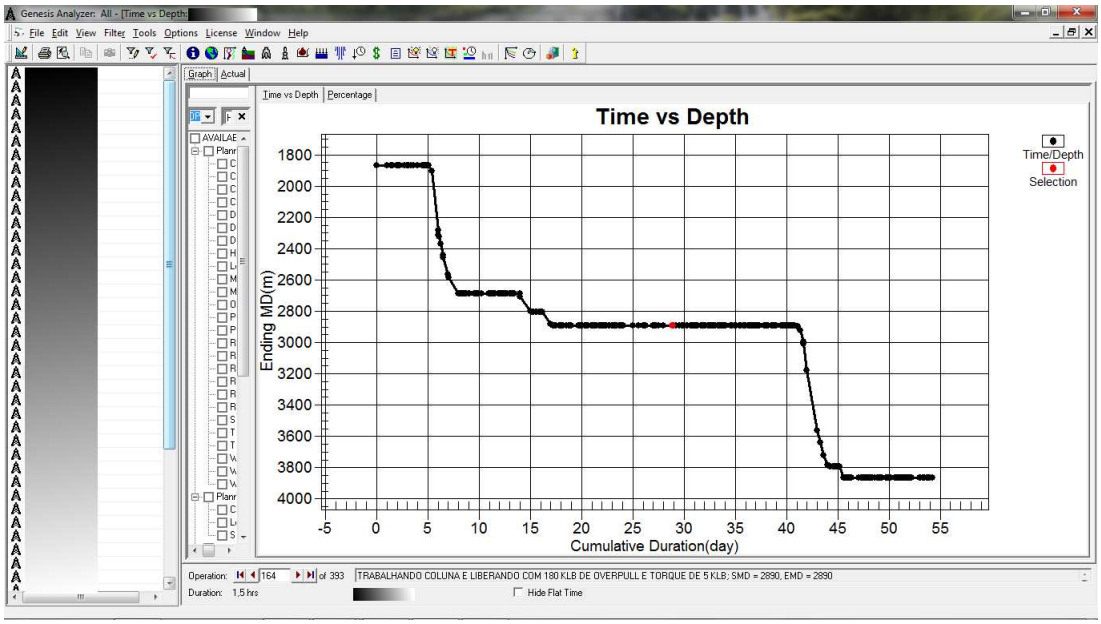

(b) Time versus Depth

Figure F.2: Well Data CASE II

Table F.6: Summary of Results

Overall BHA TSF	$h_{eff}(m)$	$h_{as}(m)$	$h\ (m)$	$\delta(mm)$	$d(cm)$	Calculated Overpull $(Klbf)$	Reported Overpull $(Klbf)$
0.67	0	103.7	69.35	0.61	3.88	195.2	180

F.3 CASE III

F.3.1 Input Data

Tables F.7 and F.8 and Fig. F.3 shows input data for Case III.

Table F.7: BHA Data

Description	**Number**	**Outer Diameter**(in)	**Length** (m)	**Cumulative Length** (m)
Drill Bit	1	17.5	0.45	0.45
STB	1	17.25	1	1.45
MOTOR	1	9.625	6.98	8.43
ADAPTER SUB	1	9.5	0.79	9.22
FLOAT SUB	1	8	0.77	9.99
LWD	1	8.25	5.87	15.86
MWD	1	8	8.42	24.28
Non-Magnetic DC	1	8	9.32	33.6
DC	9	8	84.32	117.92
DJAR	1	8	9.69	127.61
ADAPTER SUB	1	8	0.8	128.41
DC	3	6.75	28.35	156.76
HWDP	15	5	139.13	295.89

Table F.8: Summary of Operational Data for Occurrence

Well Segment ID	Well Diameter (in)	MD (m)	Reported Stuck Depth (m)	$\triangle P\,(psi)$	Pressure Curve Index H $(\frac{psi}{\exp^{sp}mm})$	Pressure Curve Index s_p	Mudcake Thickness (mm)
99	17.5	3104	2981	861	228.84	23.5	3

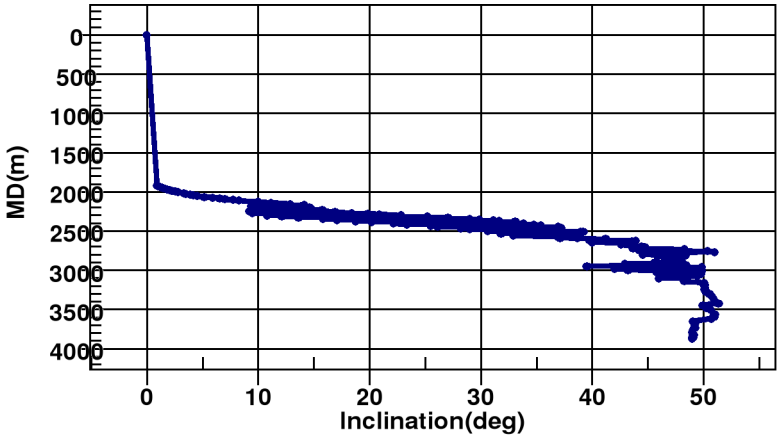

(a) Well Trajectory

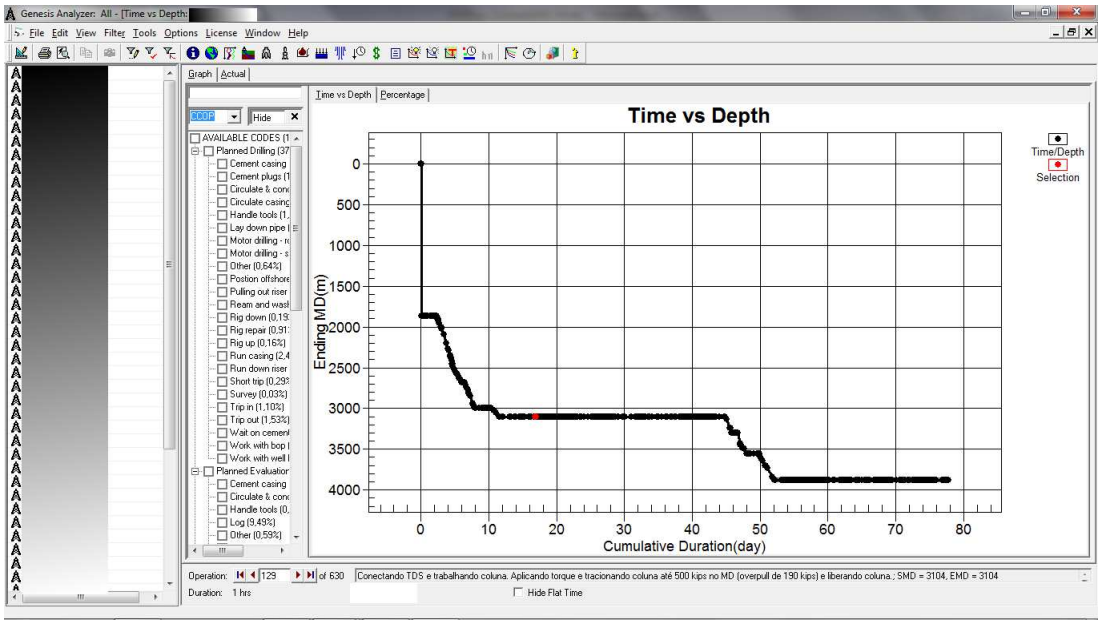

(b) Time versus Depth

Figure F.3: Well Data, CASE III

Note from drilling report before releasing drillstring (See note in Fig. F.3b in Portuguese): *"Applying torque and pulling drillstring with 500 kips at MD (overpull of*

190 KIPS) and releasing drillstring"

F.3.2 Output Data

Results for Case III are shown in Table F.9

Table F.9: Summary of Results

Overall BHA TSF	$h_{eff}(m)$	$h_{as}(m)$	$h\ (m)$	$\delta(mm)$	$d(cm)$	Calculated Overpull $(Klbf)$	Reported Overpull $(Klbf)$
0.66	0	146.4	96.8	0.06	0.9	179.8	190

Appendix G

Fuzzy Sets and Fuzzy Logic

G.1 Introduction

G.1.1 Logic Truth Tables

Fuzzy logic is a multivalued logic and is a superset of the traditional Boolean logic. Table G.1 and Fig. G.1 summarize the meaning of logical operators.

G.1.2 Fuzzy Logic Controller Example: Dinner Tip Calculator from Matlab

This section explains the major components of a fuzzy controller through the example of a fuzzy controller to calculate the tip percentage to be paid in a restaurant. This problem has two inputs, three rules, one output and five membership functions describing the two input variables.

G.1.2.1 Fuzzy Sets (Fuzzification Step)

Fig. G.3 and G.4 shows the inputs and outputs of the tip calculator fuzzy controller respectively.

G.1.2.2 Logical Operators and Related Fuzzy Methods

Table G.3 shows the details.

G.1.2.3 Run Controller: Apply Fuzzy Methods to If-Then Rules

Fig. G.5is the inference diagram of the controller where the logical operators are applied to the relevant variables according to the rules shown in Fig. G.2.

Table G.1: Logic Truth Tables and Logical Operators

(a) Boolean

A	**B**	**A *AND* B**	**A *OR* B**	**A**	***NOT* A**
0	0	0	0	0	1
0	1	0	1	1	0
1	0	0	1		
1	1	1	1		

(b) Fuzzy

A	**B**	***Min* (A,B)**	***Max*(A,B)**	**A**	***NOT* A**
0	0	0	0	0	1
0	1	0	1	1	0
1	0	0	1		
1	1	1	1		

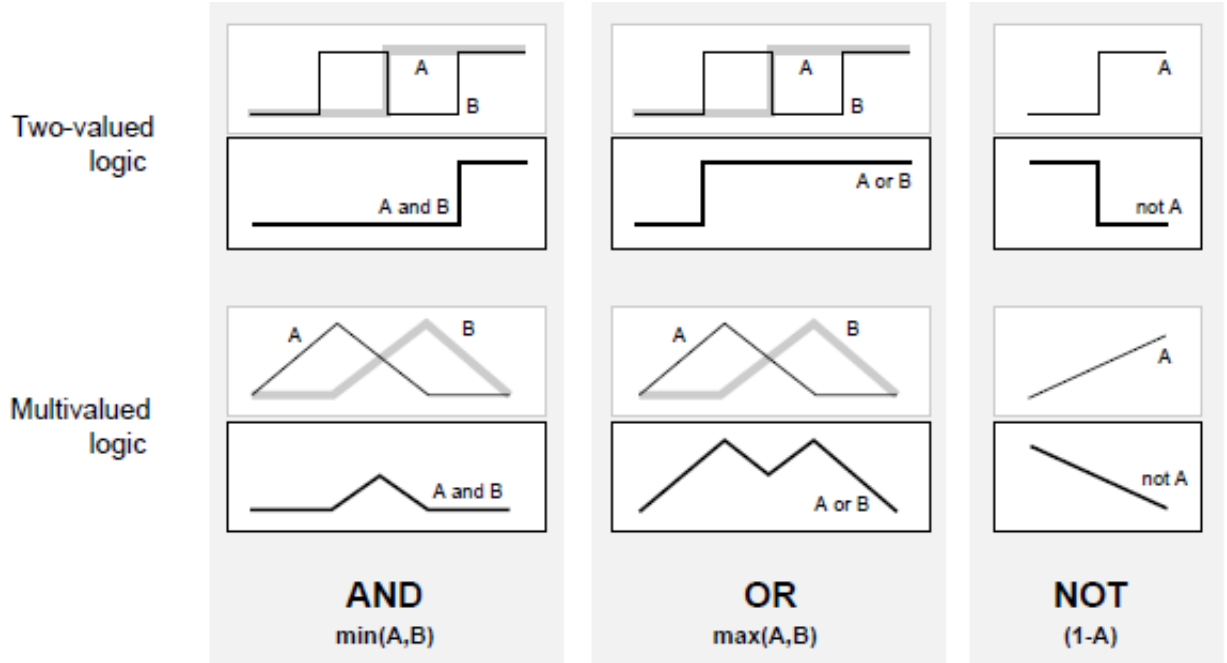

Figure G.1: Two-valued Logic and Multivalued Logic. After Matlab® Fuzzy Logic Toolbox User Manual.

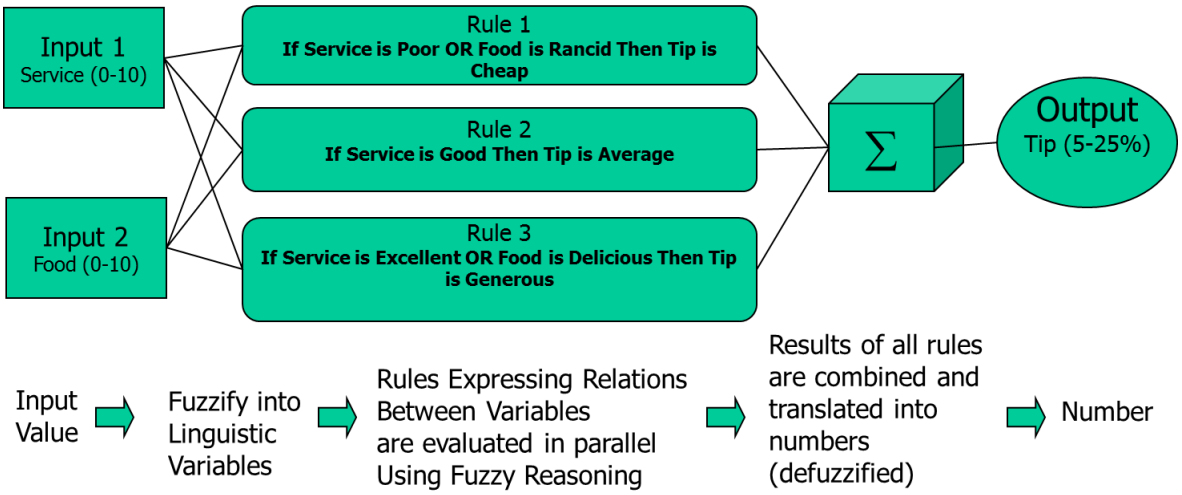

Figure G.2: Fuzzy Tip Calculator

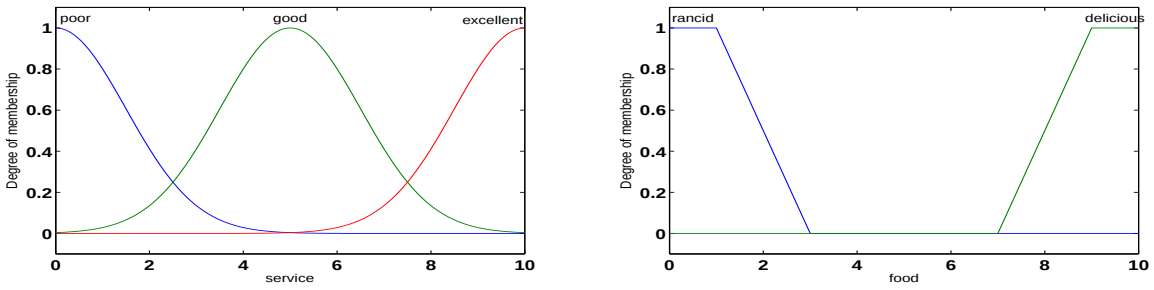

(a) Service (b) Service

Figure G.3: Inputs

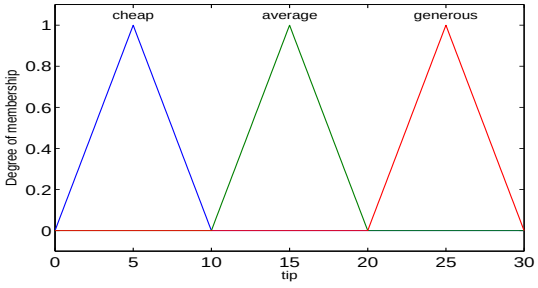

(a) Service

Figure G.4: Output

Table G.2: Logical Operators

Operator	Purpose	Method	Operation
AND	Relates two or more fuzzified variable	Min	Selects the smallest degree of membership between two fuzzy sets being related
OR	Relates two or more fuzzified variable	Max	Selects the highest degree of membership between two fuzzy sets being related
Implication	Produces the consequent part of the rule by acting on the rule's output membership function	Min	Selects the lowest degree of membership between two or more output membership functions
aggregation	Aggregates the consequent part of all rules generated by the implication step	Max	Performs the sum of maximums of each membership functions from the implication step
Defuzzification	Generates an output (fuzzy or crispy number) by computing	Centroid	Computes the centroid of the resultant area from combining membership functions from the aggregation step

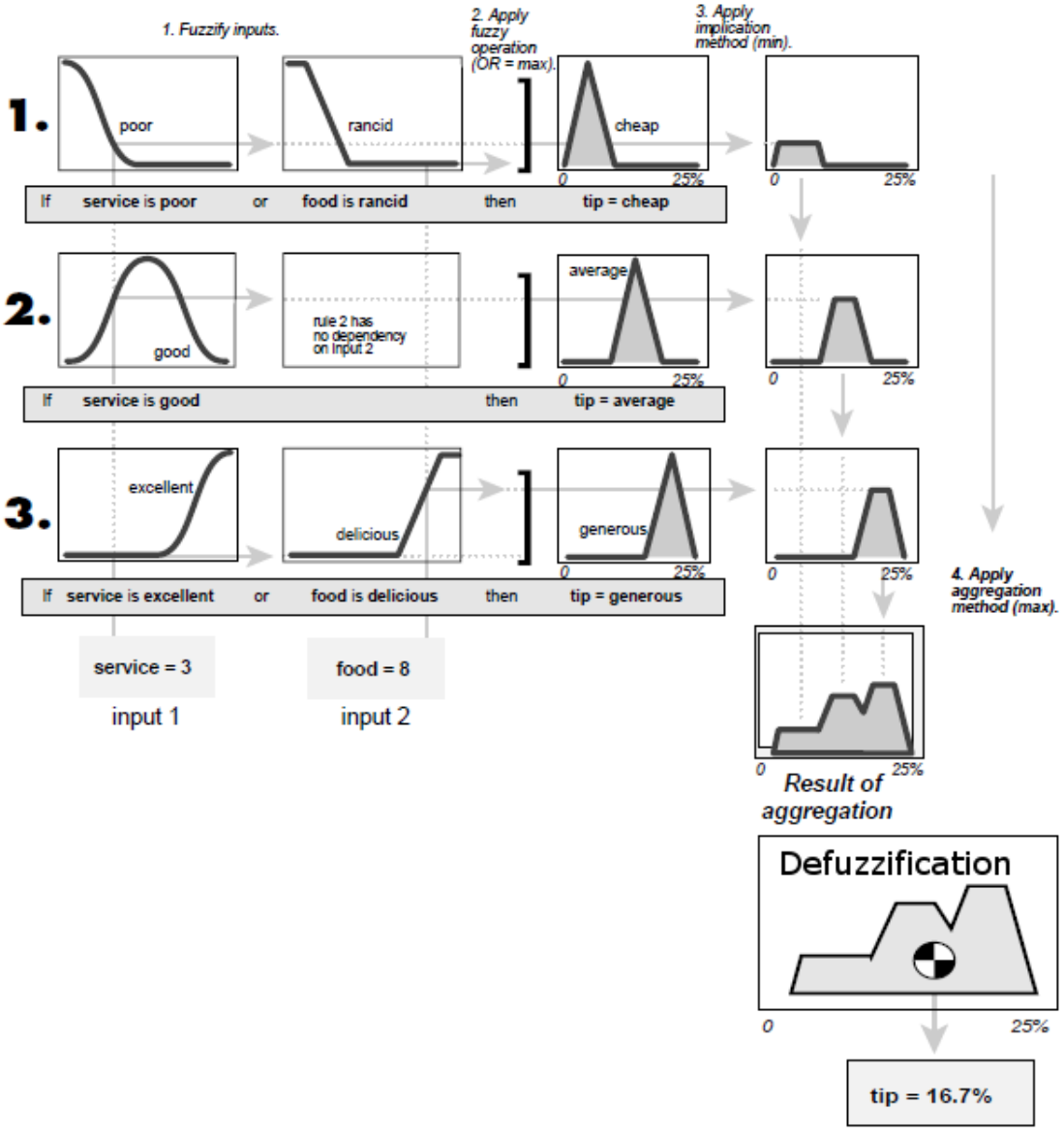

Figure G.5: Tip Controller

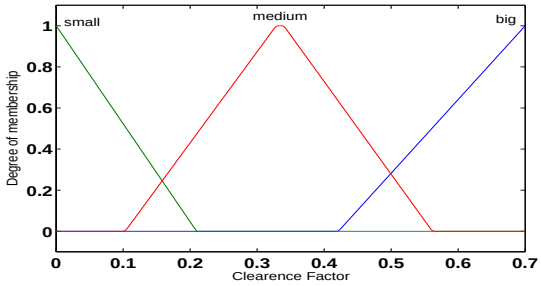

(a) Clearance Factor

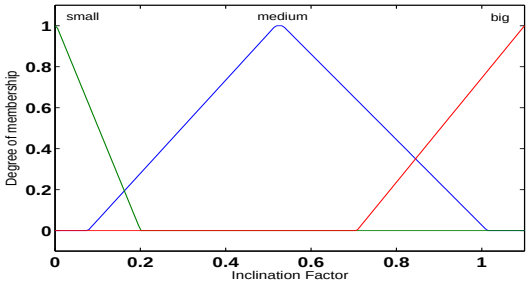

(b) Inclination Factor

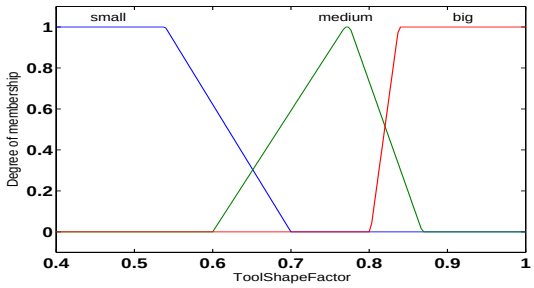

(c) Tool Shape Factor

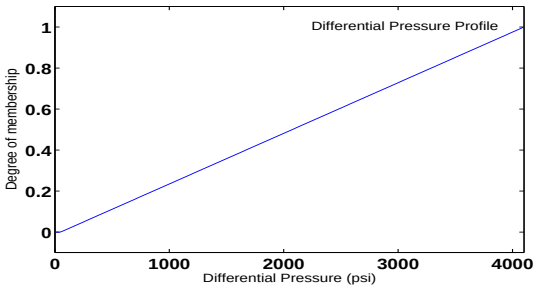

(d) Differential Pressure

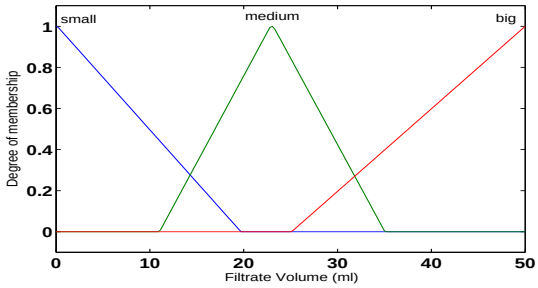

(e) Filtrate Volume

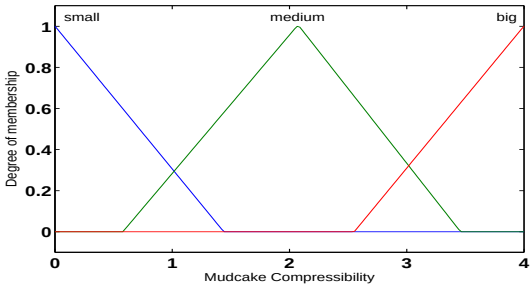

(f) API Filtrate Volume Ratio at 1000 and 500 psi

Figure G.6: Fuzzy Sets Representing Input Linguistic Variables.

G.2 Differential Sticking Fuzzy Sets

Fig. G.7 and G.6 show the fuzzified inputs and Fig. G.8 shows the outputs.

G.3 Differential Sticking Fuzzy Controller Properties

G.3.1 Overall Configuration

Fig. G.9 shows the overall controllers set up and Table G.3 the mathematical meaning of logical operators as well as implication, aggregation and deffuzification methods utilized by the fuzzy controller.

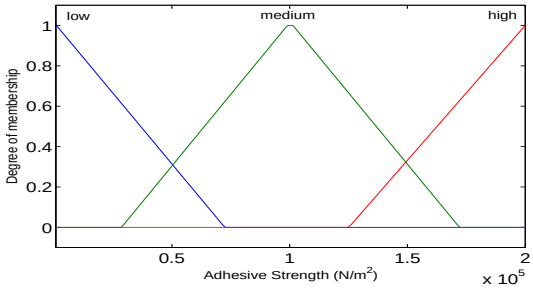

(a) Adhesion

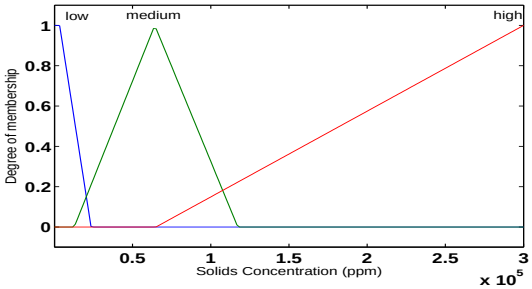

(b) Solids Concentration

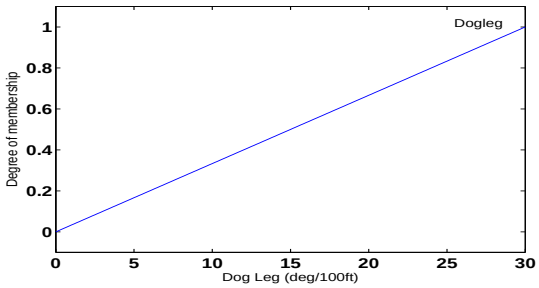

(c) Dogleg Severity

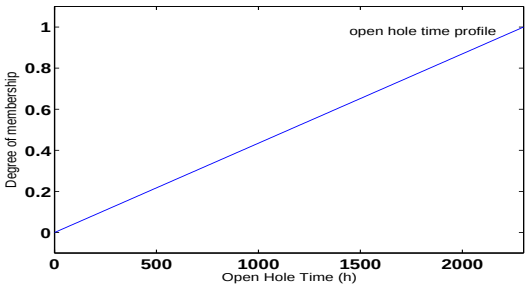

(d) Open Hole Time

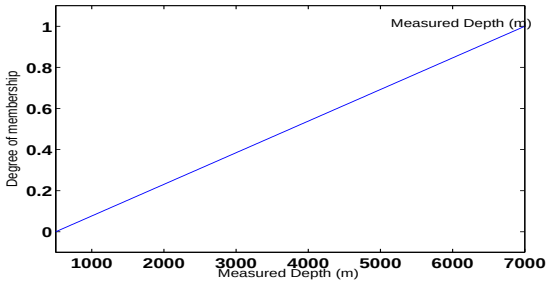

(e) Measured Depth

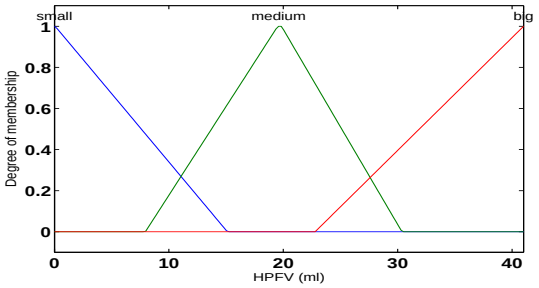

(f) API High Pressure Filtrate Volume, 500 psi.

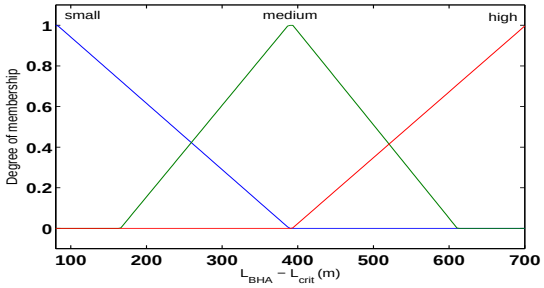

(g) $L_{BHA} - L_{CRIT}$

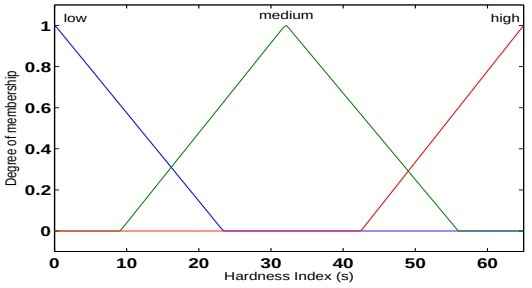

(h) Hardness

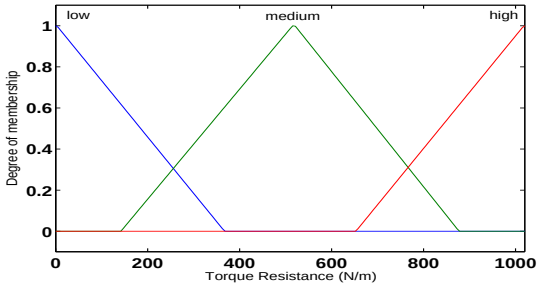

(i) Torque

Figure G.7: Fuzzy Sets Representing Input Linguistic Variables.

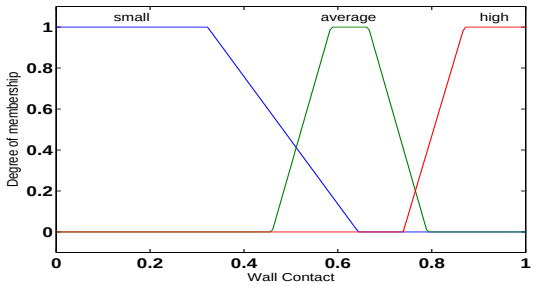

(a) Wall Contact

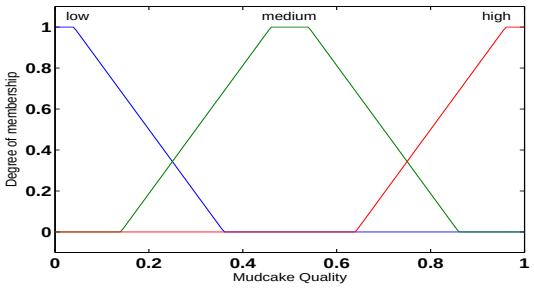

(b) Mudcake Quality

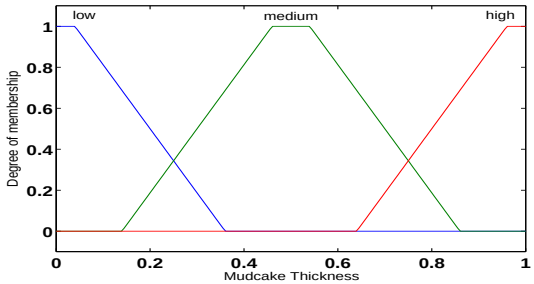

(c) Mudcake Thickness

Figure G.8: Fuzzy Sets Representing Output Linguistic Variables.

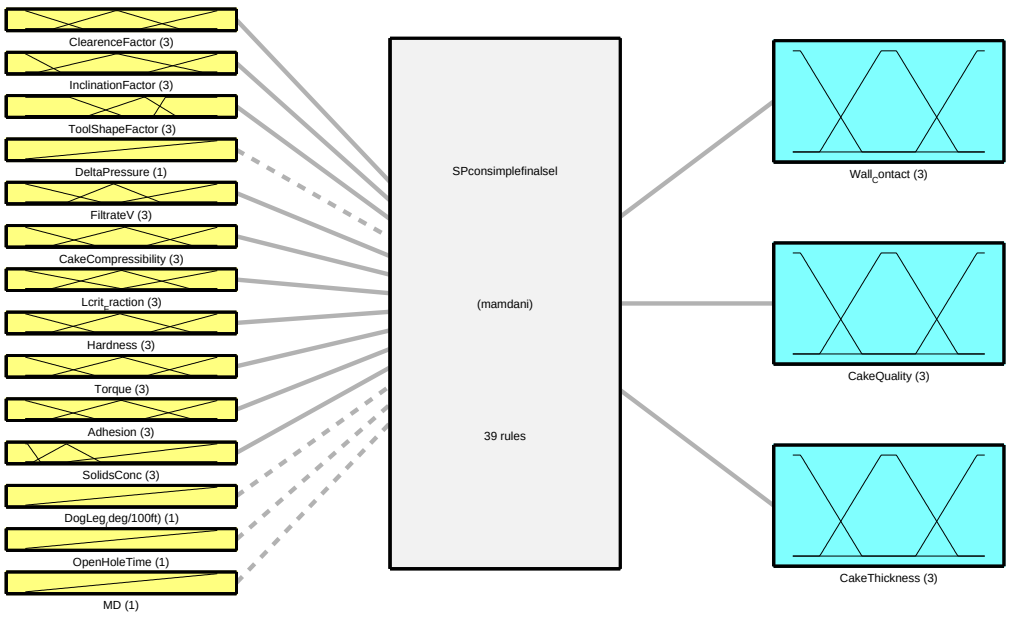

Figure G.9: Controller's Configuration

Table G.3: Logical Operators

Operator	Method
AND	Min
OR	Max
Implication	Min
aggregation	Max
Defuzzification	Centroid

G.3.2 If-Then Rules

The verbal form of fuzzy logic rules are present here.

1. If (ClearanceFactor is not small) and (InclinationFactor is small) then (Wall_Contact is small) (1)

2. If (ClearanceFactor is big) and (InclinationFactor is small) and (ToolShapeFactor is small) and (Lcrit_Fraction is not high) then (Wall_Contact is small) (1)

3. If (ClearanceFactor is big) and (InclinationFactor is medium) and (ToolShape-Factor is not small) and (Lcrit_Fraction is not high) then (Wall_Contact is average) (1)

4. If (ClearanceFactor is medium) and (InclinationFactor is medium) and (Tool-ShapeFactor is not big) and (Lcrit_Fraction is not high) then (Wall_Contact is average) (1)

5. If (ClearanceFactor is medium) and (InclinationFactor is medium) and (Tool-ShapeFactor is not small) then (Wall_Contact is high) (1)

6. If (ClearanceFactor is medium) and (InclinationFactor is big) and (ToolShape-Factor is not big) and (Lcrit_Fraction is not high) then (Wall_Contact is average) (1)

7. If (ClearanceFactor is medium) and (InclinationFactor is big) and (ToolShape-Factor is not big) and (Lcrit_Fraction is high) then (Wall_Contact is high) (1)

8. If (ClearanceFactor is medium) and (InclinationFactor is big) and (ToolShape-Factor is big) and (Lcrit_Fraction is not small) then (Wall_Contact is high) (1)

9. If (ClearanceFactor is medium) and (InclinationFactor is big) and (ToolShape-Factor is big) and (Lcrit_Fraction is small) then (Wall_Contact is average) (1)

10. If (ClearanceFactor and Tool Shape Factor is medium) and (InclinationFactor is medium) and (ToolShapeFactor is small) and (Lcrit_Fraction is high) then (Wall_Contact is high) (1)

11. If (ClearanceFactor is small) and (InclinationFactor is small) and (ToolShapeFactor is small) then (Wall_Contact is small) (1)

12. If (ClearanceFactor is small) and (InclinationFactor is small) and (ToolShapeFactor is not small) then (Wall_Contact is average) (1)

13. If (ClearanceFactor is small) and (InclinationFactor is medium) and (ToolShapeFactor is small) and (Lcrit_Fraction is small) then (Wall_Contact is small) (1)

14. If (ClearanceFactor is small) and (InclinationFactor is medium) and (ToolShapeFactor is small) and (Lcrit_Fraction is medium) then (Wall_Contact is average) (1)

15. If (ClearanceFactor is small) and (InclinationFactor is medium) and (ToolShapeFactor is small) and (Lcrit_Fraction is high) then (Wall_Contact is high) (1)

16. If (ClearanceFactor is small) and (InclinationFactor is medium) and (ToolShapeFactor is medium) and (Lcrit_Fraction is small) then (Wall_Contact is average) (1)

17. If (ClearanceFactor is small) and (InclinationFactor is not small) and (ToolShapeFactor is not small) then (Wall_Contact is high) (1)

18. If (ClearanceFactor is small) and (InclinationFactor is big) and (ToolShapeFactor is small) and (Lcrit_Fraction is not small) then (Wall_Contact is high) (1)

19. If (ClearanceFactor is small) and (InclinationFactor is big) and (ToolShapeFactor is small) and (Lcrit_Fraction is small) then (Wall_Contact is average) (1)

20. If (Hardness is HIGH) and (Torque is MEDIUM) and (Adhesion is not HIGH) then (CakeQuality is HIGH) (1)

21. If (Hardness is HIGH) and (Torque is HIGH) then (CakeQuality is MEDIUM) (1)

22. If (Hardness is HIGH) and (Torque is LOW) then (CakeQuality is HIGH) (1)

23. If (Hardness is MEDIUM) and (Torque is LOW) and (Adhesion is not LOW) then (CakeQuality is MEDIUM) (1)

24. If (Hardness is not MEDIUM) and (Torque is not LOW) and (Adhesion is not LOW) then (CakeQuality is MEDIUM) (1)

25. If (Hardness is not HIGH) and (Torque is not MEDIUM) and (Adhesion is HIGH) then (CakeQuality is LOW) (1)

26. If (Hardness is not HIGH) and (Torque is MEDIUM) then (CakeQuality is MEDIUM) (1)

27. If (Hardness is not HIGH) and (Torque is not MEDIUM) and (Adhesion is not HIGH) then (CakeQuality is MEDIUM) (1)

28. If (Hardness is LOW) and (Torque is HIGH) and (Adhesion is not MEDIUM) then (CakeQuality is LOW) (1)

29. If (Hardness is MEDIUM) and (Torque is LOW) and (Adhesion is LOW) then (CakeQuality is HIGH) (1)

30. If (FiltrateV is small) then (CakeThickness is LOW) (1)

31. If (FiltrateV is big) and (CakeCompressibility is big) and (SolidsConc is MEDIUM) then (CakeThickness is HIGH) (1)

32. If (FiltrateV is big) and (CakeCompressibility is medium) and (SolidsConc is MEDIUM) then (CakeThickness is MEDIUM) (1)

33. If (FiltrateV is medium) and (CakeCompressibility is big) and (SolidsConc is MEDIUM) then (CakeThickness is HIGH) (1)

34. If (FiltrateV is medium) and (CakeCompressibility is medium) and (SolidsConc is MEDIUM) then (CakeThickness is MEDIUM) (1)

35. If (FiltrateV is big) and (SolidsConc is HIGH) then (CakeThickness is HIGH) (1)

36. If (FiltrateV is medium) and (SolidsConc is HIGH) then (CakeThickness is MEDIUM) (1)

37. If (FiltrateV is big) and (CakeCompressibility is small) and (SolidsConc is MEDIUM) then (CakeThickness is MEDIUM) (1)

38. If (FiltrateV is medium) and (CakeCompressibility is small) and (SolidsConc is MEDIUM) then (CakeThickness is LOW) (1)

39. If (SolidsConc is LOW) then (CakeThickness is LOW) (1)

G.3.3 Relationship between Input and Output Variables

Fig. G.10shows the relationship of the controller's output and some relevant input variables.

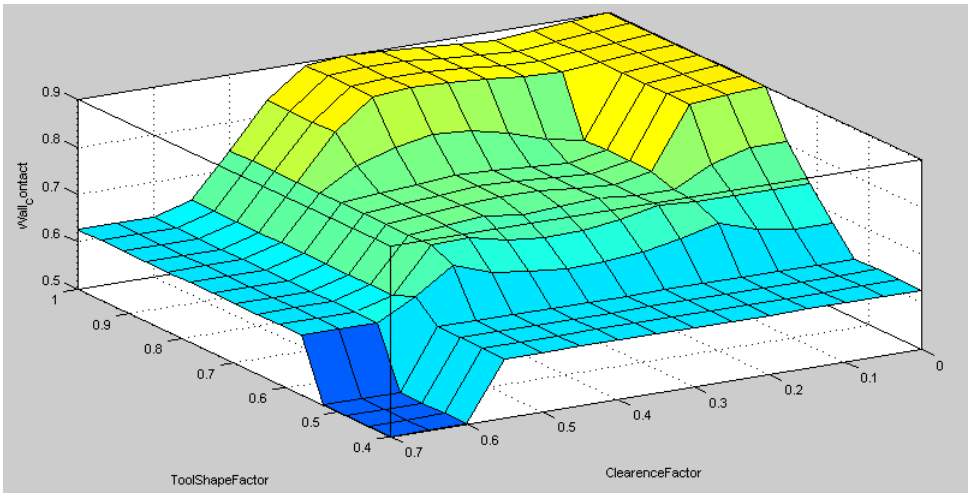

(a) Wall Contact. Inclination Factor Fixed at 0.55 and $L_{BHA} - L_{Crit}$ at 390 m

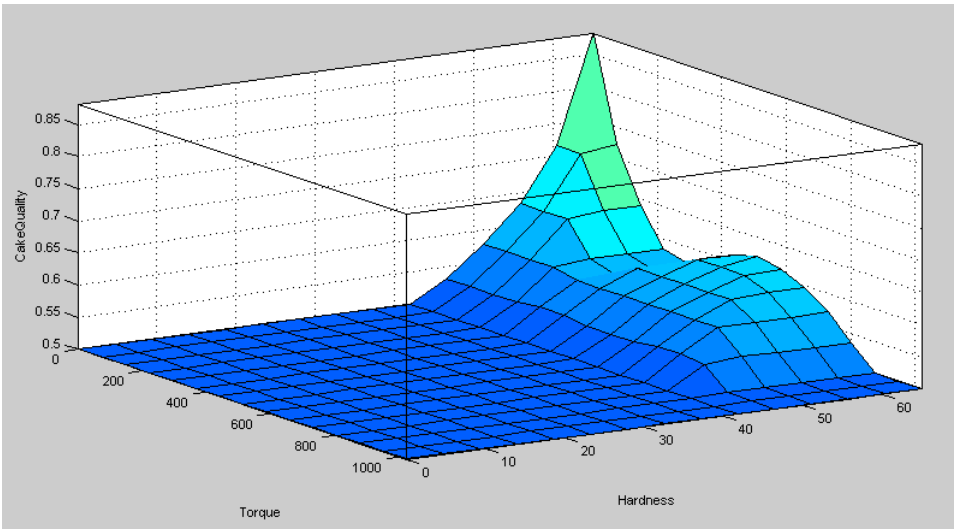

(b) Mudcake Quality. Adhesion Fixed at 1.004E+5 N/m

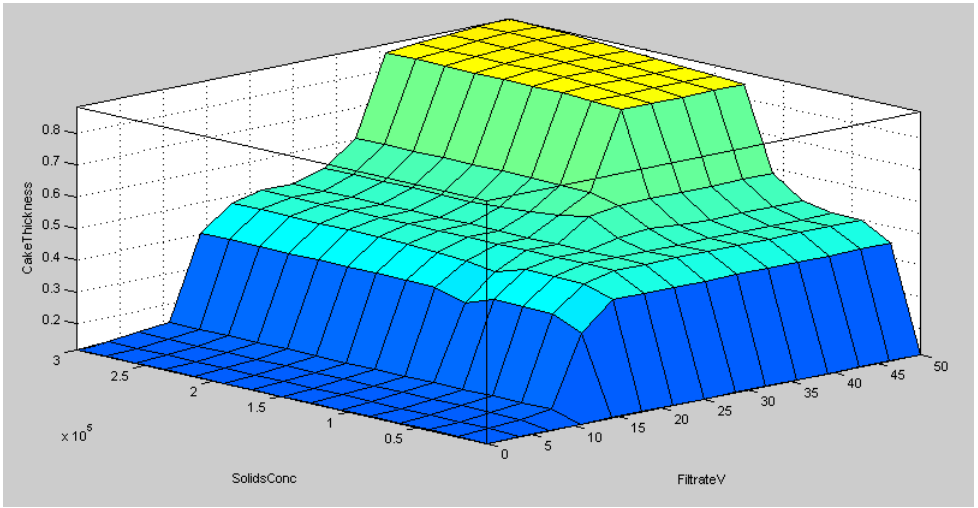

(c) Mudcake Thickness. Mudcake Compressibility fixed at 2.

Figure G.10: Examples of the Relationship Between Inputs and Outputs.